AD-A185 465 A ZONAL APPROACH FOR THE SOLUTION OF COUPLED EULER AND POTENTIAL SOLUTION..(U) INDIANA UNIV-PURDUE UNIV AT INDIANAPOLIS SCHOOL OF ENGINEERIN.. A ECER JUN 87 1/2

UNCLASSIFIED ET-S87-2 AFOSR-TR-87-1350 F49620-83-K-0034 F/G 20/4 NL

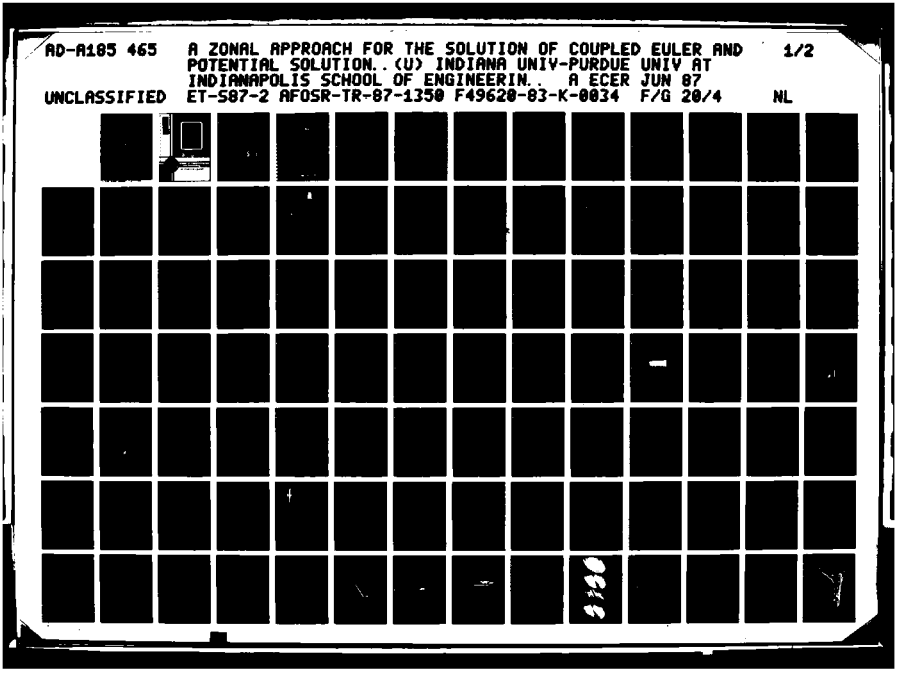

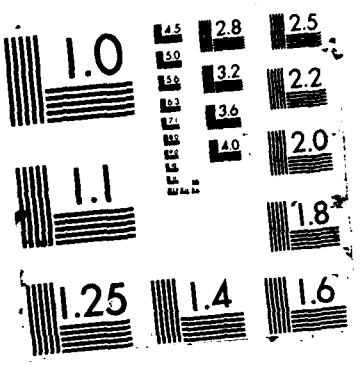
1.0
1.1
1.25
1.4
1.6
2.8
3.2
3.6
4.0
2.5
2.2
2.0
1.8

 AFOSR-TR- 87-1350

Final Report

submitted to

Air Force Office
of Scientific Research
Bolling Air Force Base
Washington, D.C. 20332

for

A Zonal Approach for the Solution
Coupled Euler and Potential Solutio
Flows with Complex Geometries

for the period of

June 1, 1983 - May 31, 1987

Purdue University
School of Engineering
and Technology
at Indianapolis

Indiana University-Purdue University at Indianapolis
IUPUI

(2)

Final Report

submitted to

Air Force Office
of Scientific Research
Bolling Air Force Base
Washington, D.C. 20332

for

A Zonal Approach for the Solution of Coupled Euler and Potential Solutions of Flows with Complex Geometries

for the period of

June 1, 1983 - May 31, 1987

by

Akin Ecer, Principal Investigator
Division of Engineering
Purdue University at Indianapolis
1201 E. 38th Street
Indianapolis, IN 46205

UNCLASSIFIED

SECURITY CLASSIFICATION OF THIS PAGE

A185 465

REPORT DOCUMENTATION PAGE

1a. REPORT SECURITY CLASSIFICATION UNCLASSIFIED	1b. RESTRICTIVE MARKINGS N/A
2a. SECURITY CLASSIFICATION AUTHORITY	3. DISTRIBUTION/AVAILABILITY OF REPORT Approved for public release, distribution unlimited
2b. DECLASSIFICATION/DOWNGRADING SCHEDULE	
4. PERFORMING ORGANIZATION REPORT NUMBER(S) ET-S87-2	5. MONITORING ORGANIZATION REPORT NUMBER(S) AFOSR-TR- 87-1350
6a. NAME OF PERFORMING ORGANIZATION Purdue University School of Eng. and Tech. at Indpolis. — 6b. OFFICE SYMBOL (If applicable)	7a. NAME OF MONITORING ORGANIZATION Airforce Office of Scientific Research N/A
6c. ADDRESS (City, State and ZIP Code) 1201 E. 38th Street, P.O. Box 647 Indianapolis, Indiana 46223	7b. ADDRESS (City, State and ZIP Code) Building 410 Bolling Airforce Base, D.C. 20332-6448
8a. NAME OF FUNDING/SPONSORING ORGANIZATION Air Force Office of Scientific Research — 8b. OFFICE SYMBOL (If applicable) NA	9. PROCUREMENT INSTRUMENT IDENTIFICATION NUMBER F49620-83-K-0034
8c. ADDRESS (City, State and ZIP Code) AFOSR/PKD Building 410 Bolling AFB, D.C. 20332-6448	10. SOURCE OF FUNDING NOS.

PROGRAM ELEMENT NO.	PROJECT NO.	TASK NO.	WORK UNIT NO.
61102F	2307	A1	

11. TITLE (Include Security Classification) A Zonal Approach for the solution of Coupled Euler and Potential Solutions of Flows with Complex Geometries

12. PERSONAL AUTHOR(S) Akin Ecer

13a. TYPE OF REPORT	13b. TIME COVERED	14. DATE OF REPORT (Yr., Mo., Day)	15. PAGE COUNT
Final Report	FROM 6-1-83 TO 5-31-87	June 1987	150

16. SUPPLEMENTARY NOTATION

17. COSATI CODES			18. SUBJECT TERMS (Continue on reverse if necessary and identify by block number)
FIELD	GROUP	SUB. GR.	Transonic Flows, Zonal Methods, Euler Equations

19. ABSTRACT (Continue on reverse if necessary and identify by block number)

A block-structured solution scheme was developed for the solution of three-dimesional Euler equations around complex geometric configurations. The overall effort included the development of a block-structured solution of both potential and Euler equations. The flow field around a complex geometry is divided into blockswith simple geometries. The computational grid is generated individually for each of the blocks and coupled automatically. For each of the blocks, either potential of Euler equations are solved independently using the finite element method. The normal mass and entropy fluxes are balanced between the blocks iterativly by using a relaxation scheme. This scheme is implemented on large computers (CRAY and IBM) using parallel precessing capabilities such as asynchronous I/O and several CPU's.

Three dimensional, airfoils, F-16 aircraft). (Keywords: Transonic flow;

20. DISTRIBUTION/AVAILABILITY OF ABSTRACT	21. ABSTRACT SECURITY CLASSIFICATION
UNCLASSIFIED/UNLIMITED ☒ SAME AS RPT. ☐ DTIC USERS ☐	UNCLASSIFIED

22a. NAME OF RESPONSIBLE INDIVIDUAL	22b. TELEPHONE NUMBER (Include Area Code)	22c. OFFICE SYMBOL
Dr JAMES WILSON	202-767-4935	AFOSR/NA

DD FORM 1473, 83 APR — EDITION OF 1 JAN 73 IS OBSOLETE.

19 2 4 6

SECURITY CLASSIFICATION OF THIS PAGE

UNCLASSIFIED

TABLE OF CONTENTS

Summary of the Project

1. Objectives

The main objective of the research project for the last two years was to develop a block-structured solution scheme for Euler equations. This work was a continuation of the effort to develop computational techniques for solving three-dimensional, transonic flow problems around complex geometries. The overall effort included the block-structured grid generation scheme and block-structured solution of potential and Euler equations. Finally, the implementation of this scheme on existing computers (CRAY X-MP and IBM-3090) was investigated.

2. Review of the Developed Block-Structured Solution Scheme

a. Introduction. A computational scheme for the block-structured solution of transonic flows was developed based on the assumption that the solution of complex flow problems requires treatment of the entire problem in terms of a number of smaller sub-regions (blocks). The solution of such a problem includes grid generation, numerical solution and display of the results. It also usually involves an iterative process where the grid is modified several times and the solution scheme is performed through several steps where the results from an initial set of runs are utilized to start the subsequent set of runs. The block-structured solution scheme was developed to provide a computational environment where all of these tasks can be performed efficiently for complex flows. One can control the solution procedure by describing particular flow regions and later modifying them

locally while these changes are automatically propogated to the remaining flow regions.

b. Block-Structured Solution Scheme. The block-structured solution of three-dimensional transonic flows may typically include the following steps:

. Design of a Block-Structure,

. Generation of a Computational Grid,

. Solution of the Equations,

. Interpretation of Results,

. Modification of the Computational Grid, (Grid Adaptation)

. Solution of the Revised Grid,

. Interpretation of Results and Comparisons.

The above list provides a realistic summary of the steps involved in solving three-dimensional problems. In most cases, the revisions of the grid are performed more than once for adopting the grid to the computed flow field. It becomes very important to be able to inspect the results in detail and implement the necessary modifications with sufficient control and ease. In the following, the description of these steps and related considerations are summarized.

c. Design of the Block-Structure. In terms of the solution of a three-dimensional problem, this step is the fundamental one. One has to decide how to divide the problem into a series of blocks. In most general terms, the blocks are chosen to identify flow structures in a complex flow field. For a simple example, such as the two-dimensional transonic flow around an airfoil, one may decide to identify the flow structures around the leading and

trailing edges of the airfoil as well as around the shocks. In some cases, these blocks may be further sub-divided providing the user the capability to control the generation and modifications of the computational grid in detail.

d. Block-Structured Grid Generation Scheme. The finite element grid generation schemes have been traditionally based on the definition of a series of blocks. Many finite element grid generation packages [1,2] employ the definition of a series of blocks as a basis of finite element grid generation process. Several years ago we have further developed some of these concepts in a form which is more suitable for analyzing complex, three-dimensional flow problems. A block-structured grid generation scheme was developed where the user specifies a block-structure as a first step before the grid generation process [3]. The convectivity of the blocks are defined as a first step. The developed procedure can model any irregular block-structures. One can define blocks which have four, five or six surfaces. The neighboring blocks can be attached, separated or coupled. Also, void blocks can be placed to model the irregularities in the block structure as necessary.

Once the block-structure is defined, the rest of the operations are performed on a block-by-block basis. A computational grid is assigned for each block. The grid can be irregular inside each block. For each flow region, an appropriate grid is designed. For example, around the leading edge of an airfoil a radial grid will provide most efficient and accurate results. The grid inside each block is defined in terms of the number of grid points on each surface and along the edges defining boundary surfaces.

As one refines the grid inside each block, the number of grid points on each surface and edge increases. The scheme automatically keeps a record of these values and provide the user with the details of these adjustments. If, for example, the user would like to reduce the level of the grid refinement away from the airfoil, special blocks are employed with irregular grid structures. The grid generation scheme can produce both structured and unstructured grids. Our strategy has been to utilize irregular (unstructured) grids away from critical regions and try to adopt a structured grid at critical flow regions. In generating structured grids inside each block, one may have to use four-noded to eight-noded, three-dimensional finite elements as necessary. Figure 1 illustrates the typical steps involved in the block structured grid generation scheme.

The use of a block-structured grid generation scheme enables the user to design appropriate computational grids without restrictions of structured grids. Once the grid is generated the solution scheme is again defined on a block-by-block basis.

e. Block-Structured Solution of Transonic Flows. A block-structured solution scheme for transonic flows was developed based on the following assumptions:

- A relaxation process is defined for each block,
- For each block, either potential, Euler or Navier-Stokes equations can be solved,
- Nodes between the neighboring blocks are matched exactly,
- The variables between the neighboring blocks are matched by using Dirichlet boundary conditions.

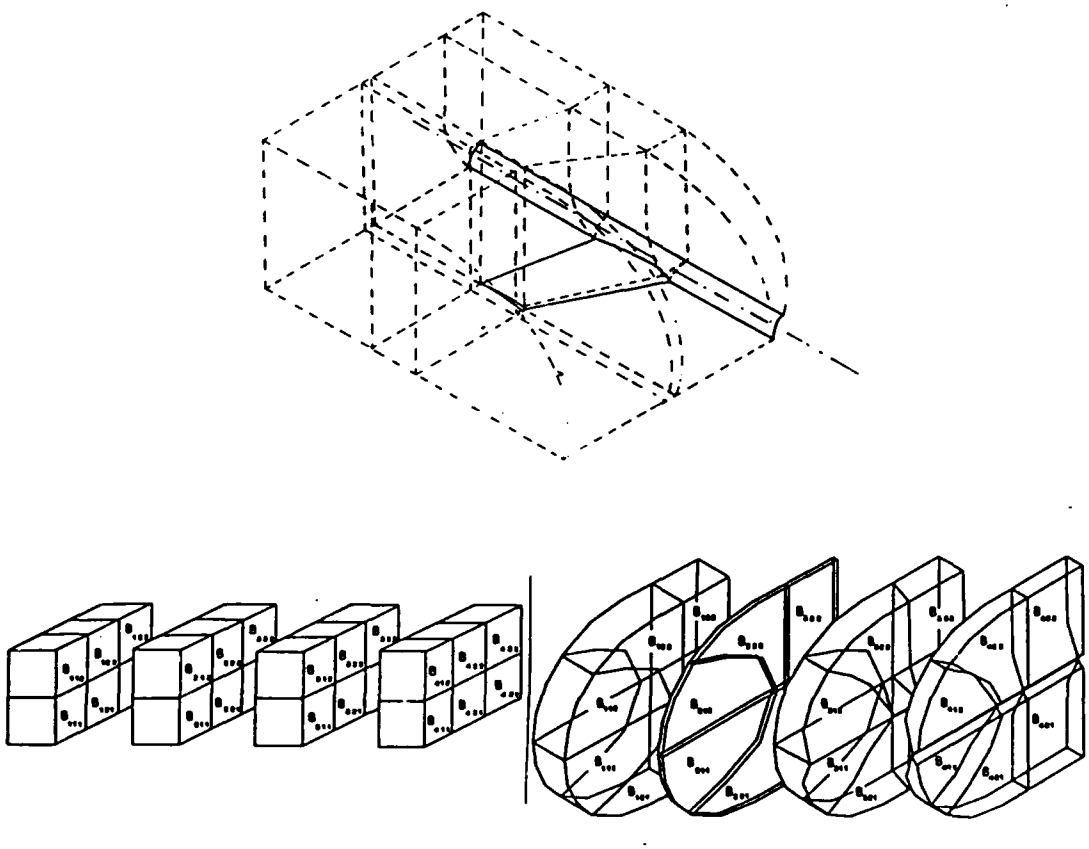

FIG. 1a. Block-Structure for the Wing-Body Problem.

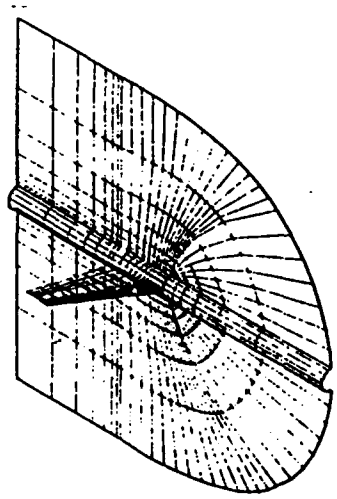

FIG. 1b. Grid Distribution over the Wing-Body.

Here, only a short summary of the solution scheme is presented [4,5].

The Navier-Stokes equations for steady, viscous, compressible flows can be written by using a Clebsch transformation of the velocity vector,

$$\underline{u} = \underline{\nabla}\phi + S\underline{\nabla}\eta + \underline{\tau} \tag{1}$$

into the following form:

$$\underline{\nabla}.(\rho\underline{u}) = 0 \tag{2}$$

$$\underline{\nabla}.(\rho\underline{u}S) = \Phi \tag{3}$$

$$\rho\underline{u}.\underline{\nabla}\eta = - p/R \tag{4}$$

where $\underline{u}$ is the velocity vector, S is the entropy, ρ is the density, p is the pressure, R is the gas constant, Φ is the viscous dissipation function and ϕ and η are the Lagrangian multiplier associated with conservation of mass and entropy equations respectively [7]. $\underline{\tau}$ is a generalized shear stress tensor which can be written in terms of the Lagrange multiplier η and the rate of strain tensor e_{ij} as follows:

$$\tau = 4\mu\eta[e_{ij} - 2\mu_i] \tag{5}$$

Equations (3-4) are cast into a second-order form by premultiplying with the convection operator. The relaxation scheme can then be summarized as follows:

. assume a velocity field

. solve equations (3) and (4) to obtain η and S distribution,

. calculate the shear stresses, $\underline{\tau}$,

. solve the conservation of mass to calculate ϕ,

. calculate a new velocity field and repeat the procedure.

In terms of a block-structured solution scheme, one has to perform the above generations for each block individually. The scheme then basically becomes a block relaxation scheme. A block relaxation scheme was defined where the operations are performed on a block basis rather than in terms of inter-block surfaces or edges. Each block is solved individually during each step of the iterations. The resulting block-surface solutions are compared along the neighboring block interfaces. Corrections are provided from each block surface which are employed to solve the individual block one more time. Before designing the details of the block-structured relaxation scheme, it is important to mention that one does not have to solve the same equations for each block. As stated before, each block represents a particular flow region. If one decides to solve Navier-Stokes equations for a particular block, all three equations (Eqs. 2-5) are solved for the primary variables ϕ, S and η. If Euler equations are required then the same set of equations are solved by ignoring the viscous dissipation term in equation (3) and the shear stresses in equation (1). No slip boundary condition is not required in this case since it only enters the formulation during the formulation of shear stresses in equation (5). For potential flows, only the velocity potential is required from the solution of conservation of mass equation in equation (2). Between neighboring blocks, ϕ, S and η values have to be matched. For blocks with potential flows S and η are known and need not to be calculated. Similarly, for blocks with Euler equations, the shear stresses are assumed to be zero and are not calculated. Thus, the formulation is general for all three types of flows. Presently, only the potential and Euler formulations are implemented although the solution schemes for Euler and Navier-Stokes equations are quite similar.

f. Block-Structured Relaxation Scheme. The block-structured relaxation scheme is applied to two sets of equations: conservation of mass equation and the transport equation for S and η. The basic procedure for this scheme is summarized below [5,6].

i) Conservation of Mass Equation. For the case of the conservation of mass equation where:

$$\underline{\nabla}.(\rho\underline{\nabla}\phi) = \underline{g}(S,\eta) \tag{6}$$

one considers the solution of the equation for each block. The relaxation scheme for each block can be written as follows:

$$\underline{A}^{o}\Delta\phi^{n} = \underline{g} - \underline{A}^{n}\underline{\Phi} \tag{7}$$

$$\underline{\Phi}^{n+1} = \underline{\Phi}^{n} + \omega\Delta\underline{\Phi}^{n} \tag{8}$$

where ω is the relaxation parameter and $\underline{A}^{o}$ represents the Laplace operator for each block calculated for incompressible flow conditions. This symmetric matrix is decomposed and stored to be used at each iteration step.

The problem is solved at two steps:

- A distribution of normal velocities is assumed for all block interfaces.
- Each block is individually solved by using the relationship in equation (6) with Neumann type boundary conditions.
- The values of Φ at interblock surfaces are compared and aver-averaged for each surface.
- Each block is re-analyzed using this time Dirichlet type boundary conditions.
- The boundary fluxes on each surface are calculated and aver-averaged.
- A new velocity field is calculated and the iteration cycle is repeated.

The above solution scheme is robust and quite efficient for transonic flows [4-6]. Generally, the block in which the shock is located determines the rate of convergence. In most cases, the number of iterations required for convergence is similar to the ones obtained by solving the same problem as a single block.

ii) Transport Equations for S and η. The solution of the two transport equations include the second order form of two equations again with symmetric operations. One can summarize the problem as follows:

Consider a transport problem with:

$$\frac{\partial}{\partial s}(gS) = \Phi \tag{9}$$

where S is the streamline direction and g is the flow speed. In this case, one has to define the entropy at the inlet as a reference value since only the changes in entropy rather than the absolute value of entropy will change the flow field.

We transfer the operator into a second order form by premultiplying with the convection operator as follows:

$$\frac{\partial}{\partial s}\left[g \frac{\partial}{\partial s}(gS)\right] = \frac{\partial}{\partial s}[g\Phi] \tag{10}$$

The original differential equation (9) becomes the additional boundary condition to be imposed at the exit boundary for this second-order differential equation. The new differential equation requires either the Dirichlet or Neumann type of boundary conditions depending whether it is a boundary point at the upstream or downstream of a streamline.

The block-structured solution of this differential equation is rather different than the first one. Dirichlet type boundary conditions are

specified on the surfaces where the flow enters the block. At other surfaces of the elements for which the flow leaves the block, only the Neumann type of boundary conditions are required. In this case, no averaging between the neighboring blocks is required. Instead, the information regarding the entropy S and η is convected in the flow direction between the neighboring blocks. These equations are solved only once during each iteration step. Figure 2 illustrates the block-structured solution of Euler equations around an airfoil.

g. Parallel Processing of Blocks. The use of block-structured solution technique allows the parallel processing of several blocks at the same time. By performing the computations on several blocks in parallel, one aims at utilizing all of the available computer resources. Important characteristics of the developed scheme, in terms of parallel processing, can be summarized as follows:

- By performing a block relaxation scheme on each of the individual blocks one decomposes two sets of banded coefficient matrices: representing the Laplace operator and the convection operator in the second-order form. Both of these operators are symmetric and are stored considering the banded form.
- When bandwidths are small for each block (≤ 80) and only a forward elimination-backward substitution is required for each block, the computation of the residual vector becomes the critical factor. In this case, all of the element information related to the geometry, such as the shape functions and their derivatives, Jacobians, etc., are calculated and stored once. The cost of computing the residuals

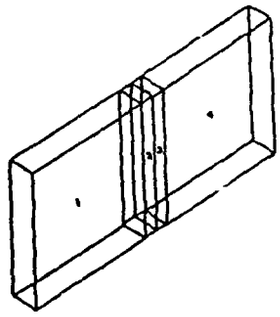

FIG. 2a. Four-Block Structure.

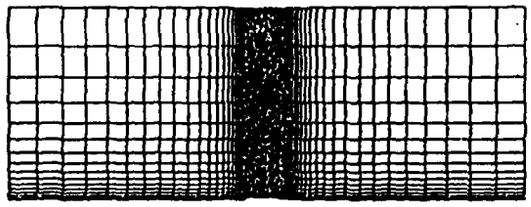

FIG. 2b. Finite Element Grid.

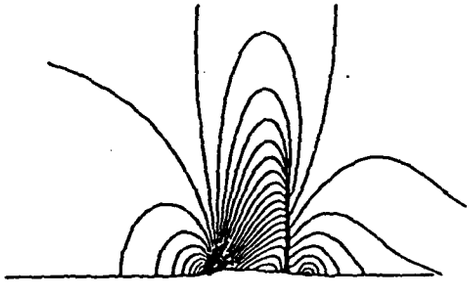

FIG. 2c. Mach Contours

FIG. 2d. Contours of Vorticity/Pressure.

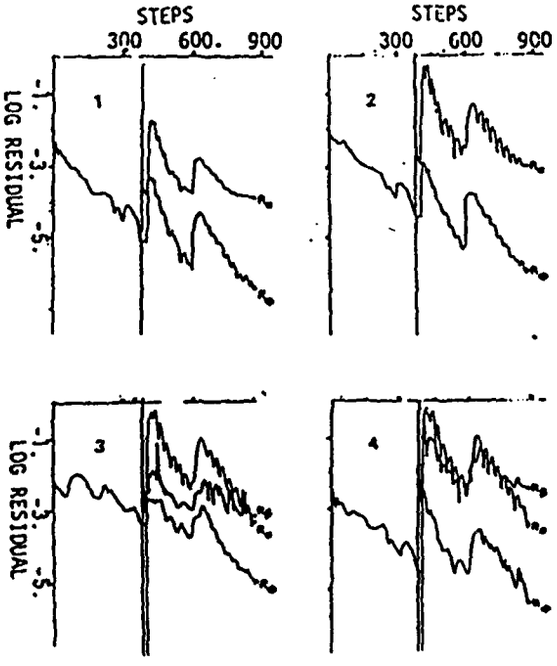

FIG. 2e. Residual History for the Euler Solution around a NACA0012 Airfoil at M_∞ = 0.85 for Different Blocks. (Potential Solution for the first two blocks, Euler Solution for the last two blocks)

and solving the equations then become comparable when the solution part is vectorized.

. The main computational concern then becomes the reduction of I/O cost such that computations still remain on the critical path i.e. no I/O wait is encountered. The scheme was implemented on two computers CRAY-XMP and IBM 3090, as shown in figure 3. On both machines, the memory is divided into parts where two or three blocks can be stored at the same time. In this case, while one block is being processed, another block can be read-in or written-out. Based on the fact that the information related to a single block can be read-in by a single read command, asynchronous I/O operations do not slow down the processors. The critical requirement for a given computer becomes the size of the memory which is available to store two or three blocks at the same time, as well as the number and speed of I/O devices. The use of high speed I/O devices improves the speed of the present process considerably. The main memory of the computer limits the maximum size of the block which can be processed. For blocks with specified wavelengths, the computational cost is linearly proportional to the number of nodes and the number of blocks.

. Currently, these studies are extended to the Intel IPSC computer which provides several processors with large memories and with many I/O channels. In this case, rather than storing all of the blocks on the disk, one keeps each block in the memory of an individual processor. Each block is coupled to several neighboring processors, each containing the neighboring block, as shown in figure 4. All geometry data and coefficient matrices are calculated and stored in

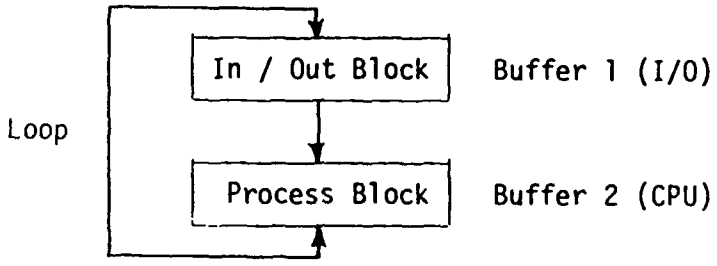

a) Two-buffer system for IBM-3090

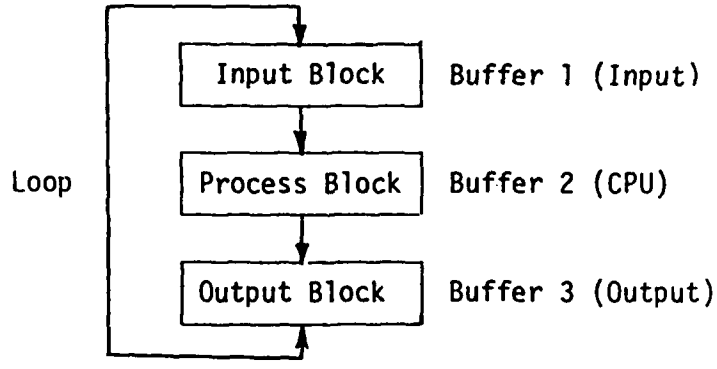

b) Three-buffer system for CRAY X-MP12

FIG. 3a. The Memory Management for the IBM and CRAY Computers

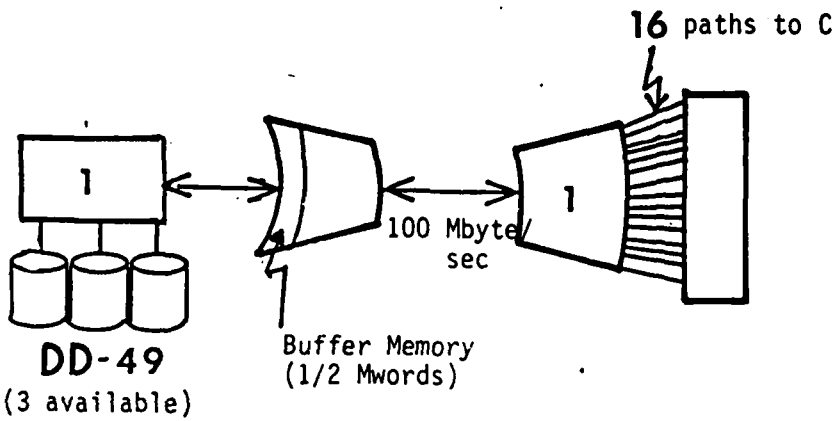

D.C.U (1 available)

I.O.S (2 IOP's)

C.P.U

C.M (2 Mwords)

1.86 Mwords
max. rotating disk
capacity

FIG. 3b. The AFWAL Cray X-MP12 System

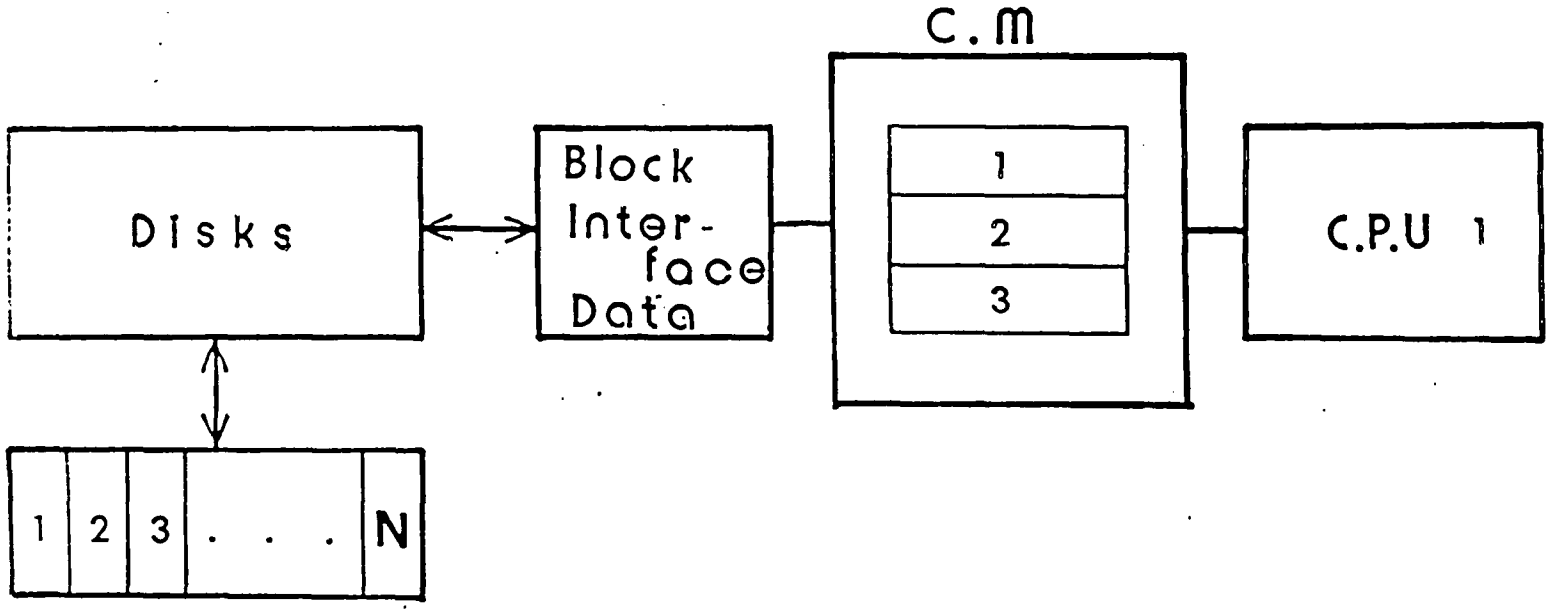

FIG. 3c. Implementation of the Block-Structural Solution Scheme on the AFWAL Cray X-MP12

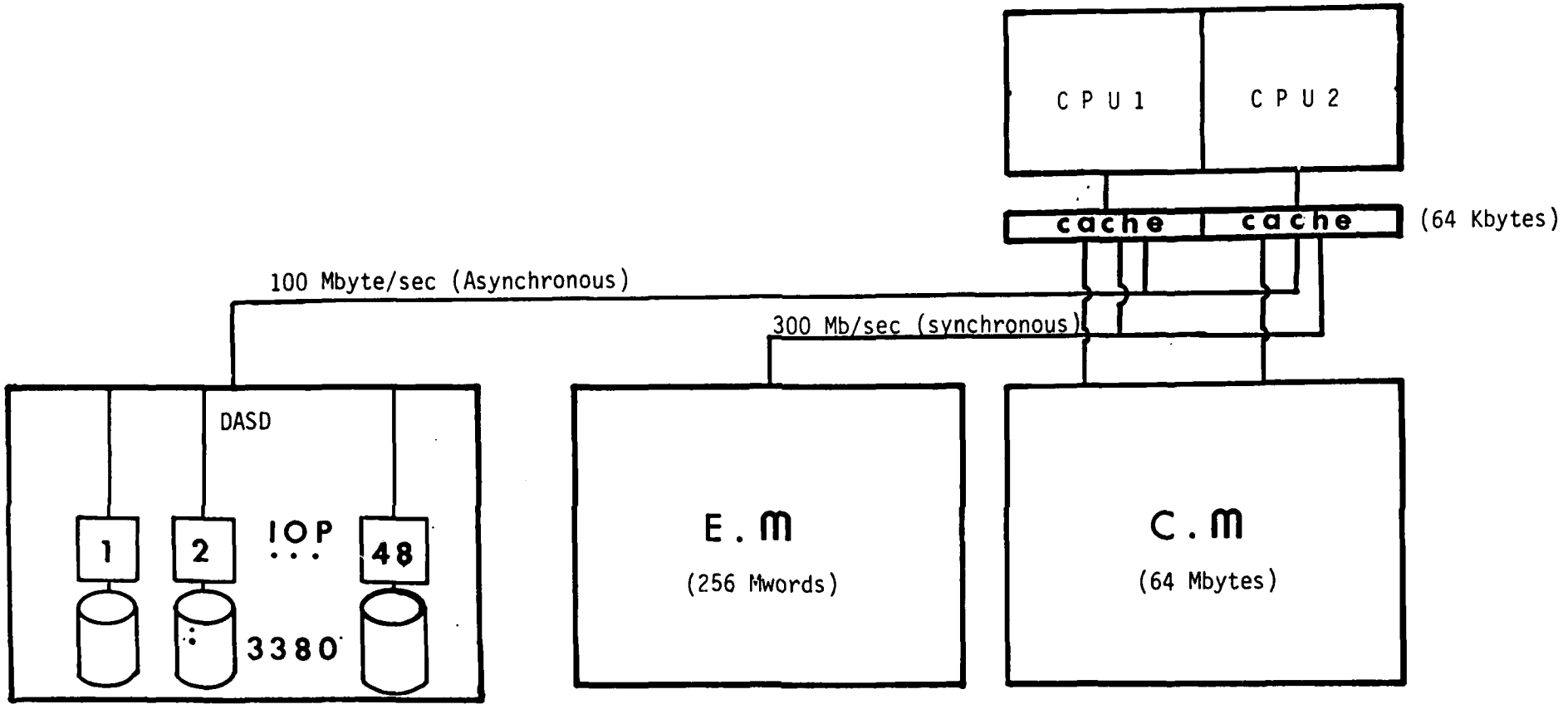

Virtual System (Automatic Memory Management)

FIG. 3d. IBM-Kingston Research Center 3090-200 System

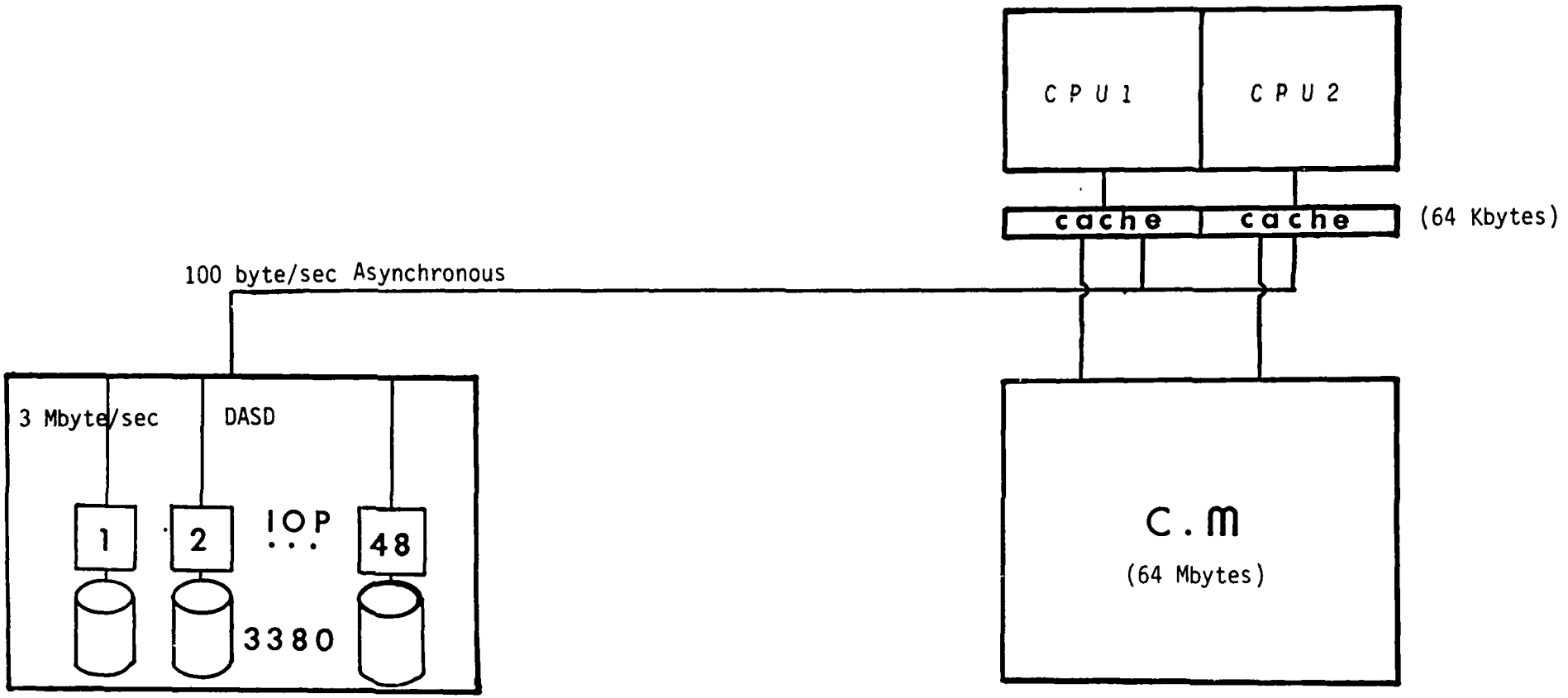

FIG. 3e. Implementation of the Block Structure Solution Scheme on the IBM 3090 System

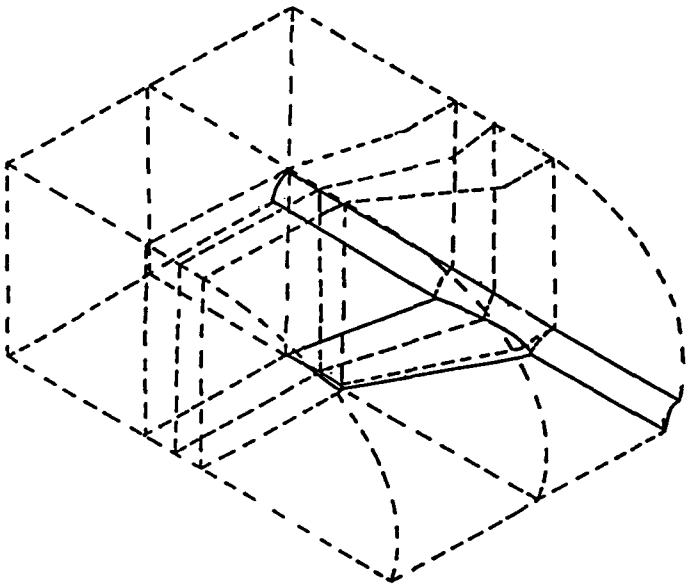

FIG. 4a. Sixteen block model for the wing-body problem

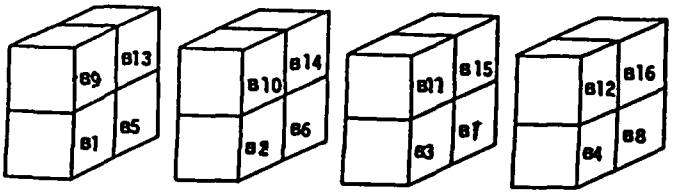

FIG. 4b. Block-structure for the sixteen block model

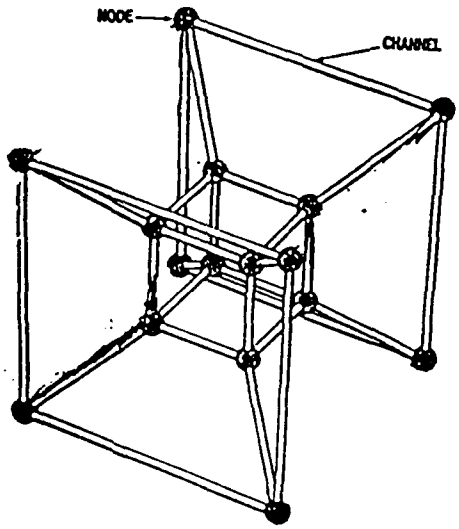

FIG. 4c. Node configuration on INTEL Computer for the sixteen block model

real memory. The only I/O operation involves the transfer of solution vectors relating the inter-block surfaces. These are balanced between neighboring blocks and the iterations continue for each block on a single processor. This type of approach requires more loosely coupled processors. For a given block-structure of different size blocks, one may like to arrange processors with different size memories to fit the topology of the block-structure.

h. Refinement of Grids. As indicated at the beginning of this paper, the analysis of a complex flow problem can be considered as an iterative process rather than a one step solution. The block-structured solution scheme provides a tool for performing such a task. We expect the user:

- to identify the block-structure,
- to generate a grid,
- to identify potential, Euler or Navier-Stokes blocks, and
- to solve the problem approximately.

Once this initial step is completed, one may:

- modify the grid in one block,
- decide to change from one of the above three formulations (potential, Euler, Navier-Stokes) to another,
- define turbulence models for viscous flow regions,
- provide special modeling of critical regions such as shocks, trailing edges, thin boundary layers, etc.

Once these modifications are made for each block, they are automatically propogated throughout the flow field. The flow field obtained from the

first step is utilized as an initial step for the second stage of the computations. It is also expected that information obtained for the analysis of particular flow structures can be employed to design better blocks for the subsequent analyses. Adaptive grid techniques again seem much more practical when considered at a block level. One can provide error estimates for a specific flow structure and provide a specific strategy for adopting the grid.

i. Concluding Remarks. The present research activity demonstrates, the advantages of block-structured solution techniques for solving large aerodynamics problems. As the complexity of the problems increase for three-dimensional problems, the cost of preparing good computational grids increases together with the time spent for actually solving the problem. One has to utilize both block-structured grid generation and solution schemes for solving such problems, as discussed in this report.

The computer hardware available for solving large problems is still limited at the present time. The use of a block-structured solution scheme allows efficient use of existing computer hardware as well as parallel processors which are under development for solving large problems. The developed scheme allows the use of secondary storage to eliminate the restrictions of main memory, while, masking the cost of performing related I/O operations. Our experience indicates that the solution of large aerodynamics problems requires accurate and efficient solution of many smaller problems which can be accomplished by using the developed scheme.

j. References

1. SDRC Inc., Supertab User's Manual, 1983.

2. PDA Inc., Patran-G User's Manual, 1984.

3. A. Ecer, J.T. Spyropoulos and J. Maul, A Block-Structured Finite Element Grid Generation Scheme for the Analysis of Three-Dimensional Transonic Flows, 23 (1985), pp.

4. A. Ecer and J.T. Spyropoulos, Block-Structured Solution Scheme for Analyzing Three-Dimensional Transonic Potential Flows, AIAA-86-0510, (1986).

5. A. Ecer , J.T. Spyropoulos and V. Rubek, Block-Structured Solution for Euler Equations for Transonic Flows, AIAA-86-1080, (1986).

6. A. Ecer, J.T. Spyropoulos and O. Atakar, Block-Structured Solution of Euler Equations for Transonic Flows, AIAA-87-0351, (1987).

7. A. Ecer, H.U. Akay and W.H. Sheu, "A Variational Finite Element Formulation for Viscous Compressible Flows", Symposium on Numerical Methods for Compressible Flows--Finite Difference, Finite element and Finite Volume Techniques, ASME Winter Annual Meeting, December 7-12, 1986, Anaheim, California.

3. Review of the Development Effort for the Last Two Years:

The research work on the block-structured solution of Euler equations progressed along five main areas:

A. Development of a Block-Structured Scheme for Three-Dimensional, Transonic Euler Equations,

B. Detailed Study of Solving Euler Equations for Lifting Airfoils with Kutta Condition for Transonic Flows.

C. Grid Generation Studies.

D. Implementation of the Procedure on Large Computers.

E. Variational Formulation of Viscous Flows.

Along the main development of the block-structured solution scheme, the other four activities also progressed. We had to determine ways of accurately calculating lift from the solution of Euler equations for transonic flows. We also continued with our activities in grid generation. Each of these activities are summarized in this report. Here, we first provide a list of the important activities, in each of these areas, which are presented together with the list of publications.

a. Block-Structured Solution Scheme:

Three papers were presented on this subject:

1. Ecer, A. and Spyropoulos, J. T., "Block-Structured Solution Scheme for Analyzing Three-Dimensional Transonic Potential Flows", AIAA-86-0510, AIAA 24th Aerospace Science Meeting, Reno, Nevada, January 1986 (to be published in the AIAA Journal).
2. Ecer, A., Spyropoulos, J. T. and Rubek V., "Block-Structured Solution of Euler Equations for Transonic Flows", AIAA-86-1080, AIAA/ASME 4th Fluid Mechanics, Plasma Dynamics and Lasers Conference, Atlanta, Georgia, May 12-14, 1986 (to be published in the AIAA Journal).
3. Ecer, A., Spyropoulos, J. and Rubek, V., "Block-Structured Solution of Three-Dimensional Transonic Flows", Sixth International Symposium on Finite Element Methods in Flow Problems, Antibes-France, June 1986.
4. Ecer, A., "A Block-Structured Solution of Transonic Flows", presented at Symposium on Domain Decomposition Methods for Partial Differential Equations, Paris, France, January 1987. (invited paper)

The first paper in fact summarizes the prior potential flow development and the last three papers summarize the Euler development. We can presently generate a three-dimensional grid on a block-by-block basis and solve the Euler equations in three-dimensions utilizing the same or modified block-structure.

A research assistants (V. Rubek) completed his masters research on this problem. Another one (R. Najmon) also worked on this problem.

b. Kutta Condition for Euler Equations

Three papers were prepared on this subject:

5. Akay, H. U., Ecer, A. and Willhite, P. G., "Finite Element Solutions of Euler Equations for Lifting Airfoils", AIAA Paper 85-0294, January 1985 (published in AIAA Journal, Vol. 24, No. 4, April 1986, pp. 562-568).
6. Akay, H. U. and Ecer, A., "Implementation of Kutta Condition for a Finite Element Formulation of Euler Equations", Fourth International Symposium on Numerical Methods in Engineering, Atlanta. Georgia. March 24-28, 1986.
7. Akay, H. U. and Ecer, A., "Solution of Transonic Euler Equations for Lifting Airfoils", Sixth International Symposium on Finite Element Methods in Flow Problems, Antibes, France, June 16-20, 1986.
8. Ecer, A. and Akay, H. U., "Computation of Steady Euler Equations Using Finite Element Method", GAMM Workshop on the Numerical Simulation of Compressible Euler Flows, INRIA, Rocquencourt, France, June 10-13, 1986. (invited paper)

A masters student (P. Willhite) completed his research on this subject, as we explained in these papers. We can calculate the lift on an airfoil accurately by imposing the Kutta condition in a correct manner. From the condition that the pressure is continuous past the sharp trailing edge, we determine the jump in the velocity distribution along a dividing streamline. We move our finite element grid to fit the dividing streamline. In this manner, we can simulate the discontinuous vorticity distribution past the airfoil as generated by two shocks on each surface of an airfoil.

Another masters student (S. Ciray) wrote a master's thesis on this same subject. He solved the axisymmetric, subsonic and transonic flows at the exhaust of an engine where two flow fields with different total pressures converge past a sharp trailing edge.

c. Grid Generation Studies

The following papers were completed in this area:

9. Ecer, A., Spyropoulos, J. T. and Maul, J., "A Block-Structured Finite Element Grid Generation Scheme for the Analysis of Three-Dimensional Transonic Flows", AIAA Journal, Vol. 23, No. 10, October 1985.
10. Pien, B., Ecer, A., Ward, P. and Bowes, C., "Application of a Block-Structured Grid Generation Scheme for Modeling Three-Dimensional Viscous Flows", 1st Int. Conf. on Numerical Grid Generation in Computational Fluid Dynamics, Landshut, Germany, July 14-17, 1986.
11. Ecer, A., J.T., Spyropoulos and H.U. Akay, "Applications of a Three-Dimensional Finite Element Grid Generation Scheme to Flow Problems", Fifth International Conference on Numerical Methods in Laminar and Turbulent Flows, July 6-10, 1987, Montreal, Canada. (invited paper)

The first paper summarizes our mesh generation scheme which was developed previously. The other two papers summarize applications of this mesh generation scheme. In the last paper, results obtained by working with Dr. J. Shang of WPAFB for generating a computational grid for the F-16 aircraft are presented. Two students worked on this problem. A presentation was made at WPAFB on this subject.

d. Application on Large Computers

The following papers were written in this area:

12. A. Ecer, J.T. Spyropoulos and O. Atakar, "Block-Structured Solution of Euler Equations for Transonic Flows", AIAA-87-0351, AIAA 25th Aerospace Sciences Meeting, January 12-15 1987, Reno, Nevada.
13. A. Ecer and J.T. Spyropoulos, "Parallel Processing Schemes for the Block-Structured Solution of Transonic Flows", 1987 Summer Computer Simulation Conference, July 1987. (invited paper)

Also a presentation was made at WPAFB on this subject.

This is a more recent activity which we are currently working on. The following progress was made in this area.

- Collaboration with IBM research center for using large IBM computers.
- NSF Grant for computer time on CYBER 205.
- Collaboration with Dr. D. Sedlock of WPAFB for running problems on a CRAY machine. Modest grants were received for running the IBM and CRAY computers, in terms of computer time and travel expenses.

The results obtained from these studies are presented in the above two papers. Also, another paper will be presented at 1988 Aerospace Sciences Meeting on this subject.

. Proposal to DOD was approved towards purchasing an INTEL CSPI computer was approved. This machine is being employed to test parallel processing aspects of the developed scheme on computers with many processors.

Finally, it should be mentioned that a Computational Fluid Dynamics Laboratory was officially established at the School. Research and Sponsored Programs of the University provided $43,000 towards purchasing additional computer terminals and graphics equipment for this laboratory.

e. Variation Formulation of Viscous Flows

We have extended the variational formulation to the solution of Navier-Stokes equations for viscous flows. One Ph.D thesis (W.H. Sheu) and three papers were written on this subject.

14. A. Ecer. H.U. Akay and W.H. Sheu. "A Variational Finite Element Formulation for Viscous Compressible Flows",Symposium on Numerical Methods for Compressible Flows--Finite Difference, Finite Element and Finite Volume Techniques, ASME Winter Annual Meeting, December 7-12, 1986, Anaheim, California. (invited paper)

15. A. Ecer, H.U Akay and P. Ward, "Variational Formulation of Viscous Flows", Computational Methods in Aeronautical Fluid Dynamics, April 1987, Univeristy of Reading, England. (invited paper)

16. H.U. Akay and A. Ecer, "Compressible Viscous Flows with Clebsch

f. Planned Future Activities for the Next Two Years:

Our recent work was mainly aimed at demonstrating the advantages of the developed block-structured solution scheme in parallel-processing environment for solving large aerodynamic problems. We have out block-structured solution scheme stabilized on the IBM and CRAY computers at this time. This has enabled us to study the basic requirements for solving large problems on a block-structured basis in detail. In fact, we hope to continue with the IBM Research Center and WPAFB on these projects for the coming year.

Our continuing work involves studying the parallel-processing environment in a more general fashion. Presently, super-computers, such as the CRAY or IBM, allow only limited main memory and a limited number of CPUs. Although these CPUs are fast and complemented with I/O resources, further developments are necessary for solving large aerodynamics problems. We expect the coming computers to improve this situation by providing large memory machines with many CPUs. Our work on the INTEL Hypercube is intended to investigate such problems. We expect to further demonstrate the utilization of block-structured solution schemes as necessary and efficient tools for solving large aerodynamics problems on these machines with many processors. During the next year, we expect to continue to work with:

. IBM-3090 at IBM Research Center (Dr. Rubin) and

. CRAY X-MP 12 at WPAFB (D. Sedlock)

on further applications of the scheme on large computers.

However, our main effort will be on the INTEL machines as an example of multiprocessor, large memory machines. We also hope to collaborate, in this area, with Dr. Shang's group at WPAFB.

A. Develoopment of a Block-Structured Solution Scheme for Three-Dimensional, Transonic Euler Equations

1. Introduction

The computation of three-dimensional transonic flows for complex configurations has been the major objective of the present research activity. This past year, a computational scheme was developed for a block-structured solution of Euler equations for three-dimensional transonic flows. This work represents a continuation of previous efforts toward building a computational capability for analyzing large flow problems around complex geometric configurations. In order to explain the basic considerations that led to the development of the present scheme, it is useful to summarize some of these previous efforts.

a. Three-Dimensional Computational Grids

The computational work performed in the area of transonic flows in the past has established the necessity for reliable grid generation procedures for performing accurate computations. Considerable work has been done on mapping techniques for designing grids appropriate to given flow fields [A1]. Since the solution schemes are based on finite element procedures, we have concentrated our efforts on generating "finite element grids", which can be classified as "unstructured grids". Although it is possible to design structured grids for simpler geometries, our assumption was that one needs unstructured grids for analyzing fully three-dimensional, complex flows.

When one works with such complex three-dimensional geometries, it also becomes apparent that controlling the generation of the grid at critical areas

is extremely important. Although it is desirable to have grid generation schemes which can automatically adapt to local flow fields, it becomes computationally expensive to provide a general capability for adaptive grid refinement for three-dimensional, transonic flows. We have chosen to develop capabilities for designing grids through an iterative process, where one can modify grids easily until the appropriate grid is generated. In generating such grids for three-dimensional problems, it was experienced that local modifications consisted a mojor portion of the total effort. Therefore, our efforts were concentrated towards developing capabilities where one can rapidly make local modifications and incorporate these changes to the iterative solution schemes.

A block-structured grid generation scheme was developed three years ago for this purpose where the grids are generated locally for each block and the blocks are automatically connected together [A2]. Although considerable work has been done for solving Euler equations by patching local flow zones with independent grid structures [A3], it was felt that it is important to ensure that the grid points are exactly matched on adjacent surfaces of neighboring blocks. Using the developed scheme, on can modify the grids locally and these changes are automatically propogated to the neighboring blocks in an organized manner.

We are continuing to apply the developed grid generation scheme for three-dimensional flow problems as described in this report.

b. Formulation of Euler Equations

In general, the unsteady Euler equations are cast in terms of the primitive variables (ρ, u, v, w, p) and numerically integrated with respect to real or pseudo-time to obtain steady solutions. The use of relaxation schemes for solving the steady Euler equations have attracted attention only during the last several years. In our efforts, we use a Clebsch transformation of the velocity field as follows:

$$\underline{u} = \underline{\nabla}\phi + S\underline{\nabla}\eta. \tag{A1}$$

For irrotational flow regions, the above expression reduces to,

$$\underline{u} = \underline{\nabla}\phi. \tag{A2}$$

Such a formulation is suitable for a block-structured solution scheme which unifies the treatment of rotational and irrotational flow regions.

Another important aspect of the present formulation is due to the fact that all equations are cast into a second-order form and solved using a standard Galerkin procedure [A4]. This is equivalent to using centered-difference approximations on second-order equations. No artificial viscosity is included, in this case, which would have been required for the solution of first-order equations.

c. Numerical Solution of the Equations

Over the years, the numerical solutions of either potential or Euler equations using relaxation schemes have been mainly restricted to the use of structured grids. For example, the use of multi-grid methods for analyzing unstructured grids has been attempted only recently [A5].

When working with unstructured grids, one has to consider a more general problem. If the computational grid can be considered as an assembly of finite elements with irregular geometries, one has to store the nodal connectivities of each element, as well as their geometries. When working with large problems, the storage of such information becomes a difficult task. If one restricts itself to developing solution schemes where all of the geometry information has to be stored as a single data set, it becomes very easy to exceed the storage limitations of a given computer.

Because of the above considerations, we have chosen a block-structured solution scheme where one divides the problem into a series of blocks. The main assumption here is that individually the blocks are small enough to be processed in the main storage, where all the geometry and solution related information can be stored at one time. Also, starting with the above assumption, we chose to employ a block-relaxation scheme, as described in references [A6] and [A7], rather than a point or line-relaxation scheme for treating unstructured grids. In fact, the point should be made that the computational efficiency of the present scheme depends mostly on transferring the data rather than processing it for irregular grids. A year ago we completed the development of a block-structured scheme for the solution of potential equations for transonic flows [A6]. In that particular development, one had to solve the conservation of mass equation in terms of velocity potential ϕ. During the past year, the same formulation was extended to the solution of complete sets of Euler equations (conservation of mass and momentum) in terms of entropy S and Lagrange multipliers ϕ and η [A7]. The computational scheme is general such that each block can be defined either

with potential or Euler equations. It should be noted that the same formulation can be extended such that one can choose between potential, Euler or Navier-Stokes equations for each block.

2. Summary of the Numerical Procedure

a. Clebsch Formulation of Euler Equations

The solution of the three-dimensional Euler equations using a block-structured solution scheme is developed in detail in reference [A7]. Here only a brief summary of the methodology and a set of descriptive numerical results are presented.

Euler equations for steady, inviscid, isoenergetic flows can be written as follows:

$$\underline{\nabla}(\rho\underline{u}) = 0 \tag{A3}$$

$$\rho\underline{u}.\underline{\nabla}\eta = -\frac{p}{R} \tag{A4}$$

$$\rho\underline{u}.\underline{\nabla}S = 0 \tag{A5}$$

where the velocity vector can be written in terms of Clebsch variables as follows:

$$\underline{u} = \underline{\nabla}\phi + S\nabla\eta. \tag{A6}$$

Here, ϕ and η are Lagrange multipliers in the variational functional employed for the above set of equations for conservation of mass and entropy respectively.

The pressure at any point can be defined in terms of local velocity and entropy. In the case of flows with shocks, the entropy generated across a shock is computed by using Rankine-Hugoniot conditions. In the case of po-

tential flows, entropy becomes a constant and velocity field can be expressed in terms of the velocity potential ϕ only.

For the finite element solution of the above equations, conservation of mass equation is solved iteratively by updating the density at each step with upwinding in the supersonic flow region. The other two equations are first-order convective equations. The finite element formulation is applied after they are cast in second-order form as follows:

$$\rho \underline{u}.\underline{\nabla}.(\rho \underline{u}.\underline{\nabla} n) = -\rho \underline{u}.\underline{\nabla}(p/R) \tag{A7}$$

$$\rho \underline{u}.\underline{\nabla}.(\rho \underline{u}.\underline{\nabla} S) = 0. \tag{A8}$$

The original equations become boundary conditions at the downstream boundary. These equations are solved by a standard finite element formulation which corresponds to centered-differencing with second-order accuracy and no artificial viscosity.

b. Block-by-Block Solution Scheme

For the solution of Euler equations, one has to be concerned with the solution of both equations (A7) and (A8). A solution scheme for the solution of conservation of mass equation was developed first [A6]. The flow region is divided into a series of blocks. Grids are generated for each block while exact matching of nodes was maintained across inter-block boundaries. An iterative solution scheme was performed in the following manner:

- Solve the conservation of mass equation with applied mass flux boundary conditions for each block independently.
- Calculate the velocity potentials ϕ between the block surfaces from

the above solution and correct these values for matching the interblock surface values.

. Solve the conservation of mass equation by using the calculated values of surface velocity potential distribution.

. Calculate the mass fluxes across the surfaces of each of the blocks and correct these values for matching the interblock surface values.

. Repeat the process until it converges.

We have experimented with this scheme for transonic potential flows and found it to be very robust. Several two and three-dimensional experiments were conducted by placing the block interfaces at critical areas around stagnation points and shocks. It was found that the scheme behaved well under such conditions. Also, it was observed that the rate of convergence for transonic flows was still basically proportional to the development of the supersonic pocket. For transonic flows, the number of iteration sweeps for a single block solution and multi-block solution was the same and dependent on the size of the supersonic pocket, the number of elements, artificial viscosity etc., which have already been studied in detail.

In the case of Euler equations, one also has to solve equations (A7) and (A8). In this case, considering the convective nature of the equations, the equations are solved block-by-block, but in a sweeping manner in the flow direction. This requires the solution of blocks in a certain order folowing the flow direction. This is more restrictive, in comparison to the solution of conservation of mass equation, where the blocks can be solved in any order. On the other hand, in this case each sweep contains the solution of single sets of equations with specified upstream boundary conditions for

S and n rather than solving the conservation of mass equation twice as described above.

In the case of shocks, it is assumed that only a single shock can occur in a single block. The entropy generated by this shock is calculated and added to the entropies coming from upstream blocks.

c. Numerical Results

The computer code was first tested for analyzing flow around two-dimensional profiles: a 10% circular bump in a channel and a NACA0012 airfoil profile [A7]. Also the three-dimensional flow filled around a wing-body configuration [A6] was tested.

Here a summary of the test case for the flow around a NACA0012 profile with $M_\infty = 0.85$ is presented.

In this case, the block structure consisted of 4 blocks as shown in Figure A1. The finite element grid employed in the analysis is shown in Figure A2. For this problem, two experiements were conducted:

i) Potential Flow Solution First a potential solution was obtained for this problem by solving the potential flow equations for all blocks. The history of relaxation factors and the artificial viscosity multiplier for the supersonic flow region are shown below:

Iteration Steps	ω_ϕ	μ
1-150	0.1	8
151-300	0.1	6
301-450	0.2	5
451-620	0.2	4.5
621-760	0.2	4.25
761-900	0.2	4.15

For high values of artificial viscosity, and by using low relaxation parameters, the shock was initially captured. The artificial viscosity was reduced for better accuracy and the relaxation parameter was increased. The residual history for this solution is shown in Figure A3. A comparison of computed pressure coefficients over the surface of the airfoil with others is shown in Figure A4. The Mach contours for the potential solution are also presented in Figure A5.

ii) Euler Solution For obtaining an Euler solution to the same problem, again the same procedure was repeated. First 380 steps of iteration were conducted by gradually lowering the artificial viscosities to obtain an approximate potential solution only. After a shock was developed, 20 iter- ation step were performed using the non-sientropic potential formulation to correct the strength of the shock. Finally, 470 steps of iteration were performed to obtain an Euler solution. The history of iterations are sum- marized below:

Iteration	ω_ϕ	ω_s, ω_η	μ	Solution type
1-150	0.1		8.	Potential
150-300	0.1	-	6.	Potential
301-380	0.2	-	5.	Potential
381-400	0.2	1.0	5.	Non-isentropic Potential
401-600	0.2	0.2	5.	Euler
601-870	0.2	0.2	4.5	Euler

The comparison of obtained surface pressure distributions with results obtained by others are shown in Figure A6. The Mach contours, equal entropy contours and vorticity/pressure contours are shown in Figure A7. The history of iterations for each block is shown in Figure A8. Finally, the vorticity pressure and Mach profiles at the shock location and at the downstream of computational grid are shown in Figure A9. As can be seen from these resuts, the convergence rates depend strongly on the artificial viscosity employed in the relaxation scheme for both potential and Euler solutions.

A block-structured solution of a three-dimensional wing body problem is in Appendix A.

References

A1. Numerical Grid Generation, Ed. by Thompson, Elsevier Science Publishing Co., 1982.

A2. Ecer, A., Spyropoulos, J.T. and Maul, J., "A Block-Structured Finite Element Grid Generation Scheme for the Analysis of Three-Dimensional Transonic Flows", AIAA Journal, Vol. 23, No. 10, October 1985.

A3. Hessenius, K.A. and Rai, M.M., "Applications of a Conservative Zonal Scheme to Transient and Geometrically Complex Problems", AIAA-84-1532, June 1984.

A4. Ecer, A. and Akay H.U., "Finite Element Formulation of Euler Equations for the Solution of Steady Transonic Flows", AIAA Journal, Vol. 21, No. 3, pp. 410-416, March 1983.

A5. Lohner, R. and Morgan, K., "Improved Adaptive Refinement Strategies for Finite Element Aerodynamic Computations", AIAA-86-0499, January 1986.

A6. Ecer, A. and Spyropoulos, J.T., "Block-Structured Solution Scheme for Analyzing Three-Dimensional Transonic Potential Flows", AIAA-86-0510, AIAA 24th Aerospace Science Meeting, Reno, Nevada, January 1986 (to be presented in the AIAA Journal).

A7. Ecer, A., Spyropoulos, J. and Rubek, V., "Block-Structured Solution of Three-Dimensional Transonic Flows", Sixth International Symposium on Finite Element Methods in Flow Problems, Antibes-France, June 1986.

A8. Rizzi, A. and Viviand, H. (Eds.), Numerical Methods for the Computation of Inviscid Transonic Flows with Shock Waves, Friedr. Vieveg & Sohn, Braunschweig/Wiesbaden, 1981.

A9. Ecer, A., Spyropoulos, J.T. and Rubek, V., "Block-Structured Solution of Euler Equations for Transonic Flows", AIAA-86-1080. AIAA/ASME 4th Fluid Mechanics, Plasma Dynamics and Lasers Conference, Atlanta, Georgia, May 12-14, 1986 (to be published in the AIAA Journal).

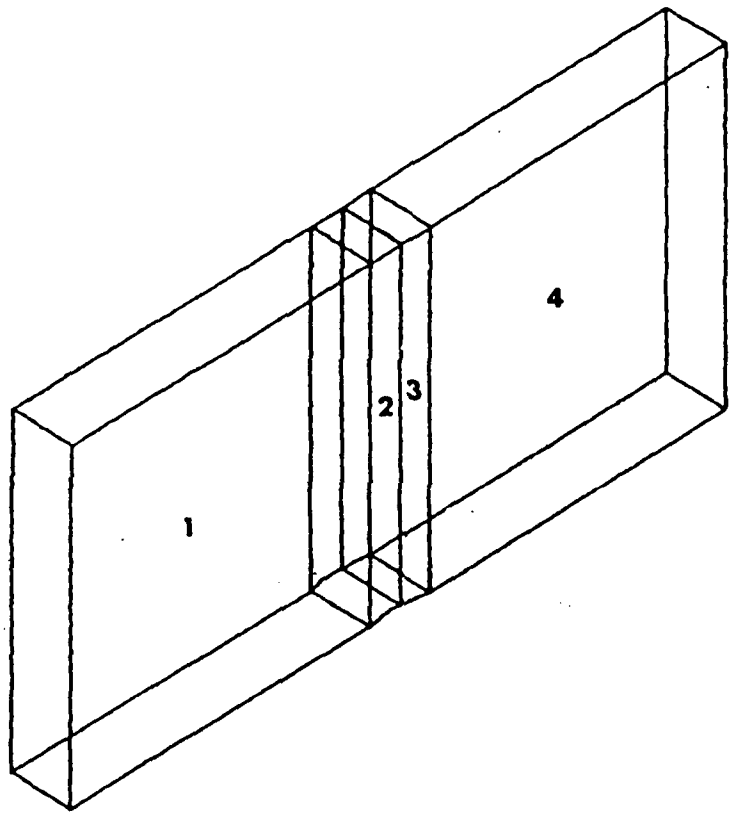

Figure A1. Computational grids that are appropriate to given flow fields.

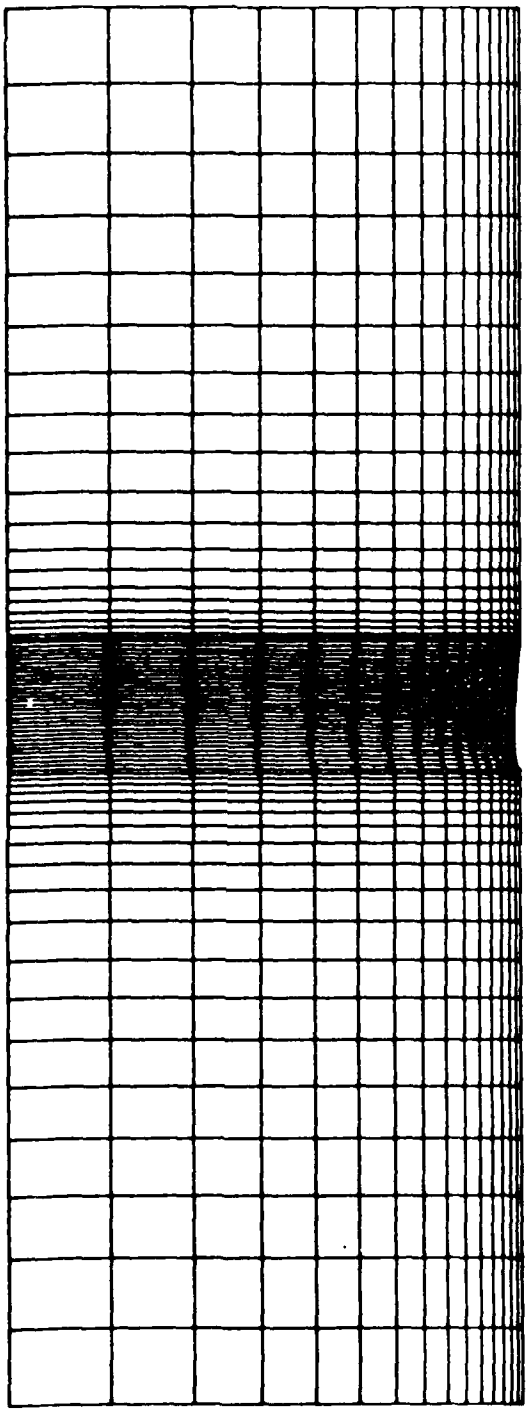

Figure A2. Block-structured grid where blocks are automatically connected together

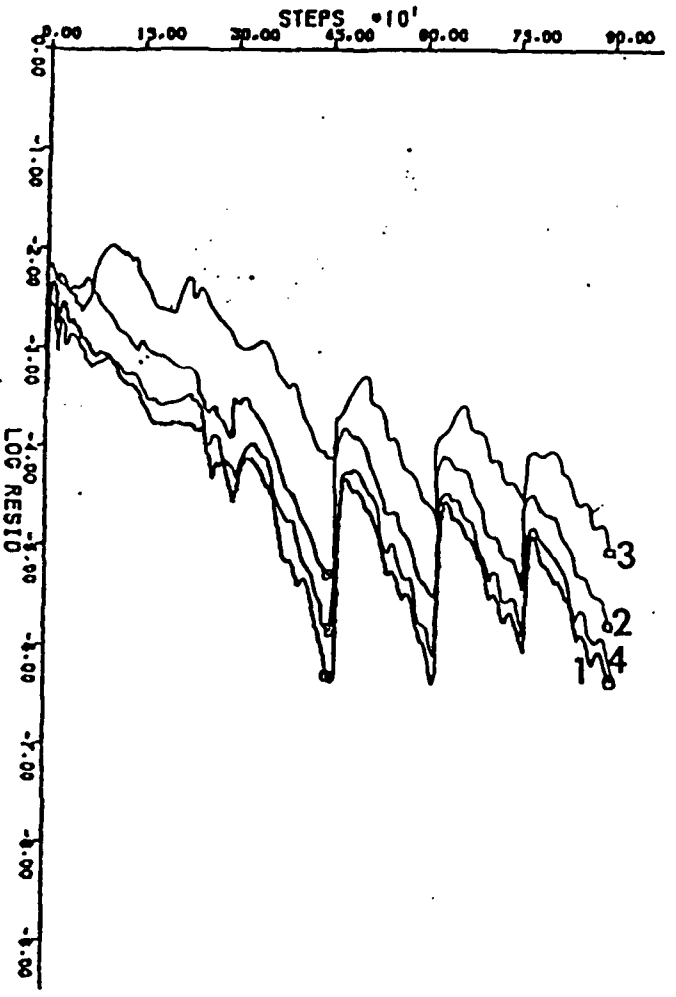

Figure A3. Local flow zones patched with independent grid structures

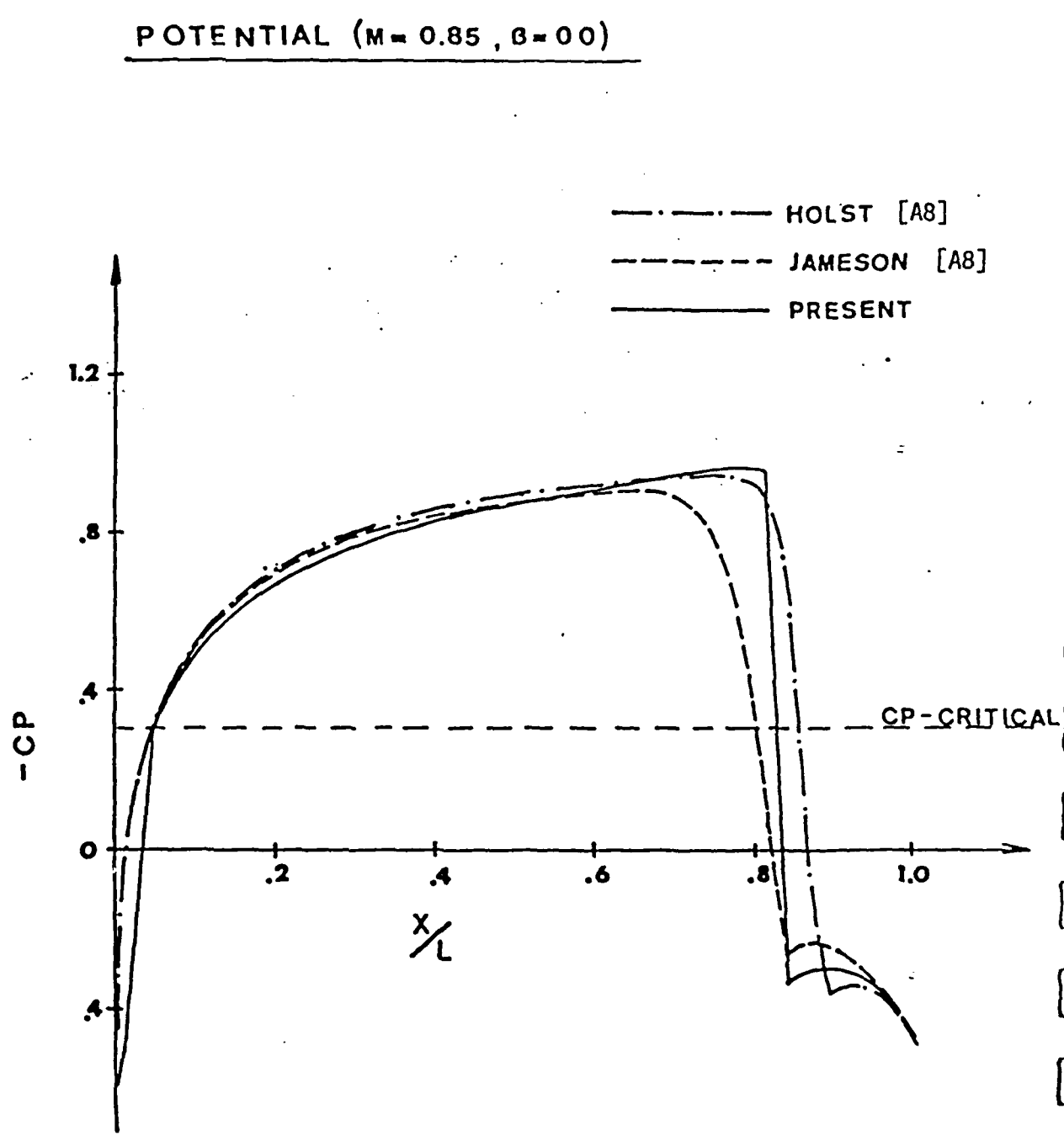

Figure A4. Comparison of pressure coefficients for present and other potential solutions (M_∞ = 0.85, β_∞ = 0.0)

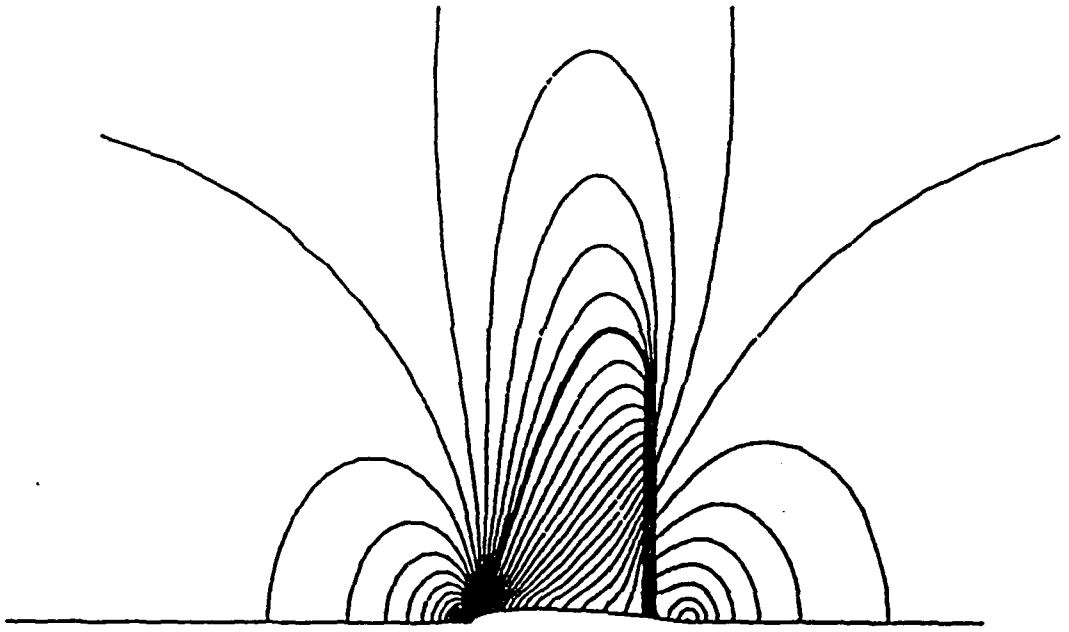

Figure A5. Mach contours for the potential flow solution

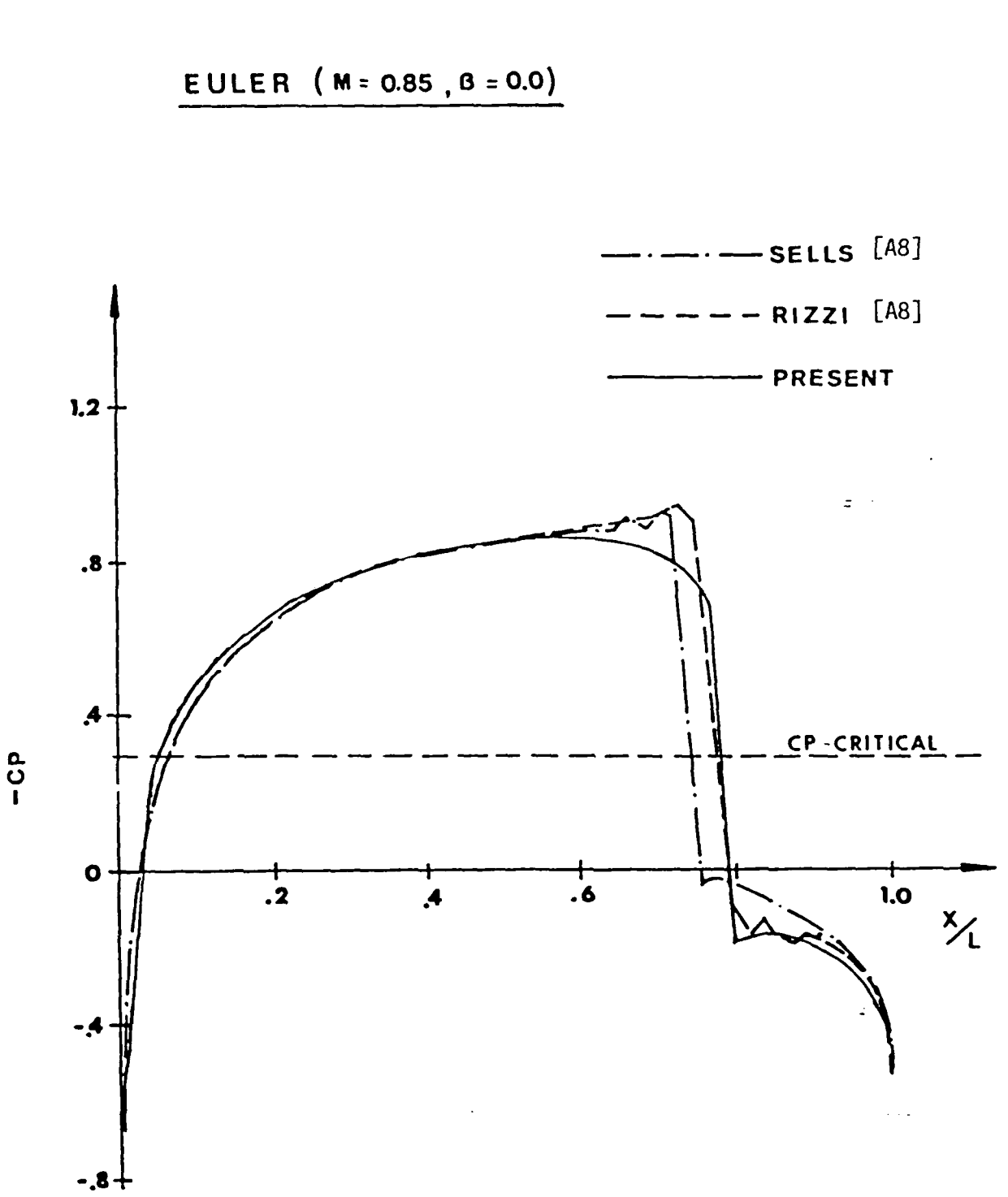

Figure A6. Comparison of pressure coefficients for present and other Euler solutions ($M_\infty = 0.85$, $\beta_\infty = 0.0$)

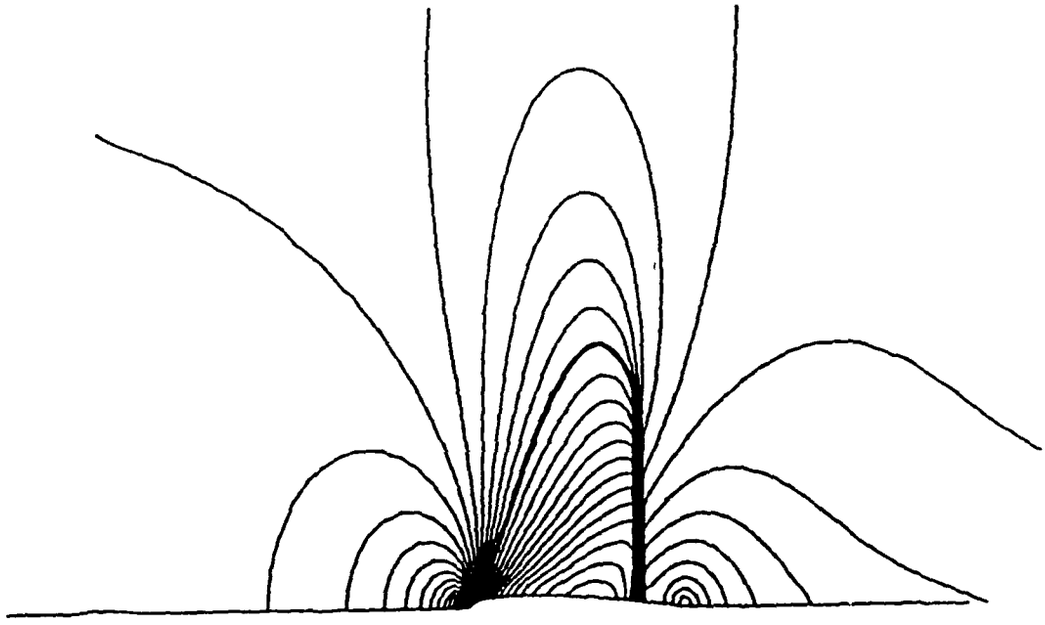

Figure A7(a). Mach contours for the Euler solution

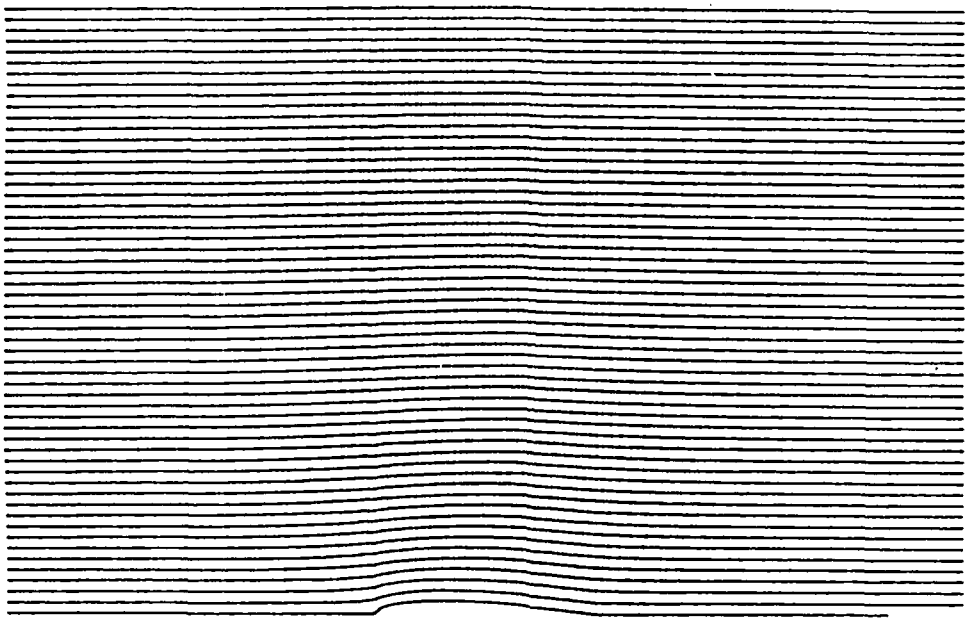

Figure A7(b). Contours for material coordinates α_1 ($\Delta\alpha_1 = 0.05$)

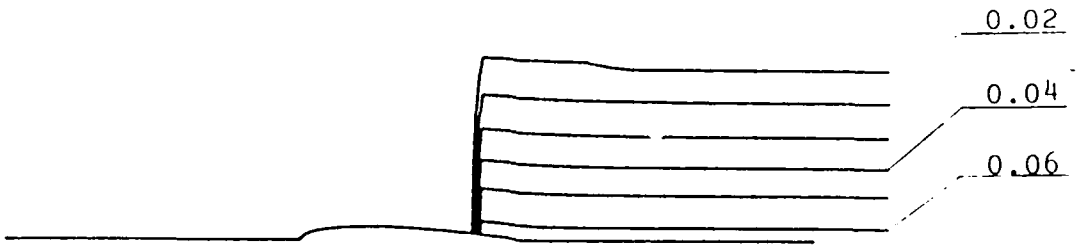

Figure A7(c). Contours for nondimensional vorticity/pressure values ($\Delta\alpha_3 = 0.01$)

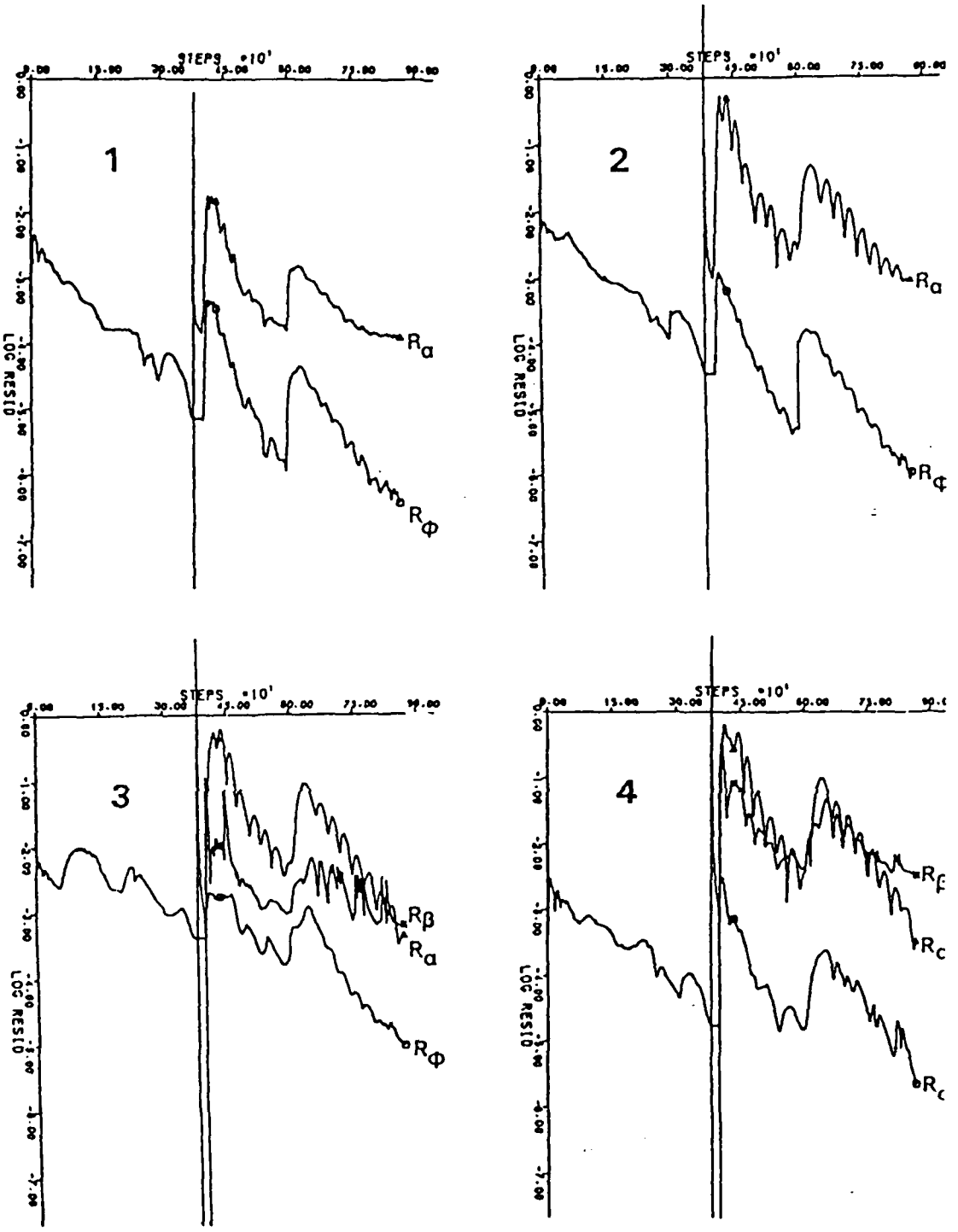

Figure A8. Residual history in each block for full Euler solution. (NACA0012)

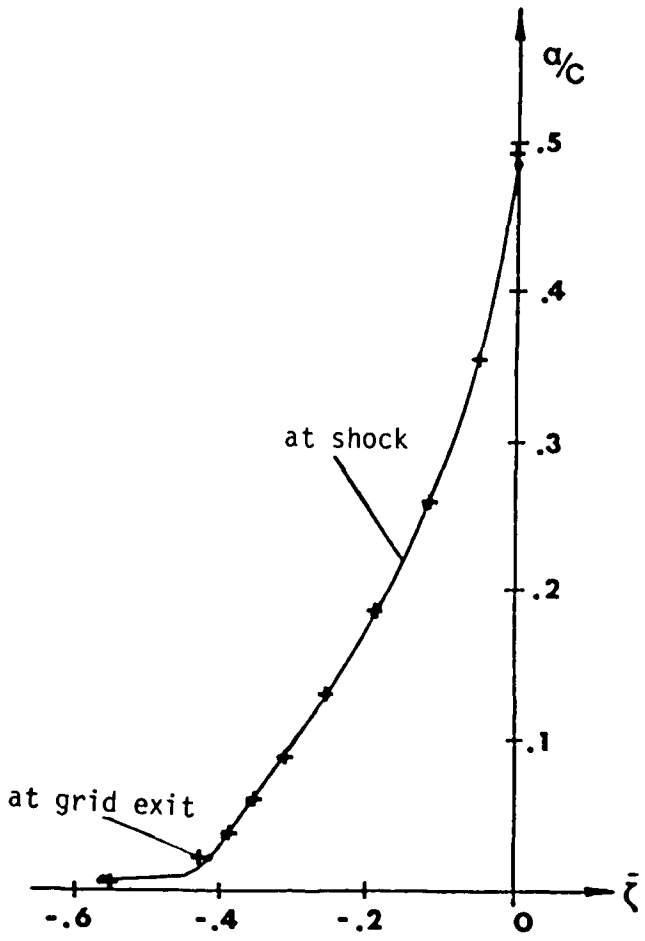

Figure A9(a). Vorticity/pressure profiles at shock location and at global grid exit (NACA0012, M = 0.85, β = 0°)

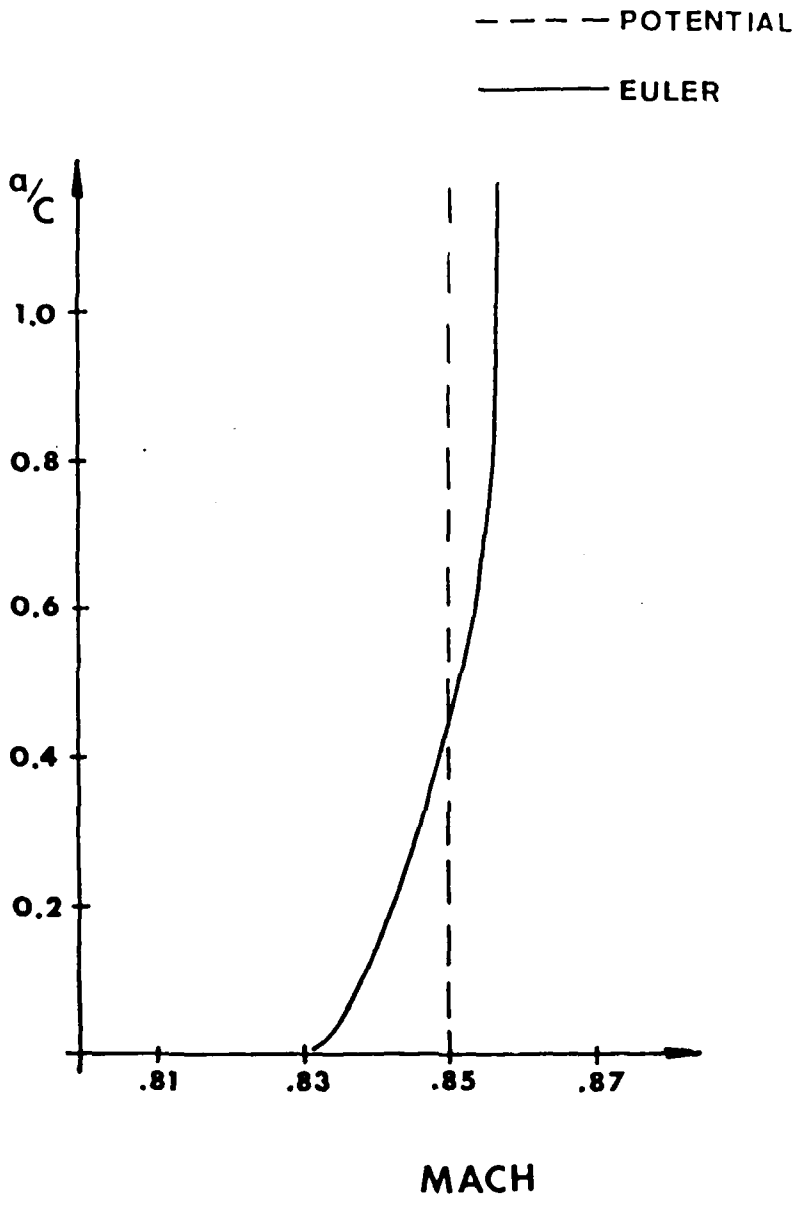

Figure A9(b). The Mach number profile at the global grid exit (NACA0012, M = 0.85, β = 0.0)

B. Detailed Study of Solving Euler Equations for Lifting Airfoils with Kutta Condition for Transonic Flows

1. Introduction

For computing transonic Euler equations around wing geometries one has to be able to model sharp trailing edges quite accurately. When one solves potential equations for the same problem, a jump is introduced to the velocity potential to include the effects of a stagnation point at the sharp trailing edge of an airfoil. In the past, when Euler equations were solved, the details of the trailing edge or the introduction of Kutta condition was not considered by other investigators.

In the present formulation, since Euler equilibriums are derived as an extension of potential flow equations, we started working on the introduction of a trailing edge Kutta condition similar to the one used for potential flows [B1, B2, B3, B4]. In the following, a summary of this activity is presented.

2. Kutta Condition for Euler Equations

In the case of potential flows, the only boundary condition is specified in terms of the normal mass flux $f = \rho \underline{u}.\underline{n}$, where $\underline{n}$ denotes an outward unit normal vector on the boundary. For the case of an airfoil in a flow field, a unique solution requires the specification of the correct circulation. For an airfoil with a sharp trailing edge, the circulation is determined from the Kutta condition which states that the flow speed at the trailing edge is finite, and the streamlines on the upper and lower surfaces of the airfoil leave the trailing edge with a continuous pressure distribution. A cut in the computational grid extending from the trailing edge to the downstream boundary is employed as shown in Figure B1. Here, the cut models a streamline which originates from the sharp trailing edge of the airfoil. In this figure, + and - respectively denote the upper and lower surfaces of the dividing streamline, E^+ and E^- are points on the surface of the airfoil closest to the trailing edge point, s and n are the tangential and normal directions on the streamlines, respectively. Using this model, the Kutta condition at the sharp trailing edge is imposed iteratively.

When the flow is transonic, the streamlines following the upper and lower surfaces of the airfoil do not convect the same entropy due to differing shock strengths. If the rotational efforts are included, a tangential discontinuity is formed along the cut (dividing streamline). It becomes important for the accurate solution of Euler equations that this discontinuity

is modeled. The definition of a streamline requires that $u_n^+ = u_n = 0$ while the balance of momentum fluxes normal to the streamline yields the condition $p^+ = p^-$ on E.G. The tangential velocity u_s, the mass density ρ and the entropy S may be discontinuous across a streamline. The exact position of the dividing streamline is unknown, however, it may be determined iteratively from the calculated for the steady flows. The tangential discontinuities in velocity can be computed from the equal pressure condition $p^+ = p^- = p$ along the dividing streamline as follows:

$$\Delta u_s = u_s^+ - u_s^- = \{2[H-(p/c)^{\frac{1}{\theta}}e^{S^+/R\theta}]\}^{1/2} - \{2[H-(p/c)^{\frac{1}{\theta}}e^{S^-/R\theta}]\}^{1/2} \qquad (B1)$$

The jump in the velocity potential across the dividing streamline shown in Figure B1 is calculated from:

$$\Delta\phi(s) = \int_o^s \Delta u_s \, ds - \int_o^s \alpha\Delta\beta_{,s} \, ds + \Delta\phi(o) \qquad (B2)$$

where

$$\Delta\phi(o) = (\phi_E^+ - \phi_E^-) \quad \text{and} \quad \beta_{,s}^- = -(pS_{,\alpha}^-) / (\rho^- u_s^- R) \qquad (B3)$$

Also along a streamline, one can write

$$\beta_{,s}^+ = -(pS_{,\alpha}^+) / (\rho^+ u_s^+ R) \quad \text{and} \quad \beta_{,s}^- = -(pS_{,\alpha}^-) / (\rho^- u_s^- R). \qquad (B4)$$

The Clebsch variables along the upper surface of the dividing streamline are thus specified as:

$$\phi^+(s) = \phi^-(s) + \Delta\phi(s) \quad , \qquad (B5)$$

$$\beta^+(s) = \beta^-(s) + \int_o^s \Delta\beta_{,s} \, ds + \Delta\beta(o) \quad , \qquad (B6)$$

$$\alpha^{+}(s) = \alpha^{-}(s) = \alpha(s) \quad . \tag{B7}$$

While ϕ and β are discontinuous across the dividing streamline, α remains continuous. The circulation around the airfoil is obtained from:

$$\Gamma = - (\phi_E^{+} - \phi_E^{-}) - \alpha(\beta_E^{+} - \beta_E^{-}) \quad . \tag{B8}$$

A simple numerical intergration scheme is employed to perform the integral in Equations (B2) and (B6) along the dividing streamline.

3. Numerical Results

Transonic flow around a NACA0012 airfoil with inflow conditions $M_\infty = 0.85$ and $\beta_\infty = 1.0°$ was considered as a test case, where M_∞ and β_∞ denote the Mach number and angle of attack at the farfield upstream, respectively. A C-type computational grid with 124 x 26 grid points (74 placed on the airfoil (surface), shown in Figure B2, was used.

The obtained pressure distribution over the airfoil surface and the comparison with other available solutions in the literature are shown in Figure B3. Here, additional details of the solution are presented to illustrate the accuracy in predicting the involved discontinuities.

Contours of Mach numbers around the airfoil are given in Figure B4. Distribution of non-dimensionalized vorticity/pressure contours which extend from shocks to the downstream are shown in Figure B5. As can be seen from this figure, the vorticities are convected in the streamwise direction with no apparent diffusion. Shown in Figure B6 are the entropy, vorticity/pressure and Mach number variations across the cross-flow direction at two selected sections on the dividing streamline. The convection properties of entropy and vorticity/pressure values as well as discontinuity of these and velocities across the dividing streamline can be observed clearly.

Since the angle of attack was small, the dividing streamline remained almost horizontal in this case. Results of a higher angle of attack case, in which the mesh modifications needed to move the cut to align with the dividing streamline becomes apparent, as can be seen in Figure B7.

A second example of the same problem was the solution of flow around an exhaust duct, as shown in Figure B.8. In this case, two flows: from the exhause and the surrounding air stream, combine where each has a different constant total pressure. One starts with an initial grid, as shown in Figure B.9 and modifies the grid as the streamlines are calculated. For the accurate solution of Euler equations, one has to align the grid with the streamline to obtain accurate solutions. As can be seen from Figure B.10, the grid is modified automatically to obtain the transonic flow solution in Figure B.11 by using such an adaptive scheme. In this case, the Kutta condition is applied for an accurate solution of the problem. Without proper implementation of the Kutta condition and adaptation of the grid, it is very difficult to obtain accurate solutions to the above problem.

References

B1. Akay, H.U., Ecer, A. and Willhite, P.G., "Finite Element Solutions of Euler Equations for Lifting Airfoils", AIAA Paper 85-0294, January 1985 (published in AIAA Journal, Vol. 24, No. 4, April 1986, pp. 562-568).

B2. Akay, H.U. and Ecer, A., "Implementation of Kutta Condition for a Finite Element Formulation of Euler Equations", Fourth International Symposium on Numerical Methods in Engineering, Atlanta, Georgia, March 24-28, 1986.

B3. Akay, H.U. and Ecer, A., "Solution of Transonic Euler Equations for Lifting Airfoils", Sixth International Symposium on Finite Element Methods in Flow Problems, Antibes-France, June 16-20, 1986.

B4. Ecer, A. and Akay, H.U., "Computation of Steady Euler Equations Using Finite Element Method", GAMM Workshop on the Numerical Simulation of Compressible Euler Flows, INRIA, Rocquencourt, France, June 10-13, 1986.

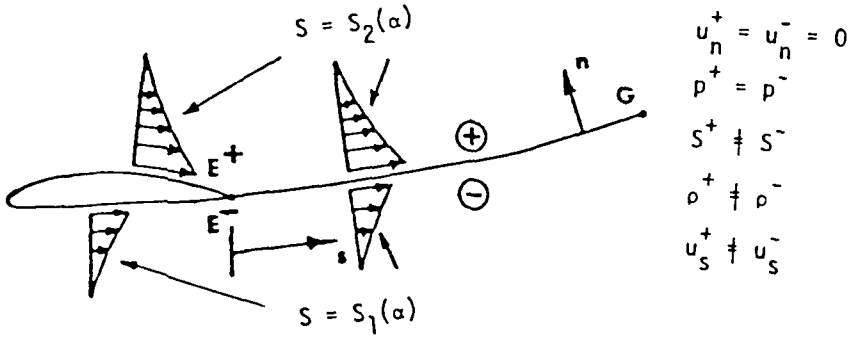

Figure B1. Dividing streamline model

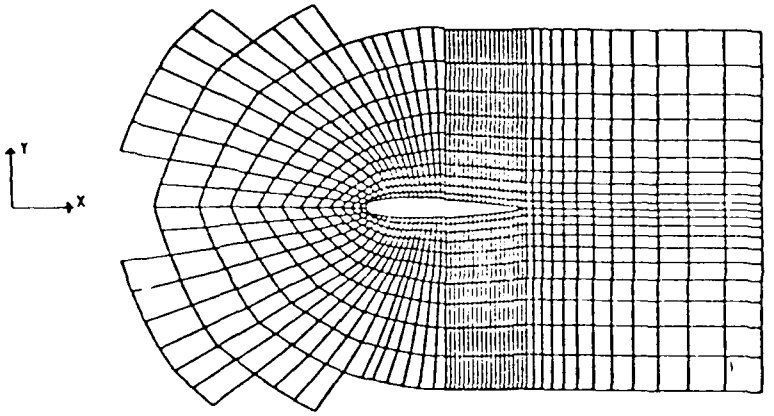

Figure B2. C-type computational grid

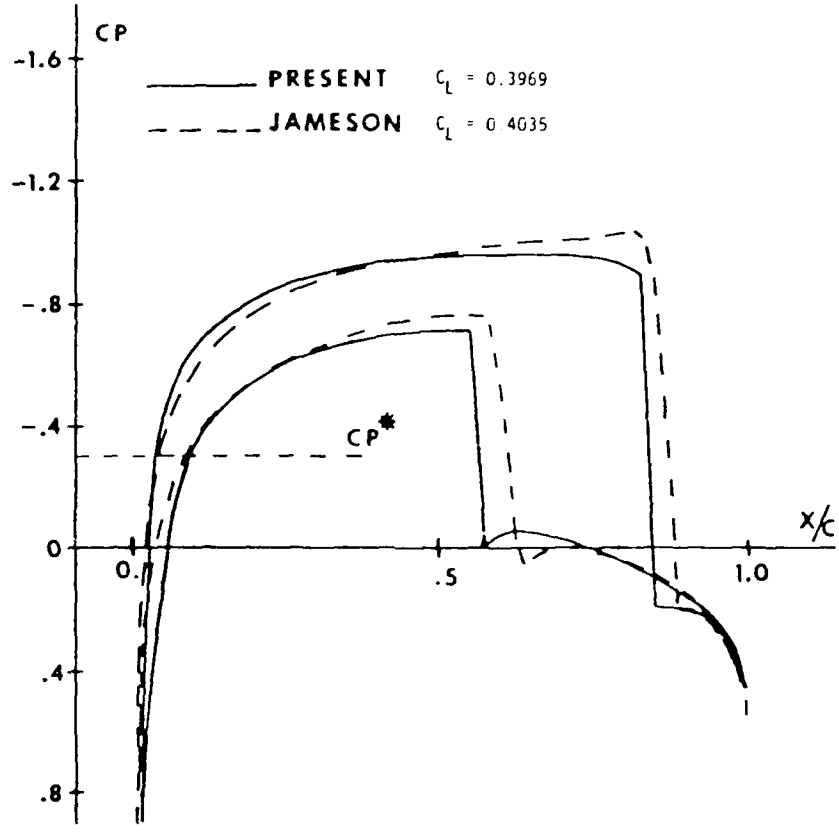

Figure B3. Pressure coefficients (M_∞ = 0.60, β_∞ = 5.0°)

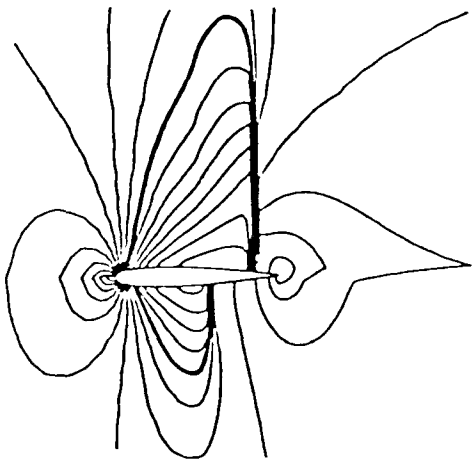

Figure B4. Mach contours (M_∞ = 0.85, β_∞ = 1.0°, ΔM = 0.05)

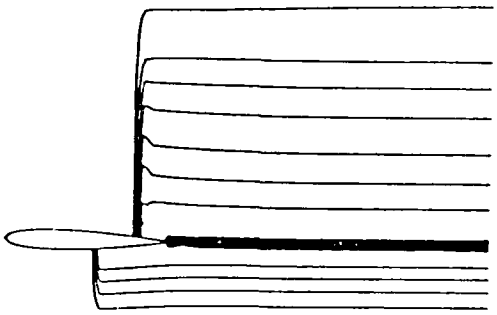

Figure B5. Contours of non-dimensionalized vorticity/pressure values (M_∞ = 0.85, β_∞ = 1.0°, $\Delta\bar{\zeta}$ = 0.01)

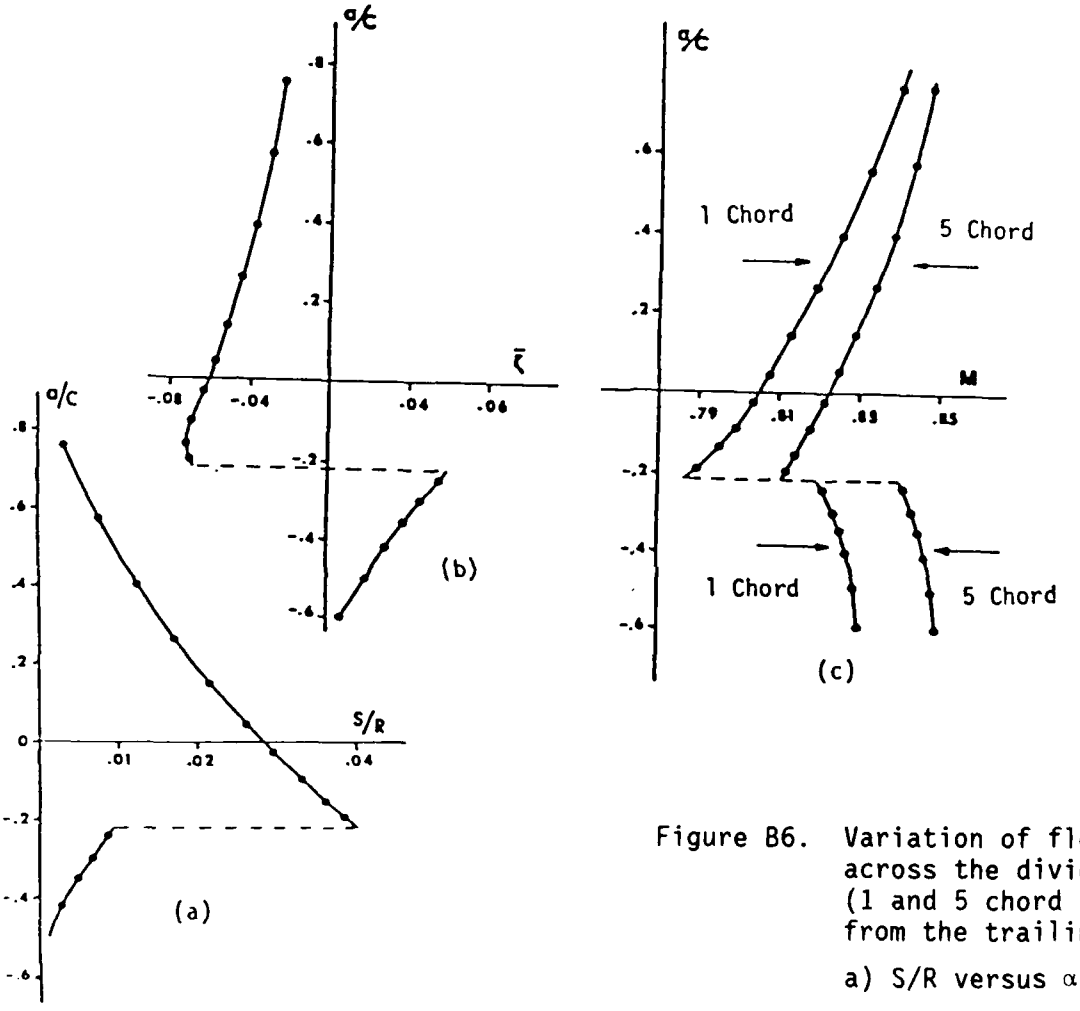

Figure B6. Variation of flow properties across the dividing streamline (1 and 5 chord length distances from the trailing edge)

a) S/R versus α

b) $\bar{\zeta}$ versus α

c) M versus α

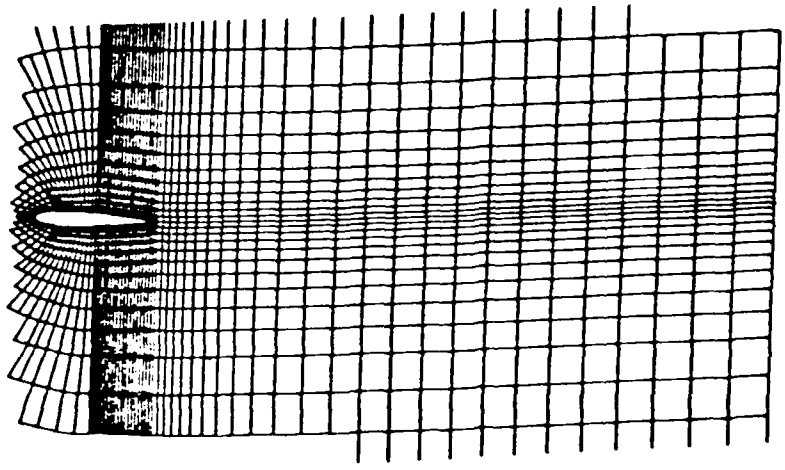

Figure B7(a). The modified grid

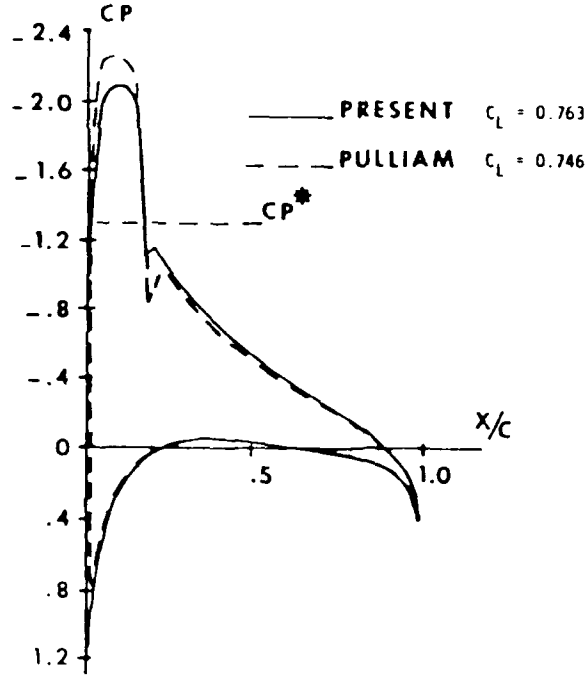

Figure B7(b). Pressure coefficients (M_∞ = 0.60, β_∞ = 5.0°)

... EXHAUST PROJECT , 6-BLOCK GRID , JAN-89 ...

CL= -488.7000
CD= 149.8000
CM= 3625.0000

RMULG= 5.00
RMUGP= 5.00
SMULG= 1.00
SMUGP= 1.00

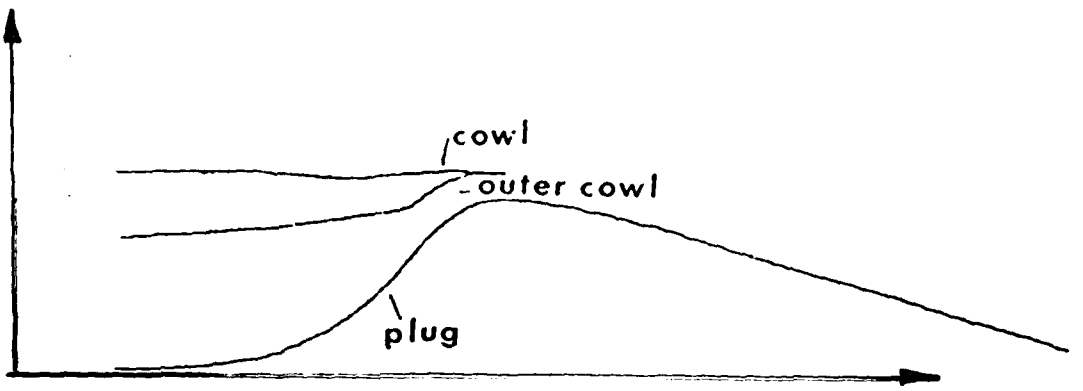

Figure B8. Exhaust duct problem

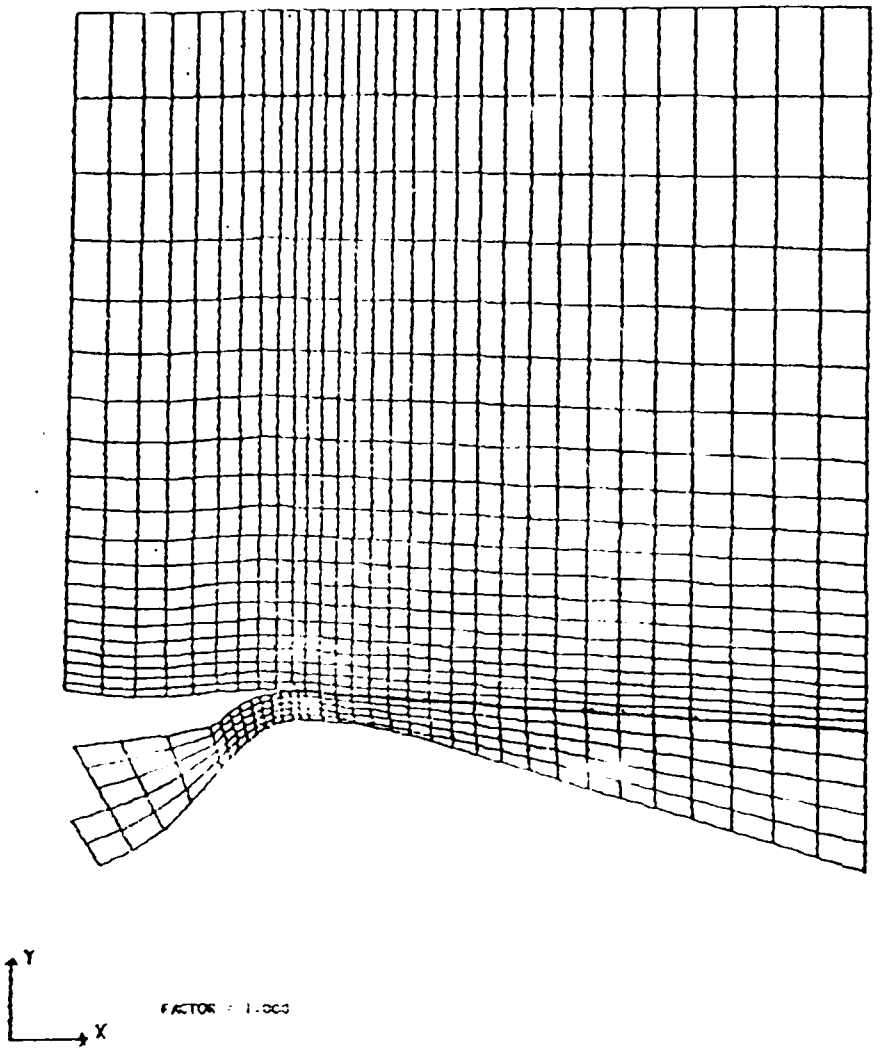

Figure B9. Initial finite element mesh

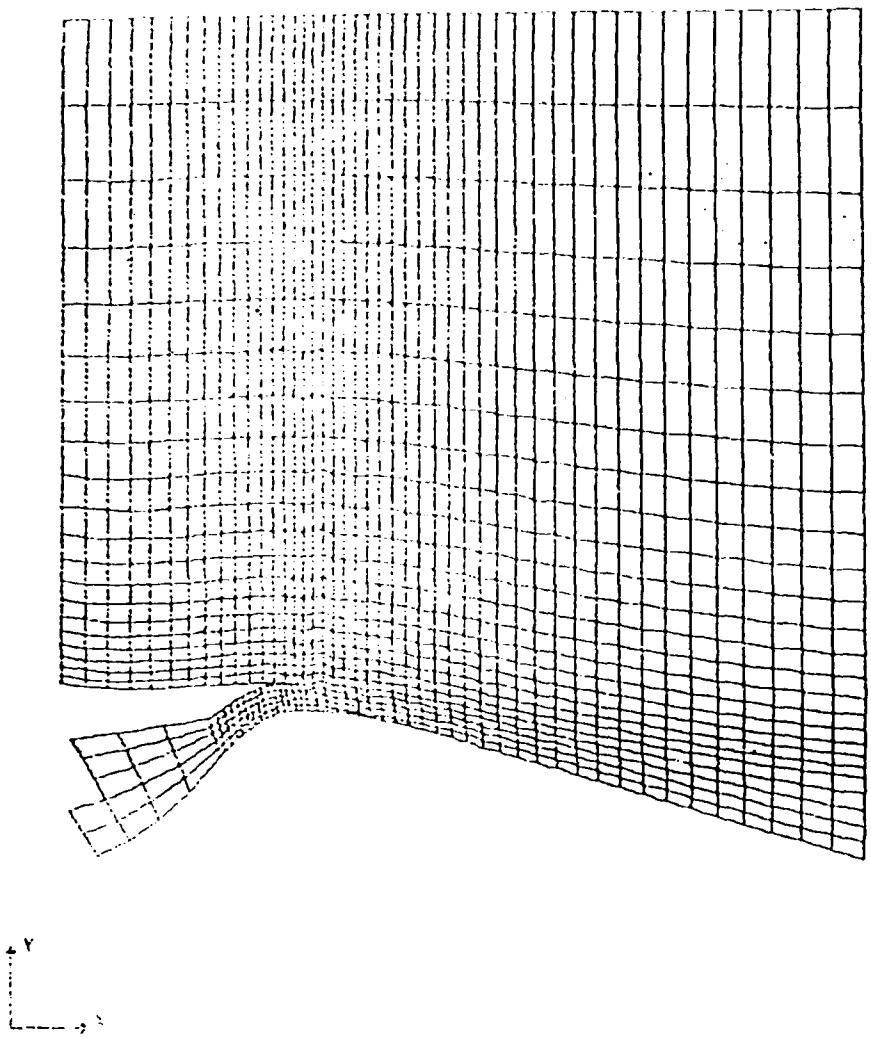

Figure B10. Modified finite element mesh

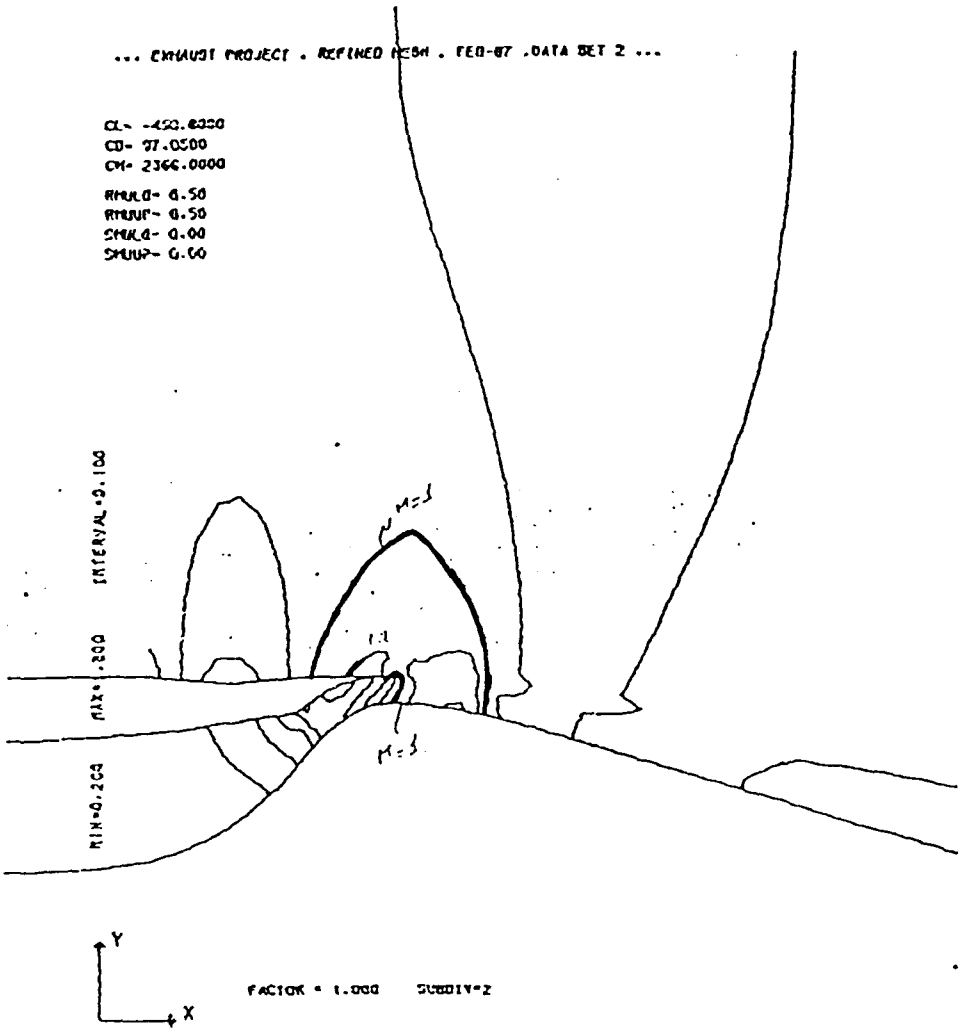

Figure B11. Mach number contours

C. Grid Generation Studies

1. Introduction

The block-structured grid generation scheme was completed three years ago. Since then, we have been employing this scheme for solving different types of three-dimensional flow problems. In the following, the grid-generation related activities are summarized.

2. Grid Generation for F-16

Over the years, the grid generation for an F-16 aircraft was employed as a test case. A finite element grid was generated by assembling several C-type grids around the aircraft and its wing through a unified block-structure [C1], as shown in Appendix B. During the last twelve months, we have worked with Dr. J. Shang's group at WPAFB for generating a computational grid for the same problem to be analyzed by using finite difference/finite scheme type algorithms. The block-structure for this grid is shown in Appendix C. It will be basically an H-type grid designed according to the specifications of Dr. Shang's groups where the aircraft is modeled with a series of "void" blocks embedded in a regular block-structure. In fact, a structured grid was produced for every block and connected in terms of an "irregular" block-structure. We hope to continue working with this grid for the next year in terms of improvements and also analyzing the flow.

References

C1. Ecer, A., Spyropoulos, J.T. and Maul, J., "A Block-Structured Finite Element Grid Generation Scheme for the Analysis of Three-Dimensional Transonic Flows", AIAA Journal, Vol. 23, No. 10, October 1985.

C2. Pien, B., Ecer, A., Ward, P. and Bowes, C., "Application of a Block-Structured Grid Generation Scheme for Modeling Three-Dimensional Viscous Flows", 1st Int. Conf. on Numerical Grid Generation in Computational Fluid Dynamics, Landshut, Germany, July 14-17, 1986.

D. Implementation of the Developed Procedure on Large Computers

1. Summary of the Activity

This activity was started during 1986 and involved a major portion of our efforts during 1987. A short summary of the work in this area is summarized below.

a. Collaboration with the IBM Research Center

For the last twelve months, we have been working with Dr. Rudin of IBM Research Center on the application of our block-structured Euler solver on large IBM machines.

IBM has supported our travel to IBM Research Center in Kingston, New York, as well as providing us with free computer time on their IBM 3090. Main areas of interest on this computer where the vectorization of the code, availability of large virtual memory and asynchronous I/O operations. The objective of this study was to demonstrate that the present block-structured solution scheme is flexible in terms of efficient utilization of all of the computer resources mentioned above. The configuration of IBM 3090 computers and the implementation of the Euler solver on this machine are shown in Appendix F. Recently, further support was obtained from IBM in terms of computer time and a research assistant to continue this work for the coming twelve months.

b. NSF Support on CYBER 205

A proposal submitted to NSF was funded two years ago for 80 hours of CYBER 205 computer time on Purdue's computer. We had a masters student who adopted the code on this machine and used most of the available computer time. His work included an introduction of Kutta condition in 3-D environment and accurate modeling of complex shock configurations as well as testing the efficiency of the scheme on this machine. We decided not to work on this machine any further when the NSF account had to be switched from Purdue's computer to another machine. When we started to work with the CRAY computer at the University of Illinois, the inefficiency in working with their time-sharing operating system, which was completely different from the one at WPAFB became apparent. We decided to concentrate our efforts on the CRAY computer at WPAFB and transported the developed capabilities to this machine as described below.

c. Cooperation with WPAFB

A cooperative work was conducted with Dr. D. Sedlock of WPAFB which involved working on the CRAY computer at WPAFB. Computer time and travel support was provided by WPAFB. A researcher stayed at the base for a total of two months and making frequent trips for implementing and running the code. We implemented the Euler code on their machine running the standard wing-body. We are currently working to complete another test case. The results of this work will be presented under a separate report. The implementation of the block-structured code on the CRAY-XMP computer are also illustrated

in Appendix F. We have plans to continue also with this activity during 1987-1988.

d. Planned Future Activities in this Area

Our recent work is mainly aimed at demonstrating the advantages of the developed block-structured solution scheme in parallel-processing environment for solving large aerodynamic problems. We have our block-structured solution scheme stabilized on IBM and CRAY computers at this time. This has enabled us to study the basic requirements for solving large problems on a block-structured basis in detail. In fact, we hope to continue with IBM Research Center and WPAFB on these projects for the coming year.

Our continuing work involves studying the parallel processing environment in a more general fashion. Presently, Super Computers, CRAY or IBM allow limited main memory, limited number of fast CPU's and large and fast disk I/O reserves. We expect the coming computers to improve this solution by improving large memory machines with many CPU's. Our proposal to DOD for purchasing a CSPI machine was approved. We have started to work on this machine. We expect to show that block-structured solution schemes are necessary and efficient tools for solving large aerodynamics problems on these machines.

APPENDIX A

THREE-DIMENSIONAL BLOCK-STRUCTURED SOLUTION SCHEME FOR TRANSONIC FLOWS

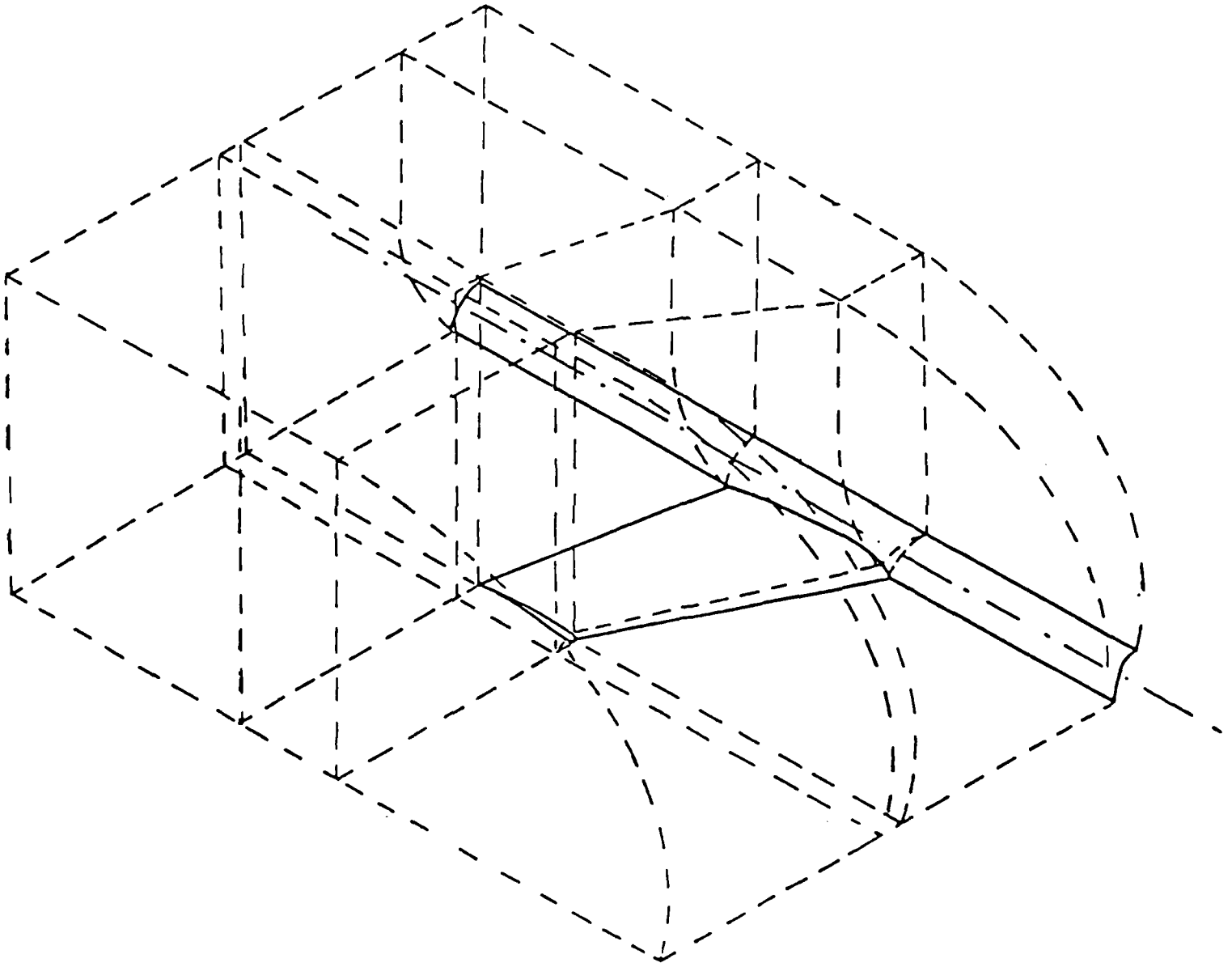

Figure 1. Upper-half block-structure for analyzing the transonic flow around the wing-body configuration.

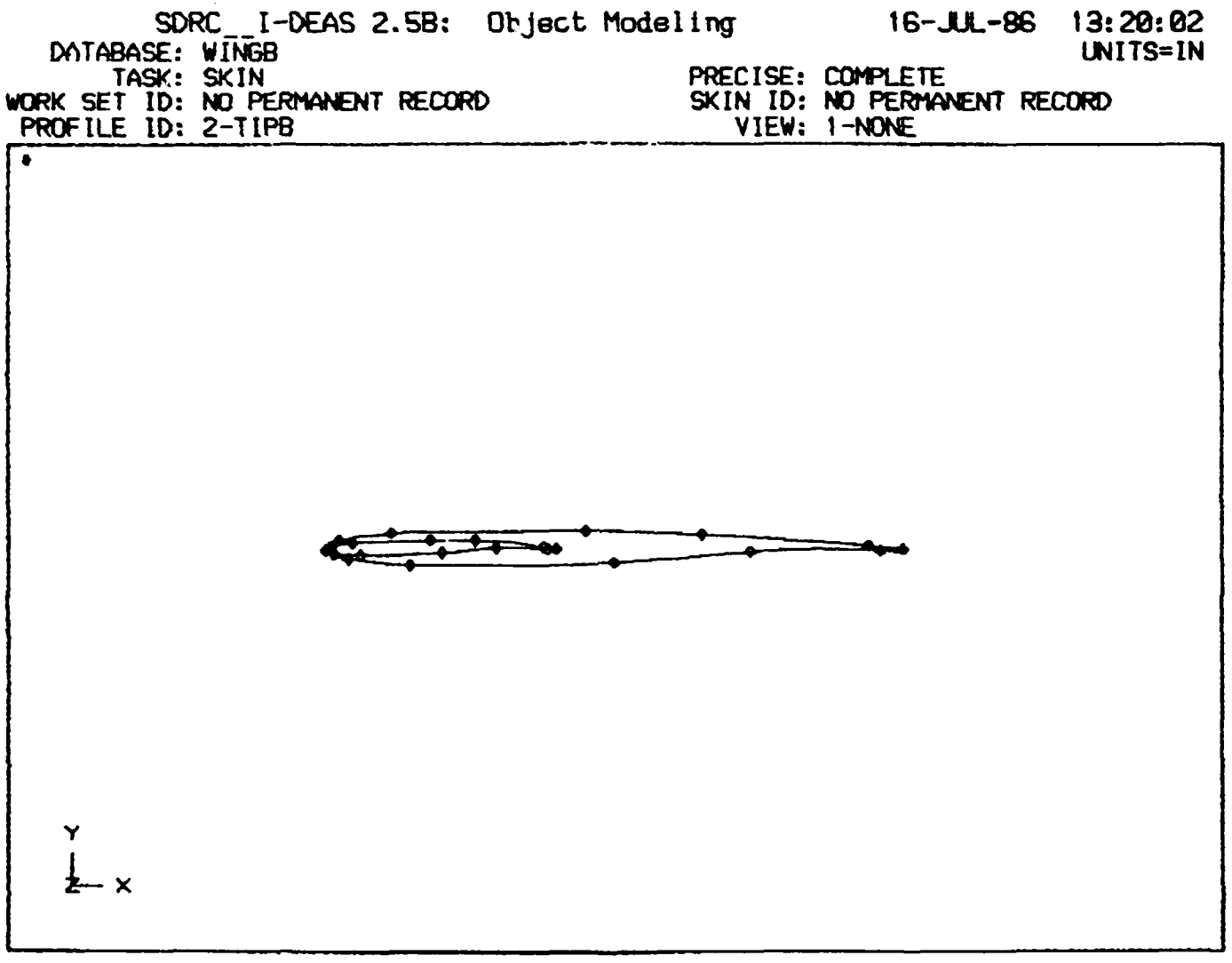

Figure 2. Root and tip sections of the wing.

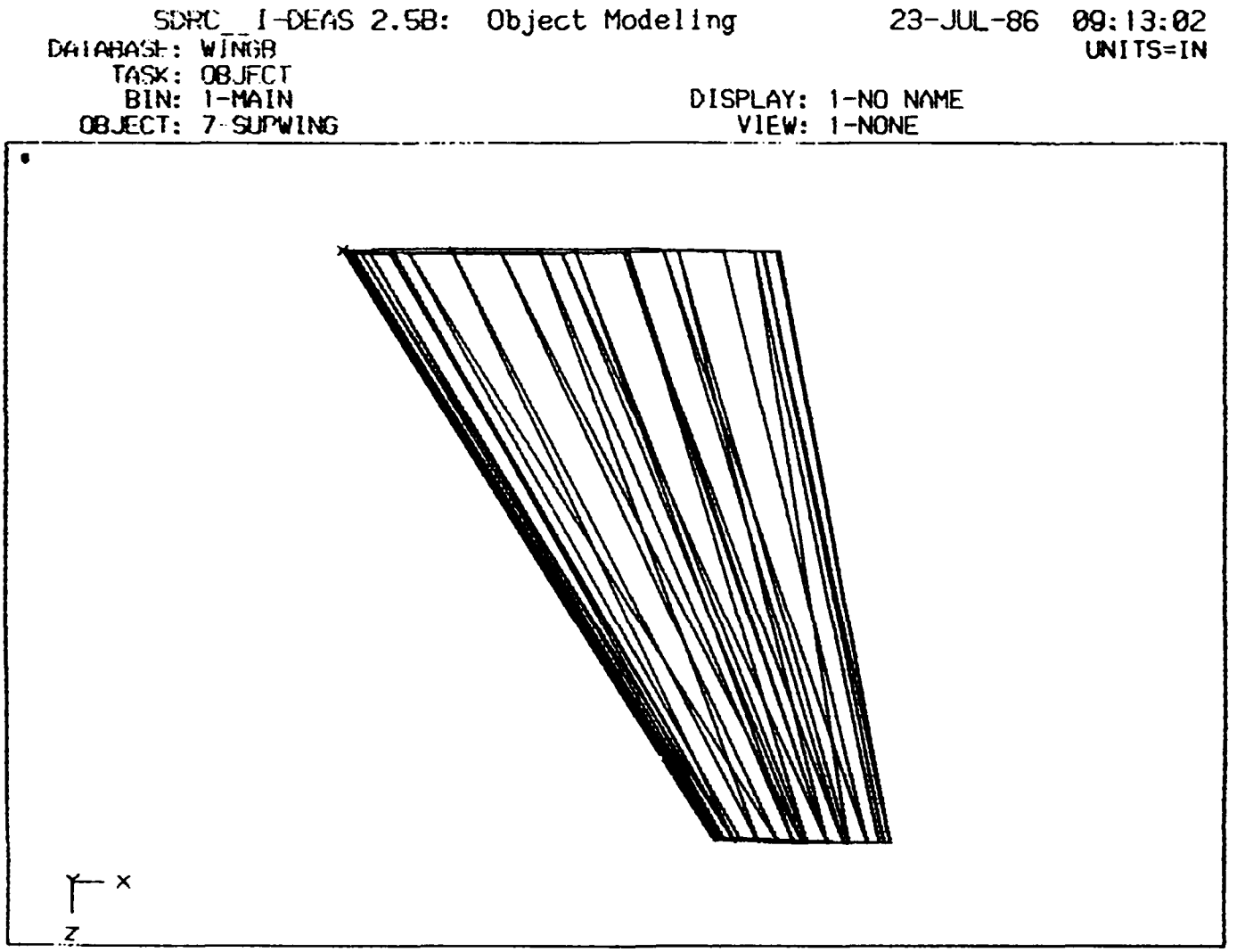

Figure 3. Planview of the wing defined by extrusion of the root and tip sections.

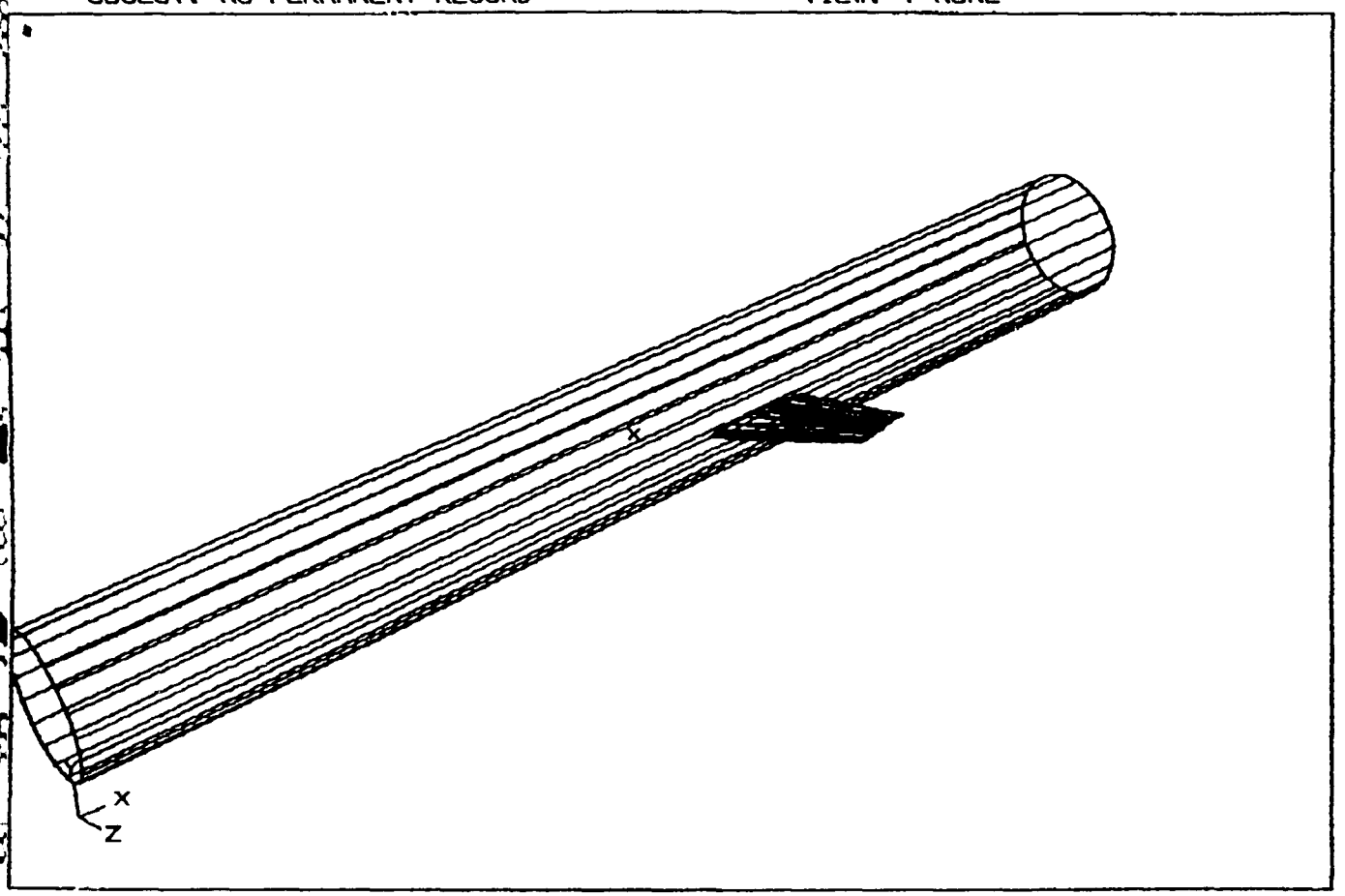

Figure 4. Wing attatched to the cylindrical fuselage geometry.

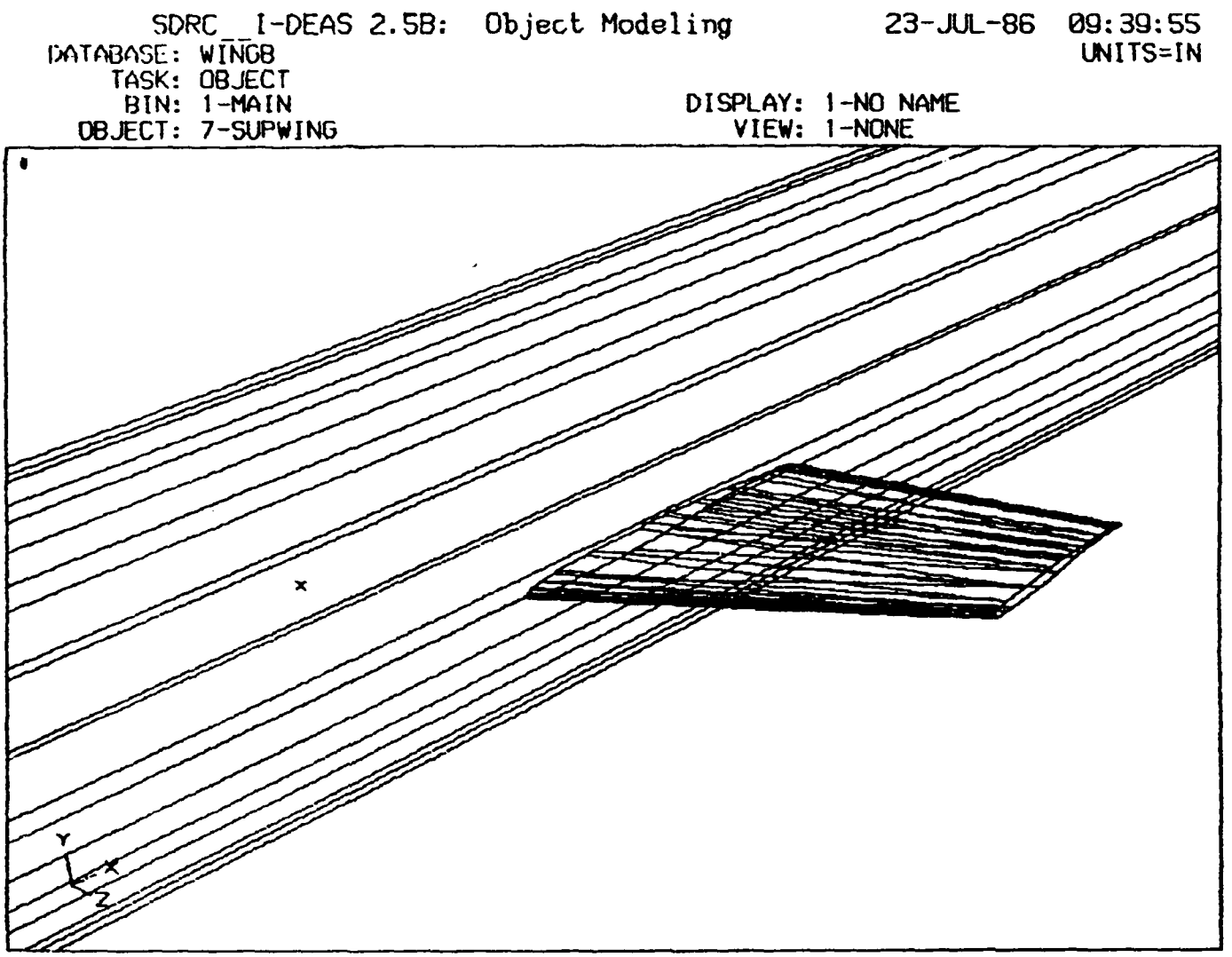

Figure 5. Detail of the wing-fuselage intersection.

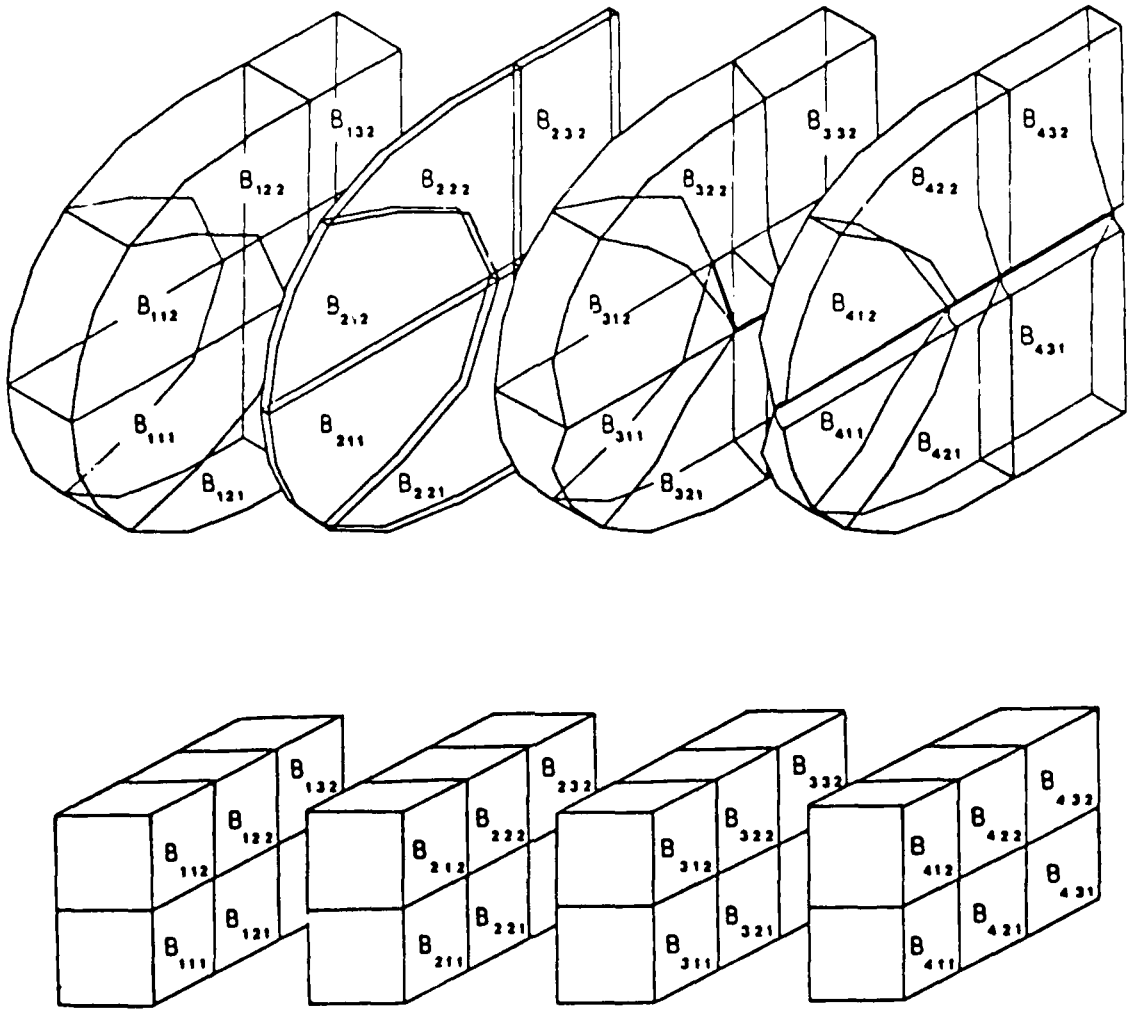

Figure 6. Twenty-four block representation of the flow domain in the real and computational spaces for the wing-body problem.

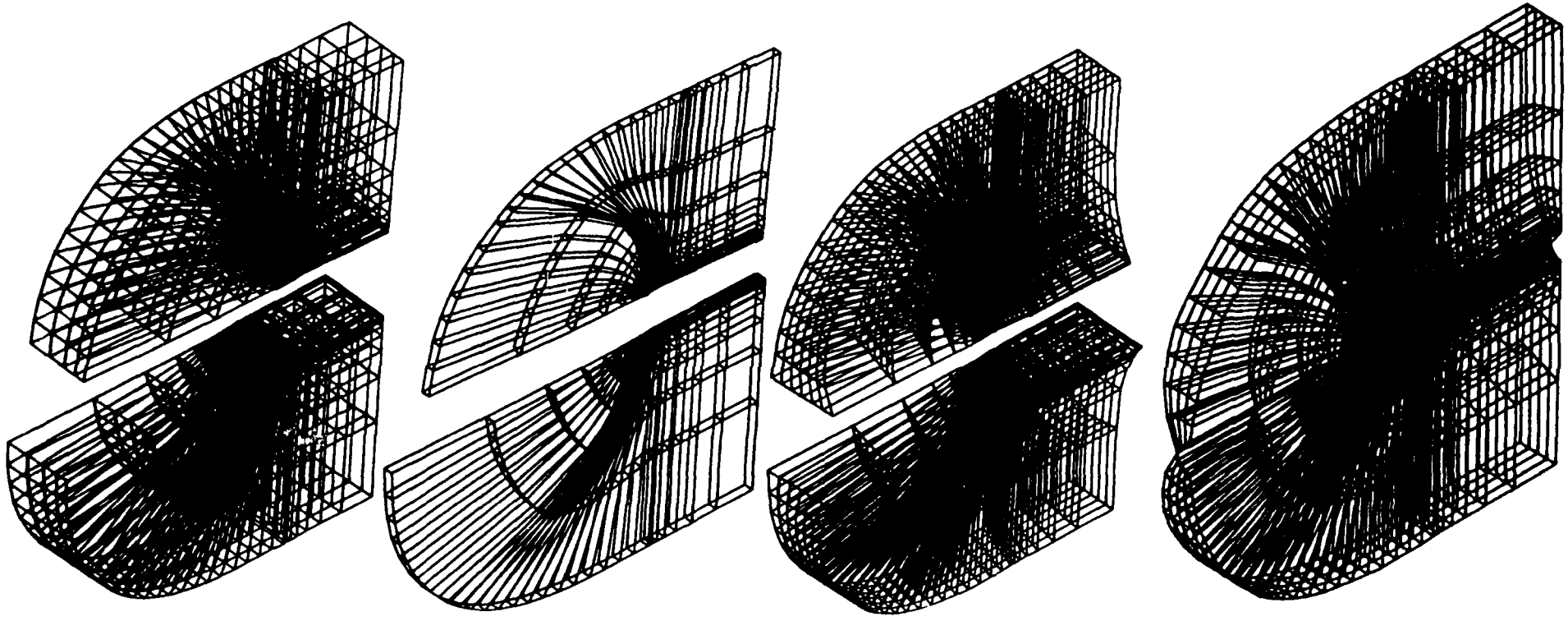

Figure 7. Finite element grids for the blocks in the wing-body problem.

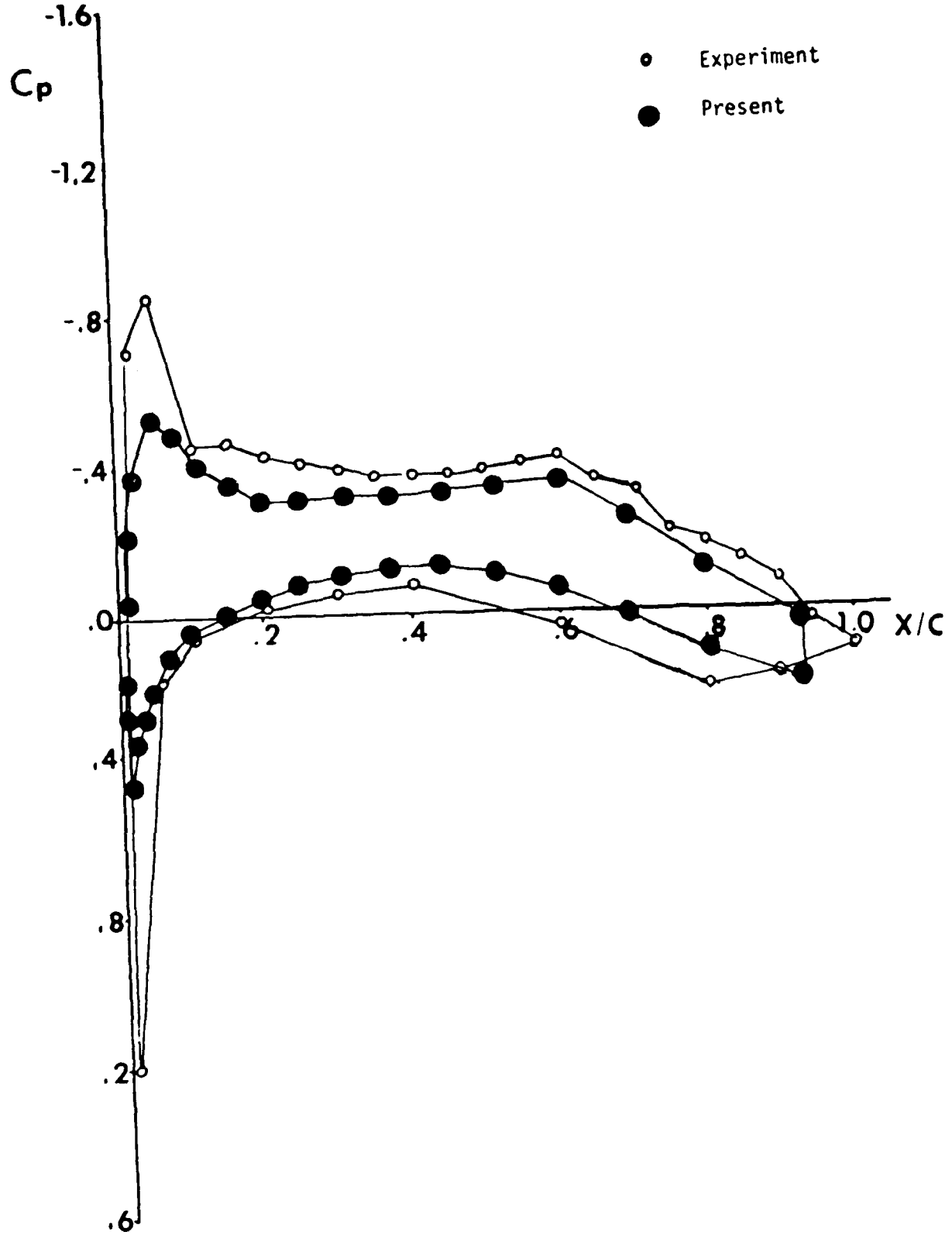

Figure 8. Variation of pressure coefficients along the root for the wing-body problem.

APPENDIX B

THREE-DIMENSIONAL FINITE ELEMENT GRID GENERATION FOR F-16 AIRCRAFT

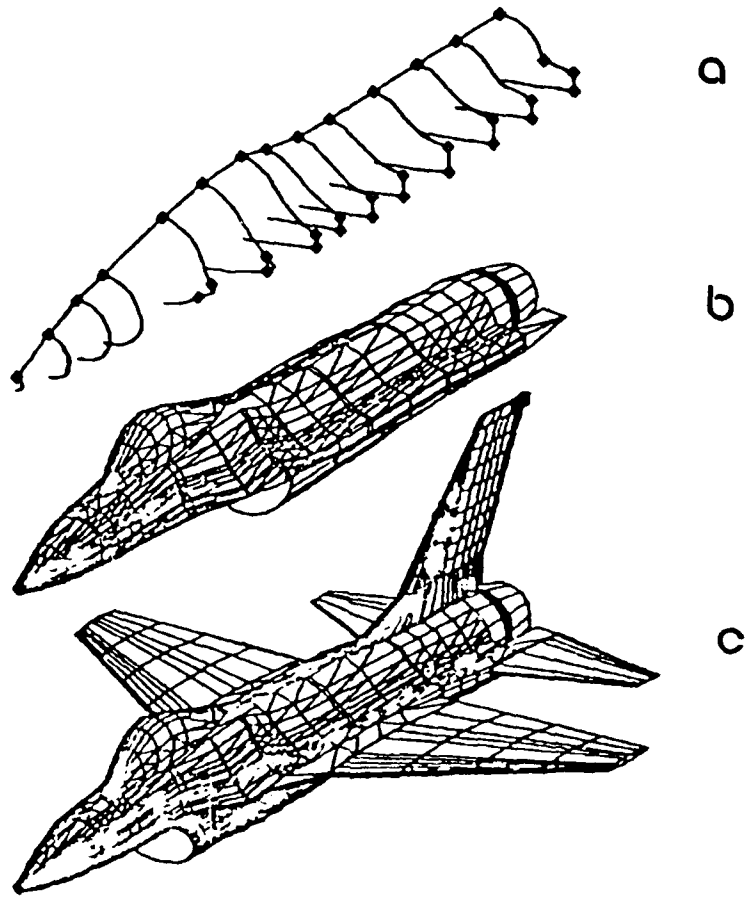

Figure 9. Aircraft geometry defined by skinning of individual fuselage cross-sections and adding of the wings end tail.

SDRC__I-DEAS 2.0: Object Modeling 24-FEB-84 12:06:48
UNITS=IN

DATABASE:
TASK: OBJECT
BIN: 2-BIN2
OBJECT: 5-BODYM

DISPLAY: 1-NO NAME
VIEW: 1-NONE

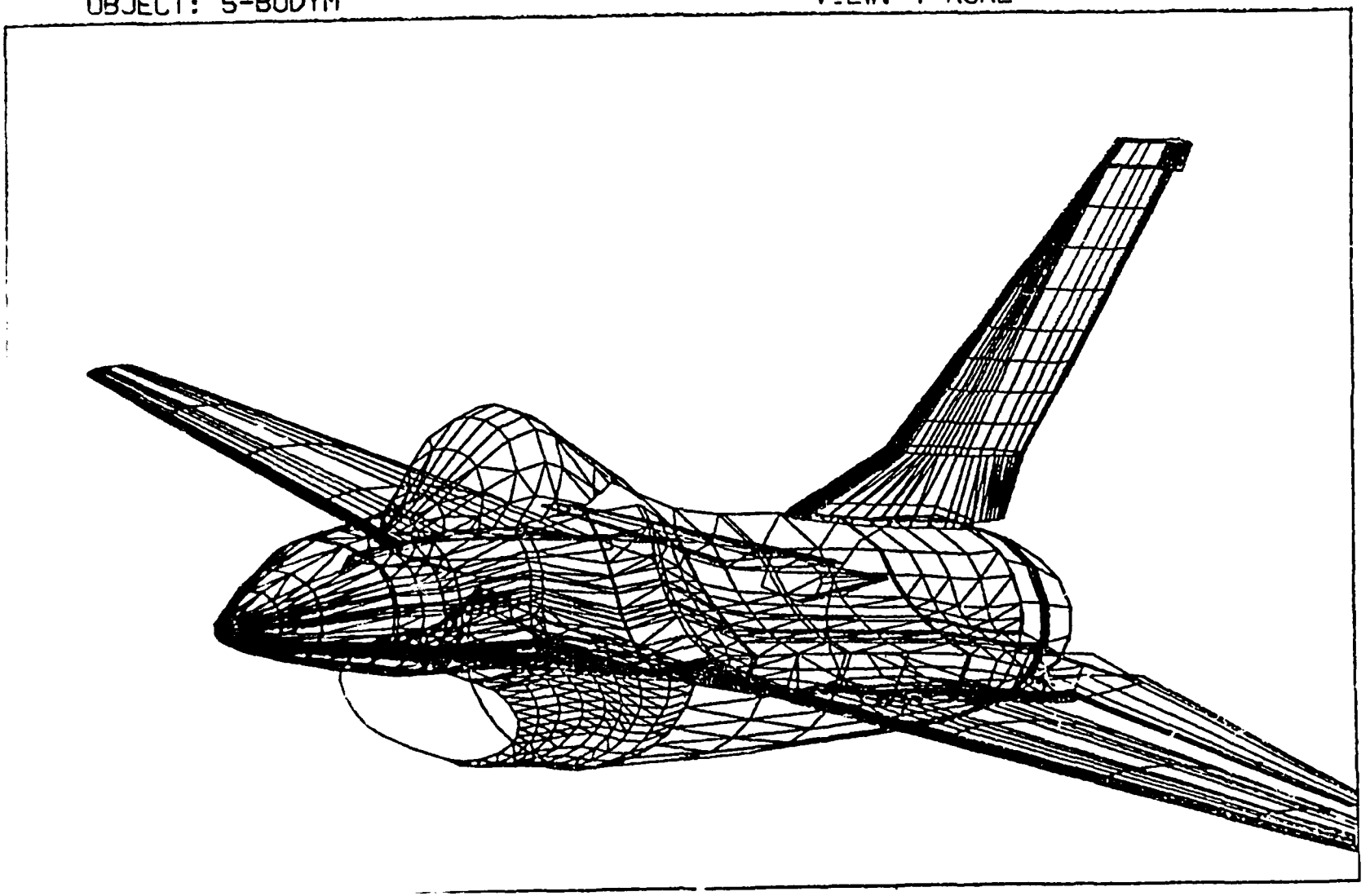

representation of the F-16 geometry.

AD-A185 465 A ZONAL APPROACH FOR THE SOLUTION OF COUPLED EULER AND POTENTIAL SOLUTION..(U) INDIANA UNIV-PURDUE UNIV AT INDIANAPOLIS SCHOOL OF ENGINEERIN.. A ECER JUN 87 2/2

UNCLASSIFIED ET-S87-2 AFOSR-TR-87-1350 F49620-83-K-0034 F/G 20/4 NL

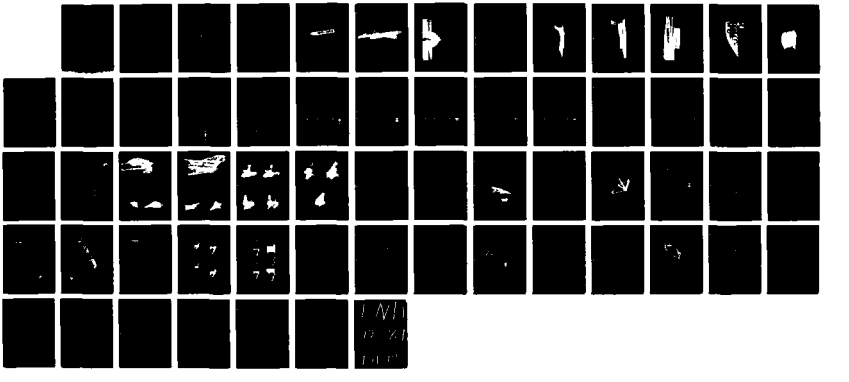

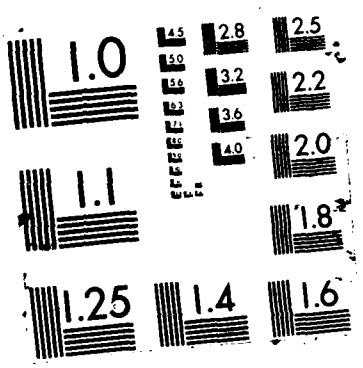
1.0
1.1
1.25
1.4
1.6
1.8
2.0
2.2
2.5
2.8
3.2
3.6
4.0
4.5
5.0
5.6
6.3
7.1
8.0
9.0

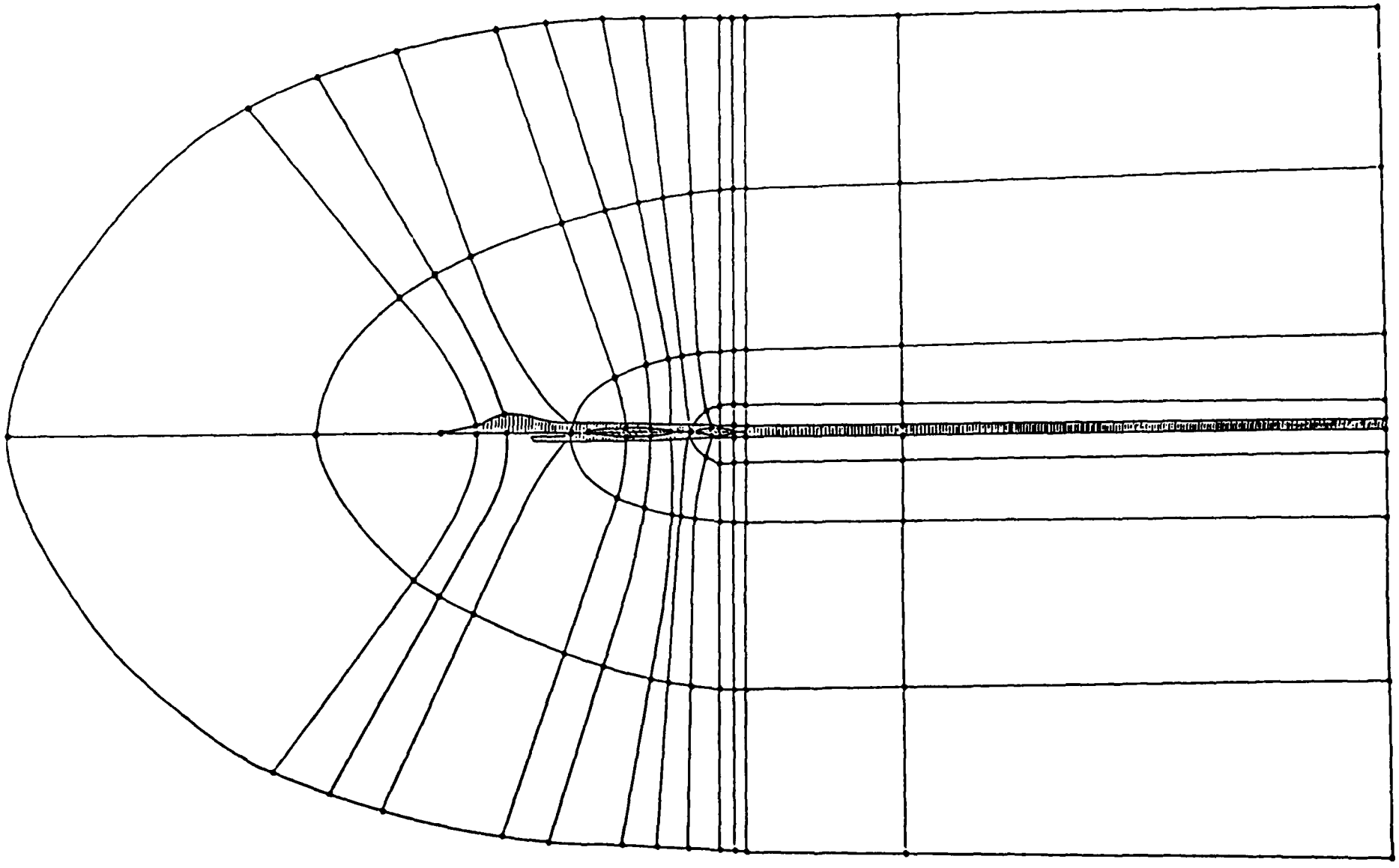

Figure 11. Cross-section of the F-16 block-structure employing C-type grids around the wings and horizontal stabilizer.

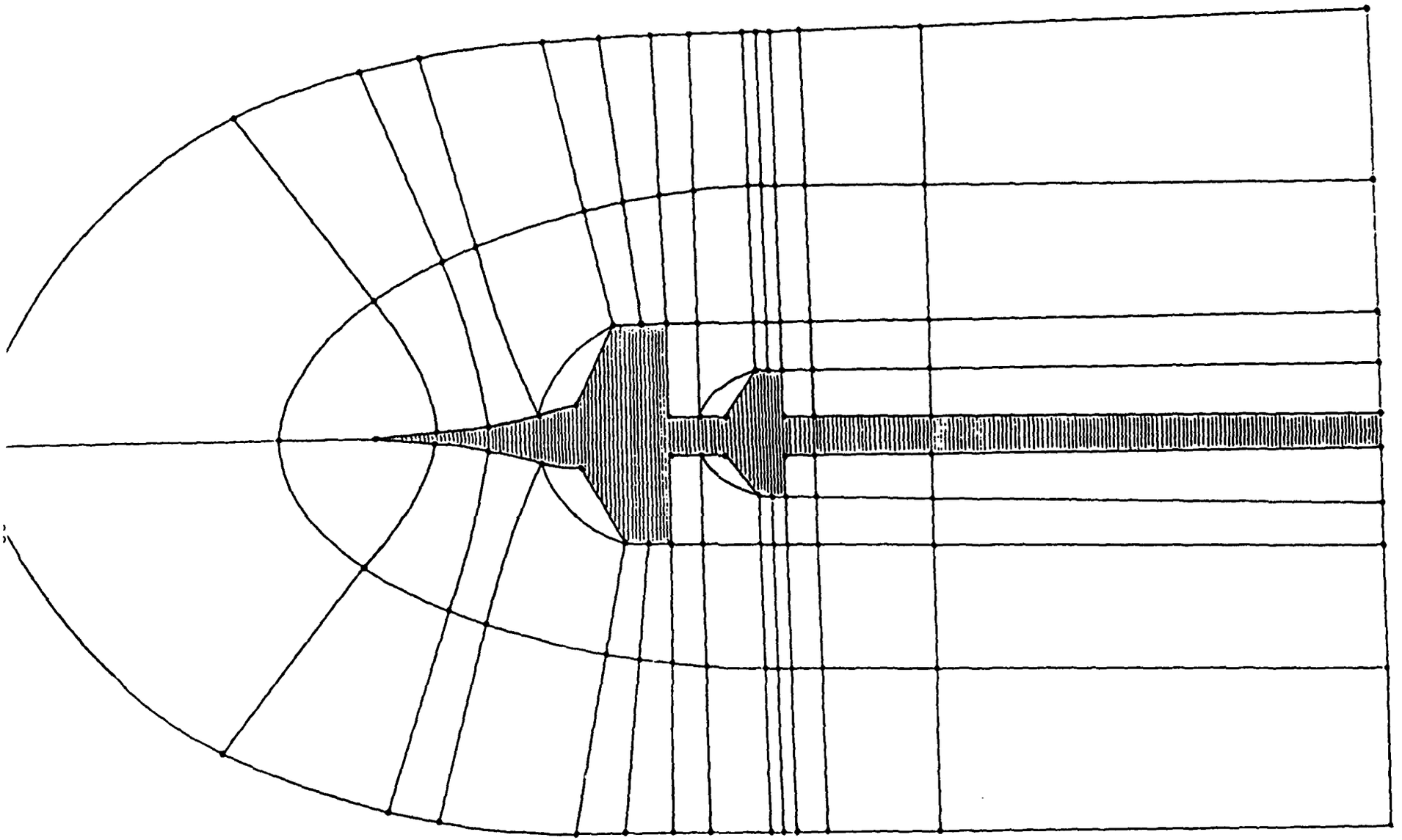

Figure 12. Top view of the F-16 block-structure employing C-type grids around the wings and tail.

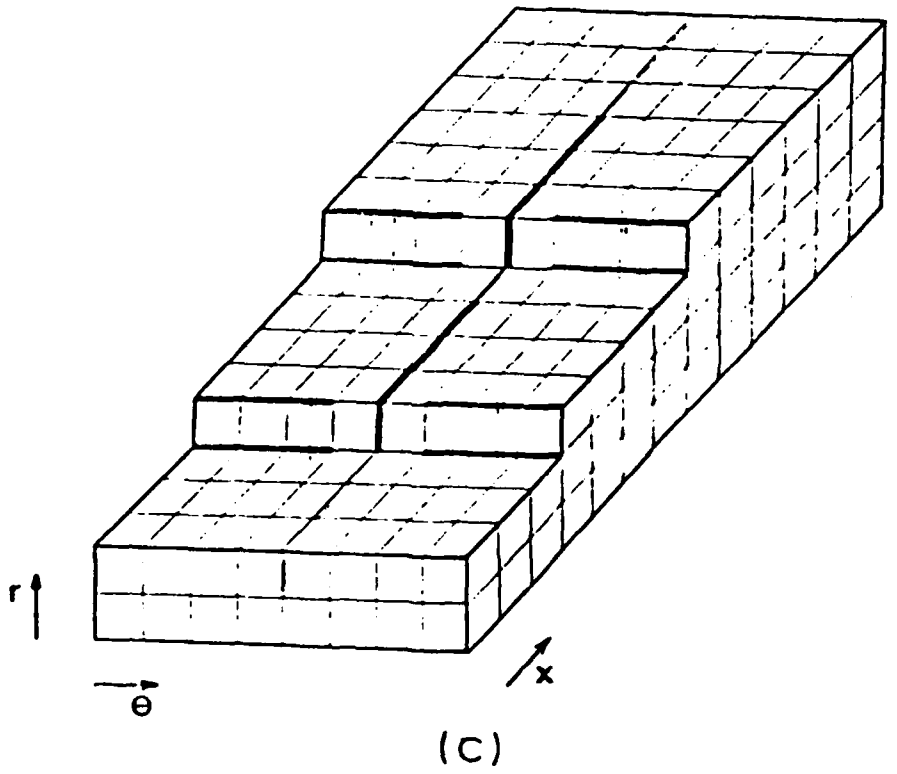

Figure 13. F-16 block-structure in the computational space.

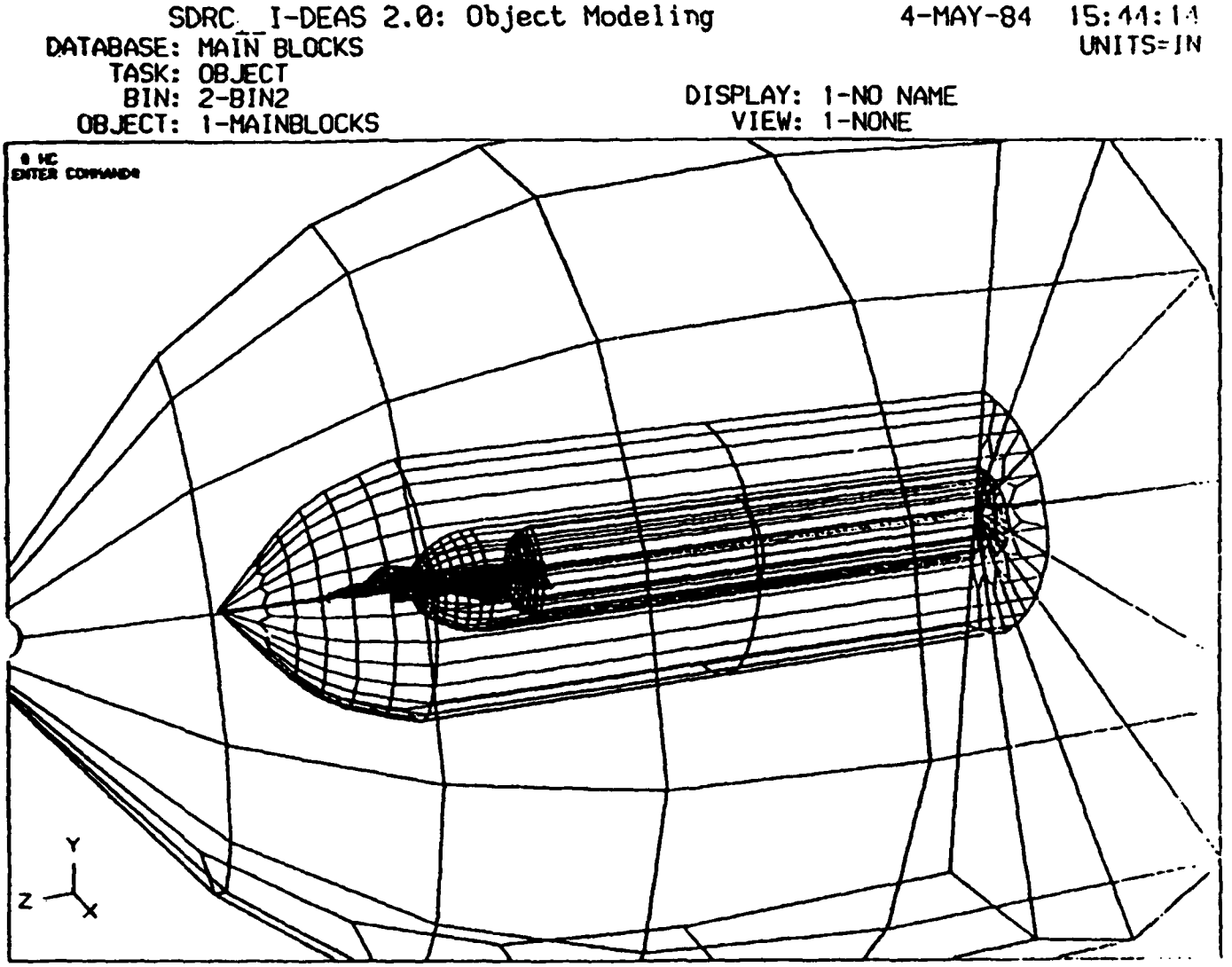

Figure 14. Definition of the radial block shells around the *F-16 geometry.*

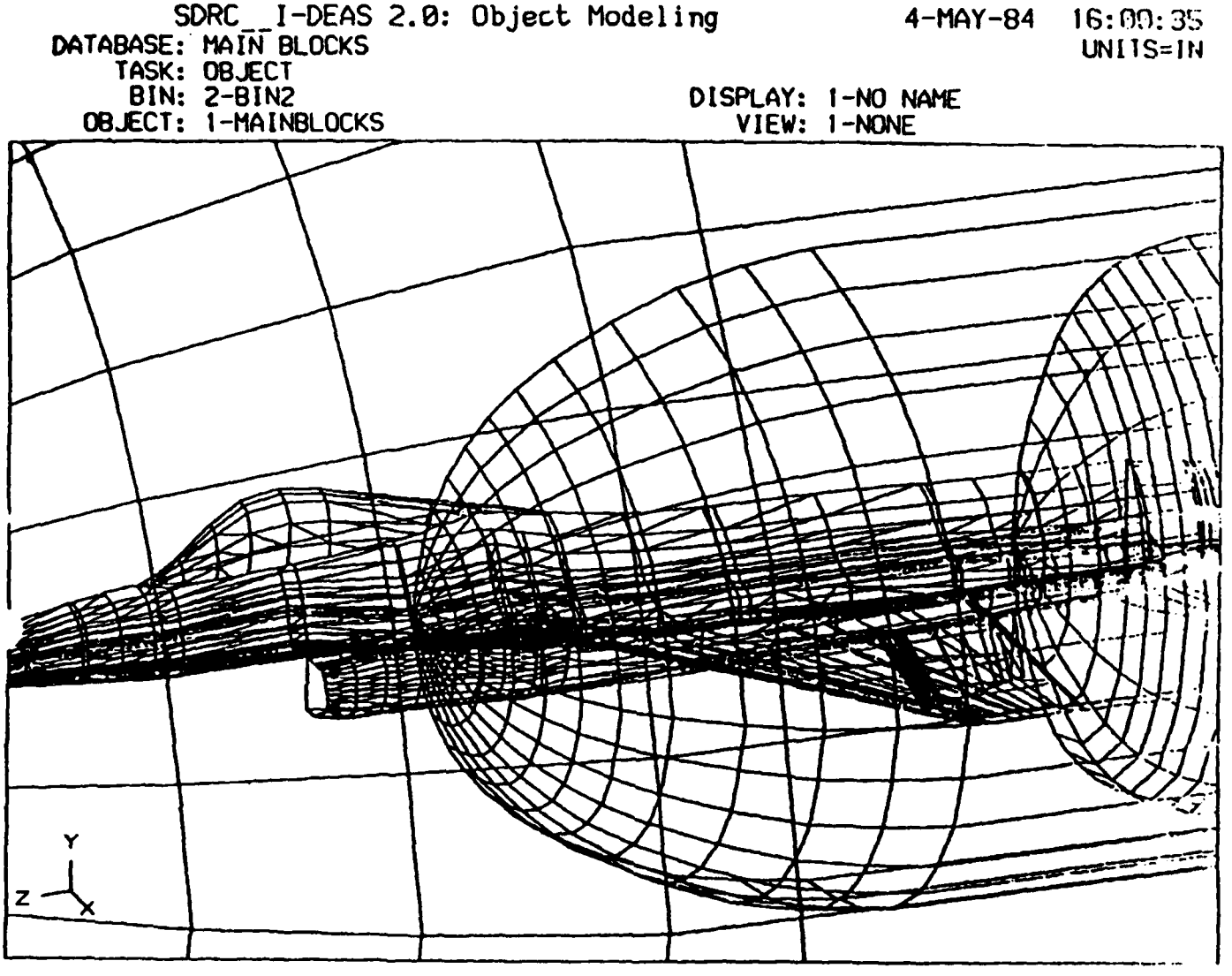

Figure 15. Detail of the block shells around the wings and tail section.

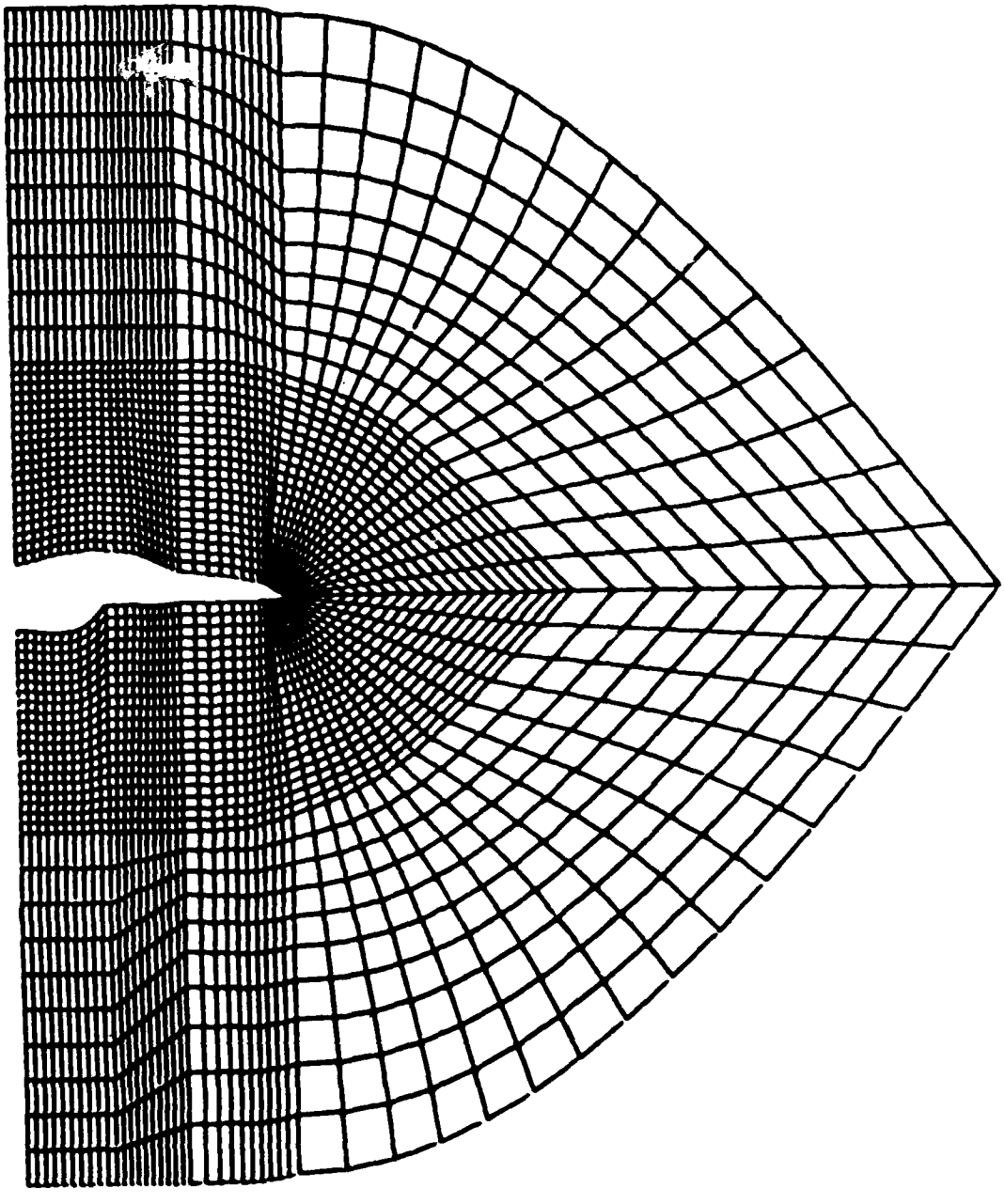

Figure 16. C-type grids for the blocks around the nose section.

APPENDIX C

F-16 GMD DEVELOPMENT FOR WPAFB (DR. SHANG)

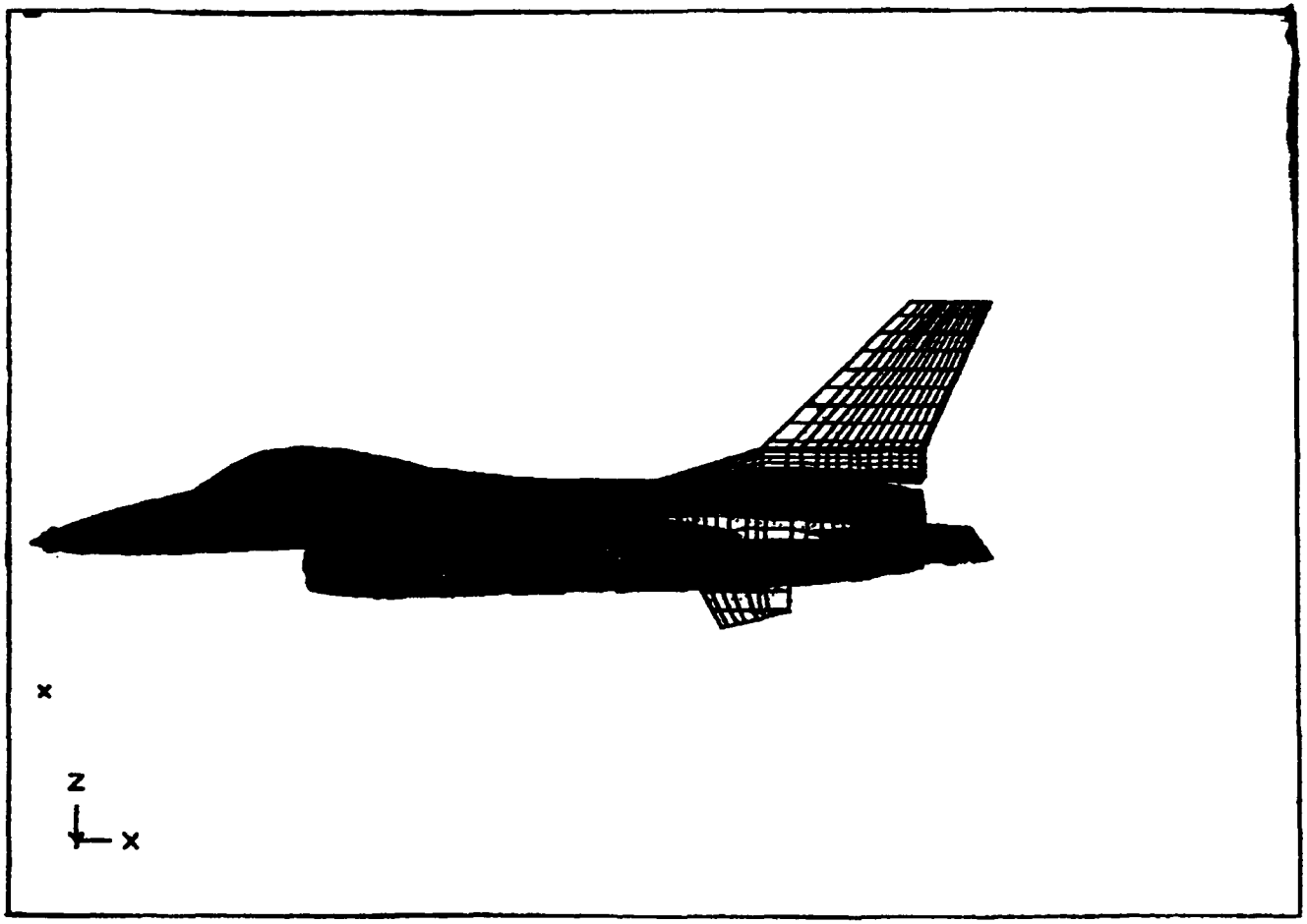

Figure 17. F-16 precise geometry employing panels from General Dynamics.

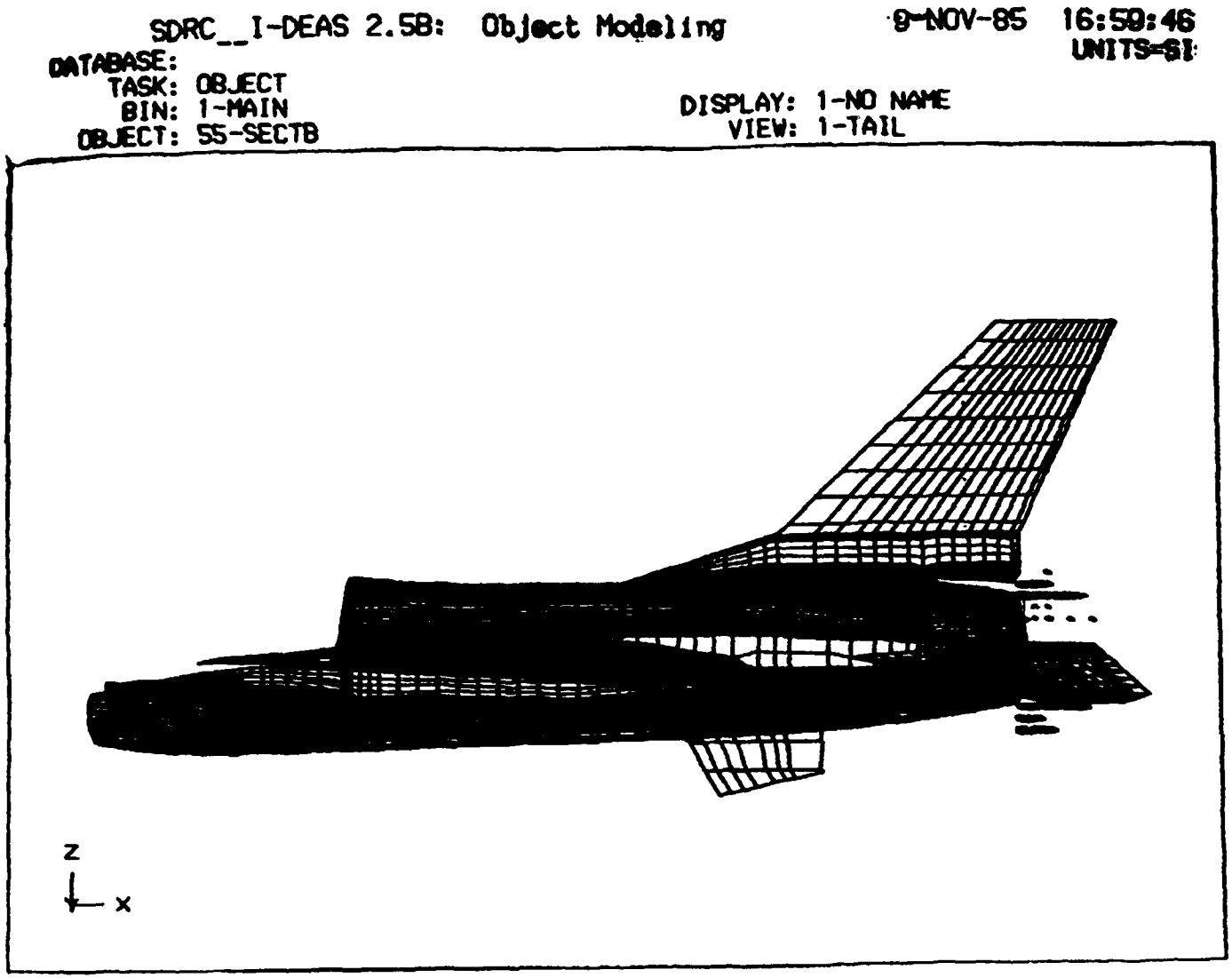

Figure 18. Panel description of the F-16 rear section.

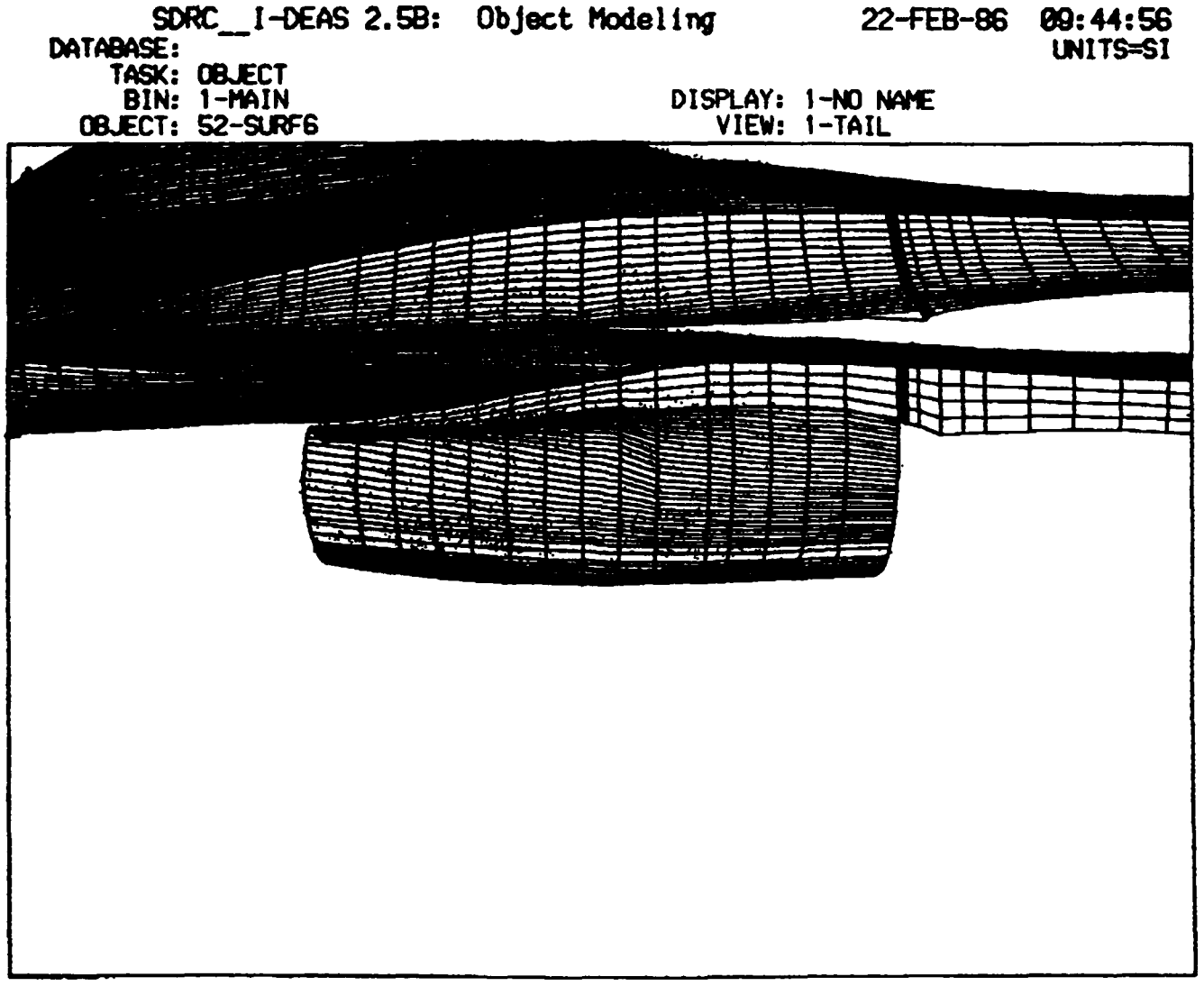

Figure 19. Detail of panel representation around engine inlet section.

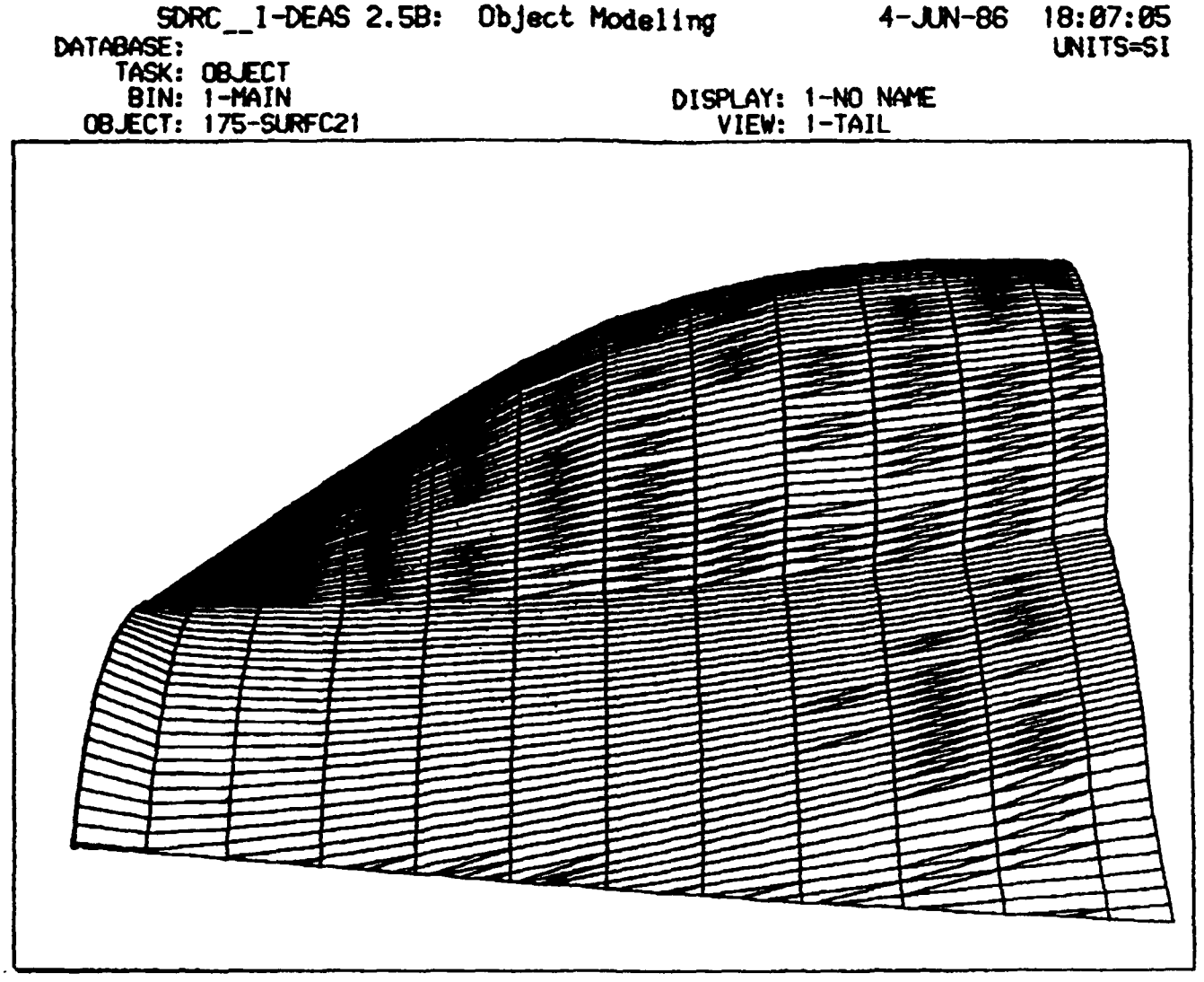

Figure 20. Geomod precise surface representation of the F-16 canopy section from panel data.

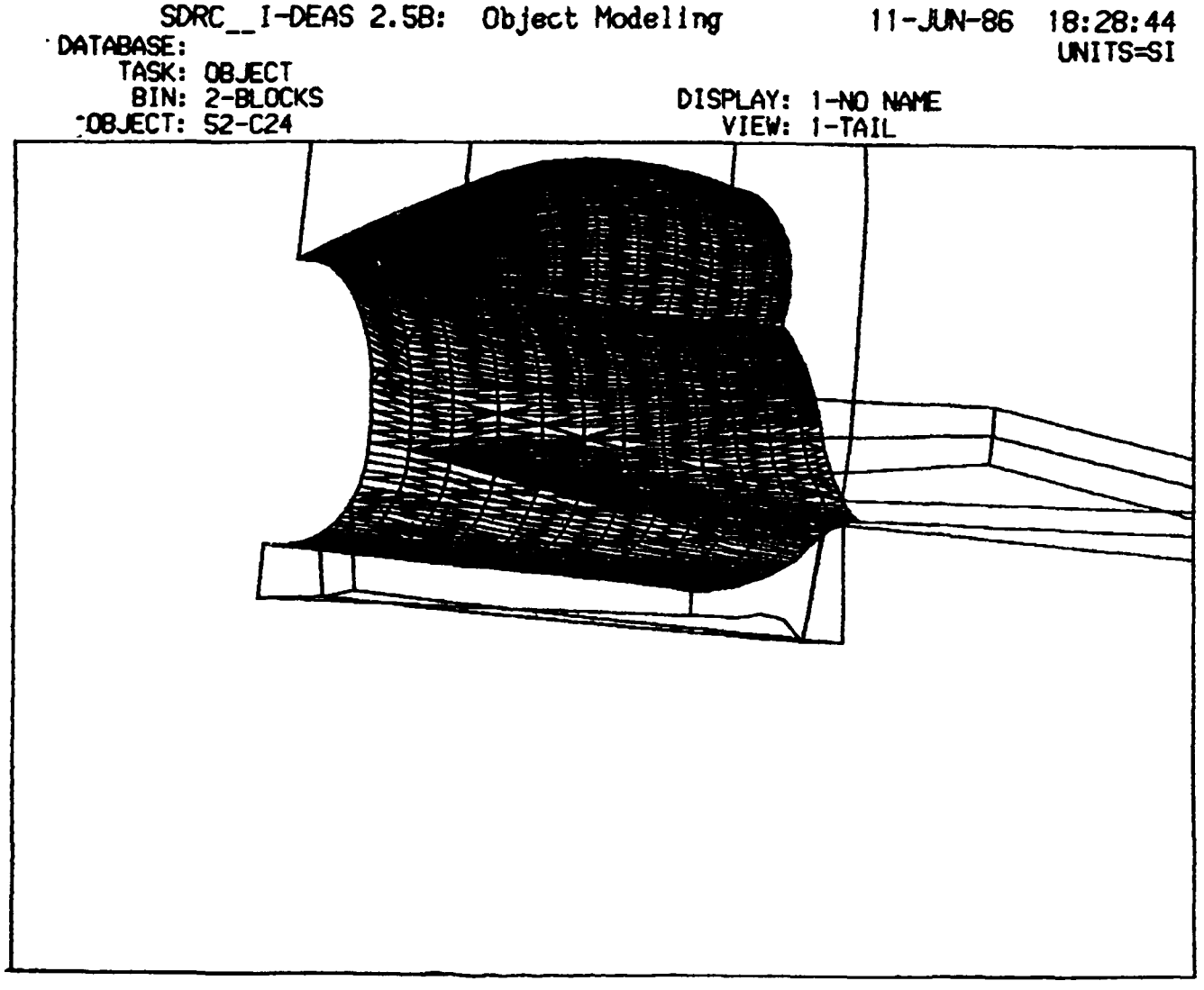

Figure 21. Blocks around the canopy section.

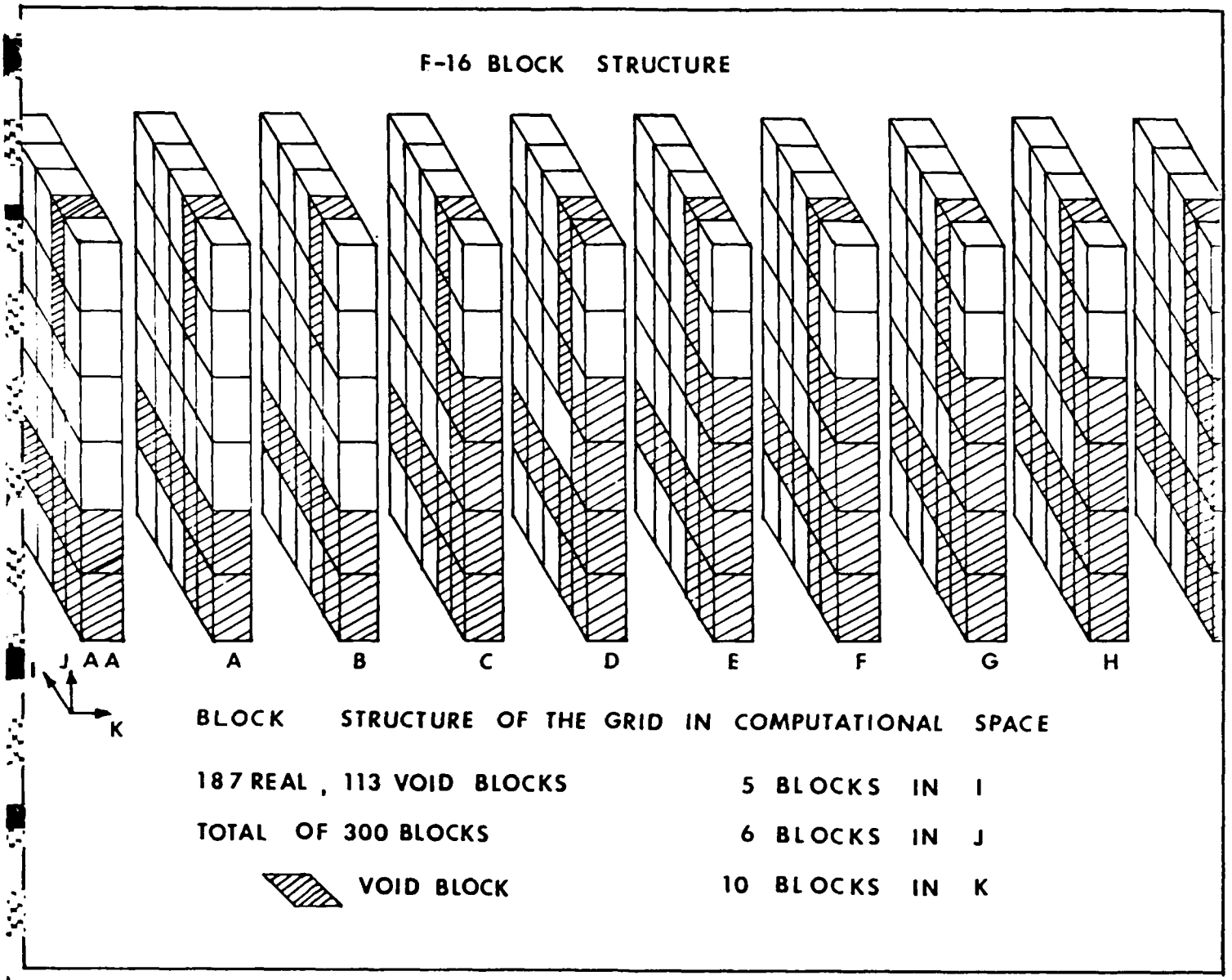

Figure 22. F-16 block-structure in the computational space.

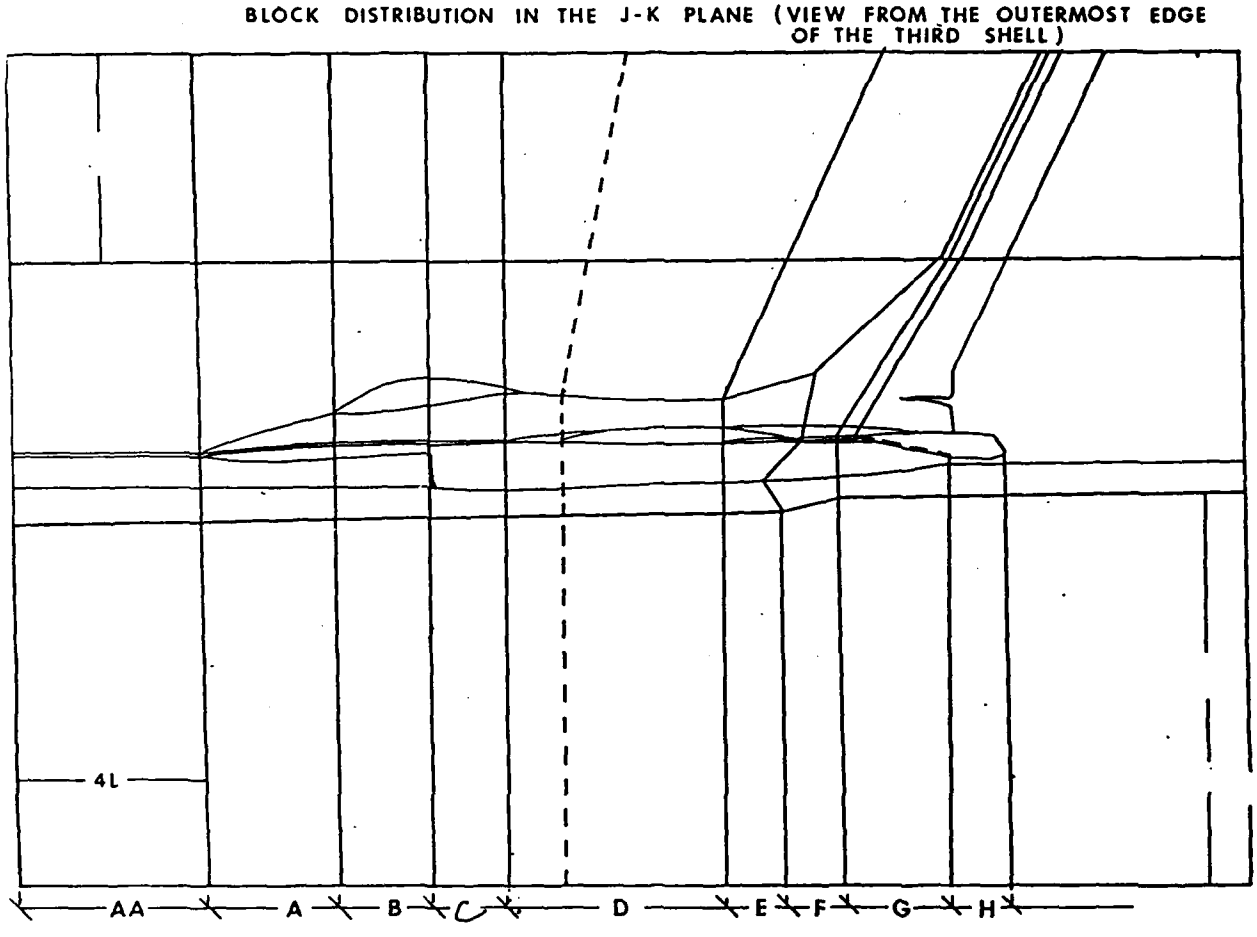

Figure 23. Cross-section of the F-16 block-structure employing H-type grids around nose and wing sections.

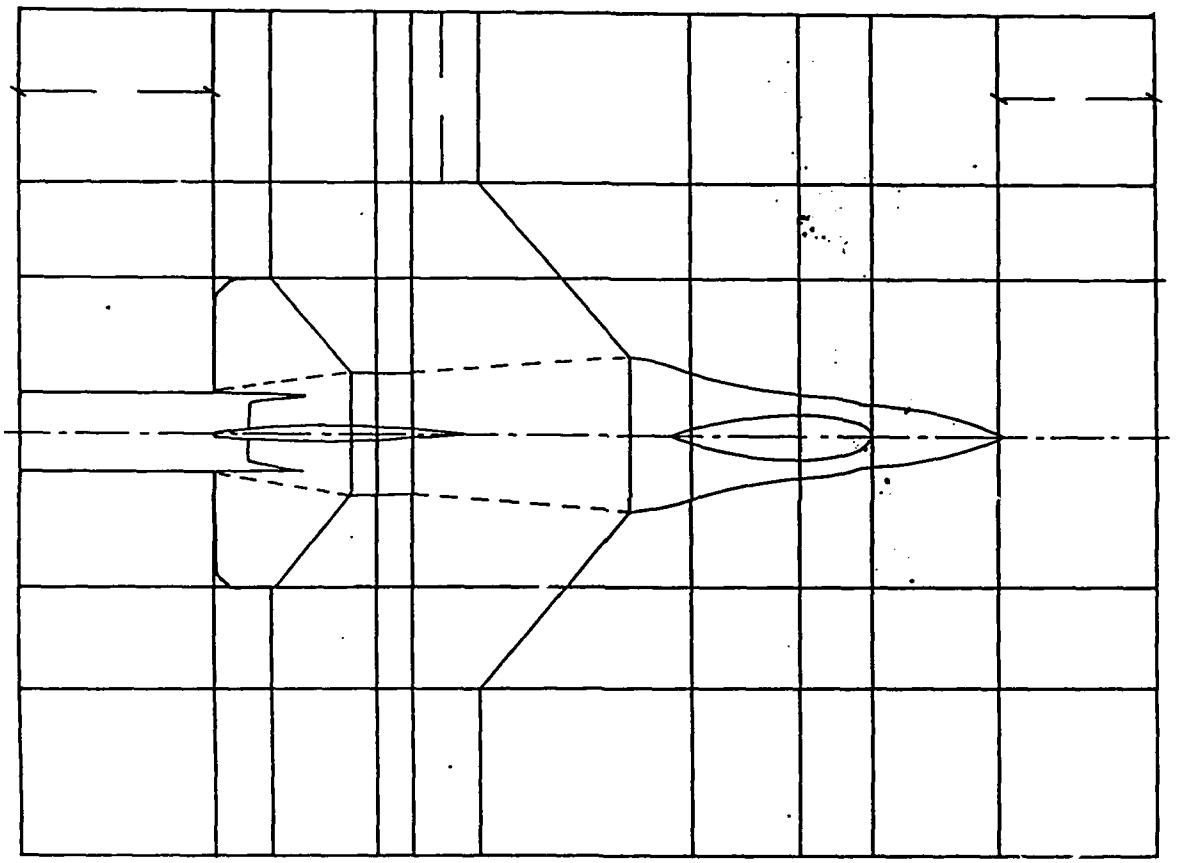

Figure 24. Top view of the F-16 block-structure employing H-type grids around the nose and wing sections.

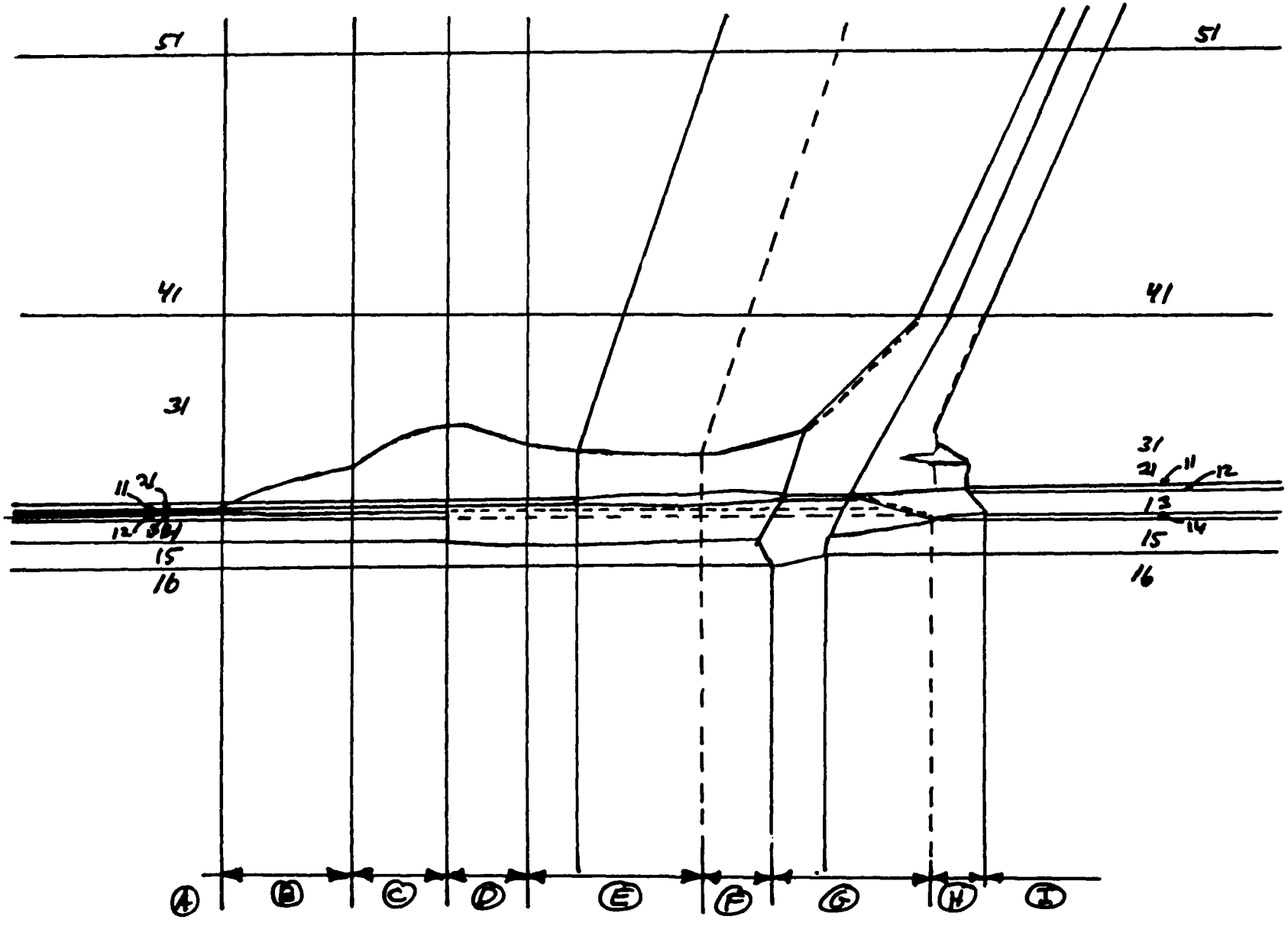

Figure 23. Cross-section of the F-16 block-structure employing H-type grids around nose and wing sections.

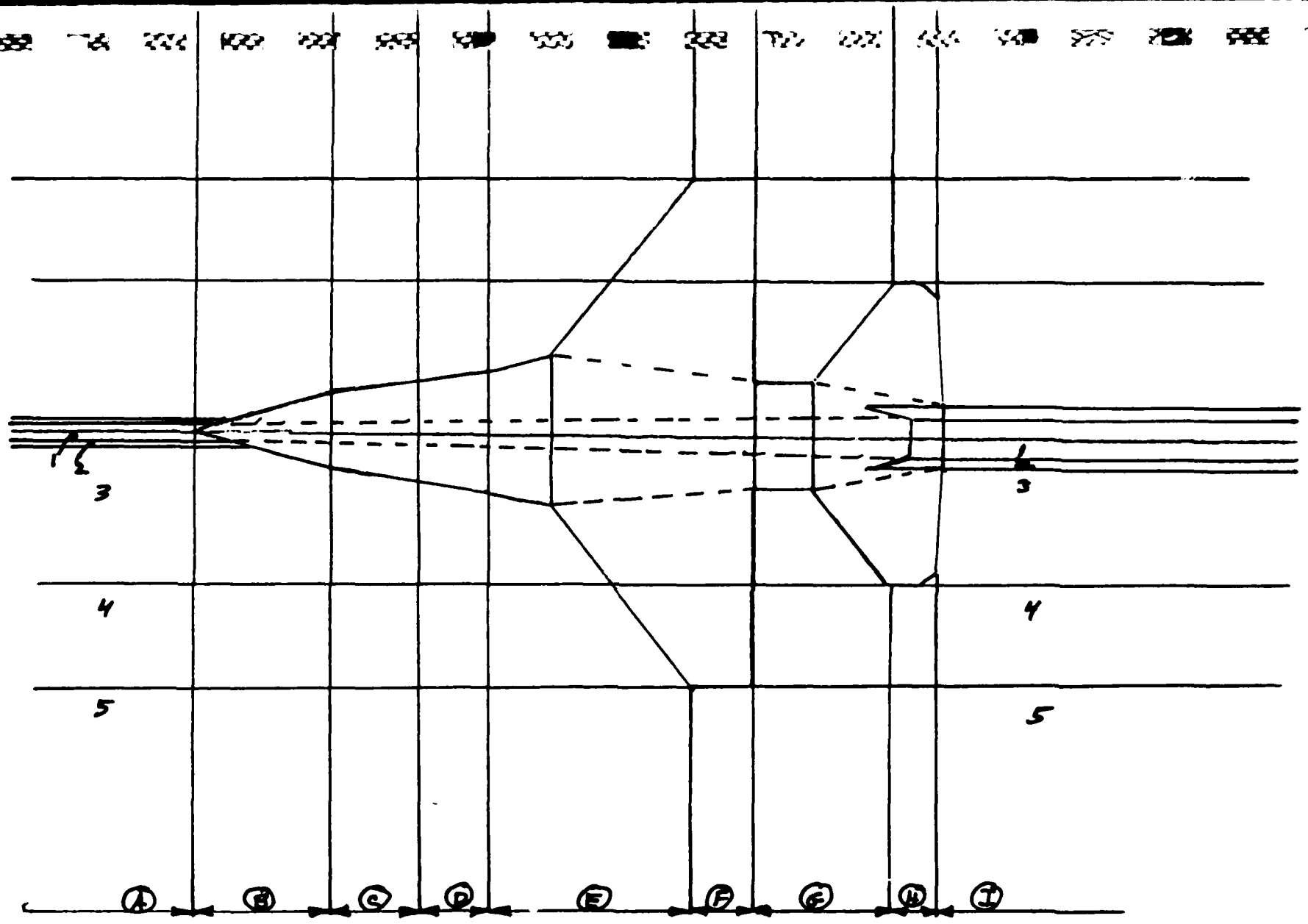

Figure 24. Top view of the F-16 block-structure employing H-type grids around the nose and wing sections.

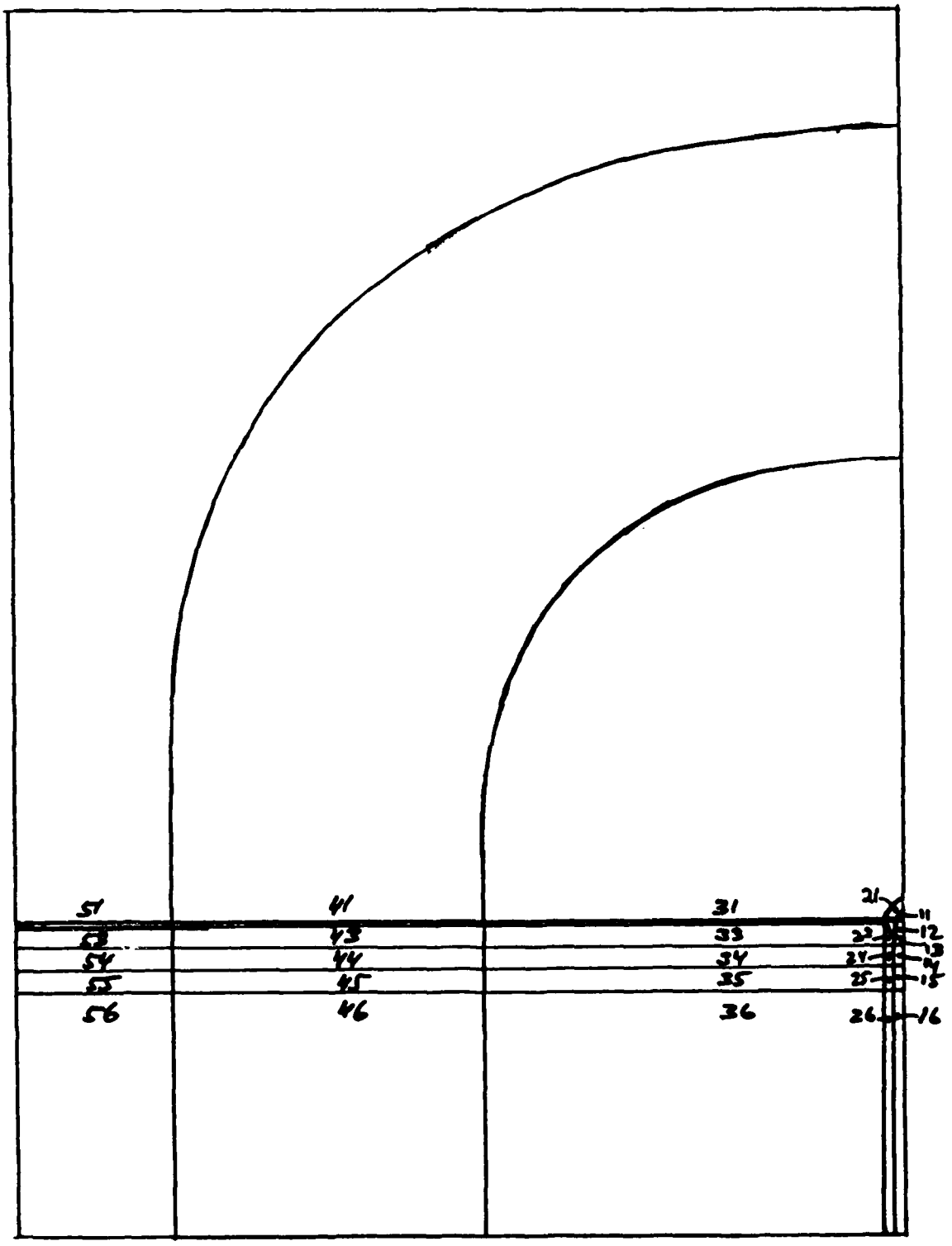

Figure 25. Block-structure at section x = 0.0" (tip of nose).

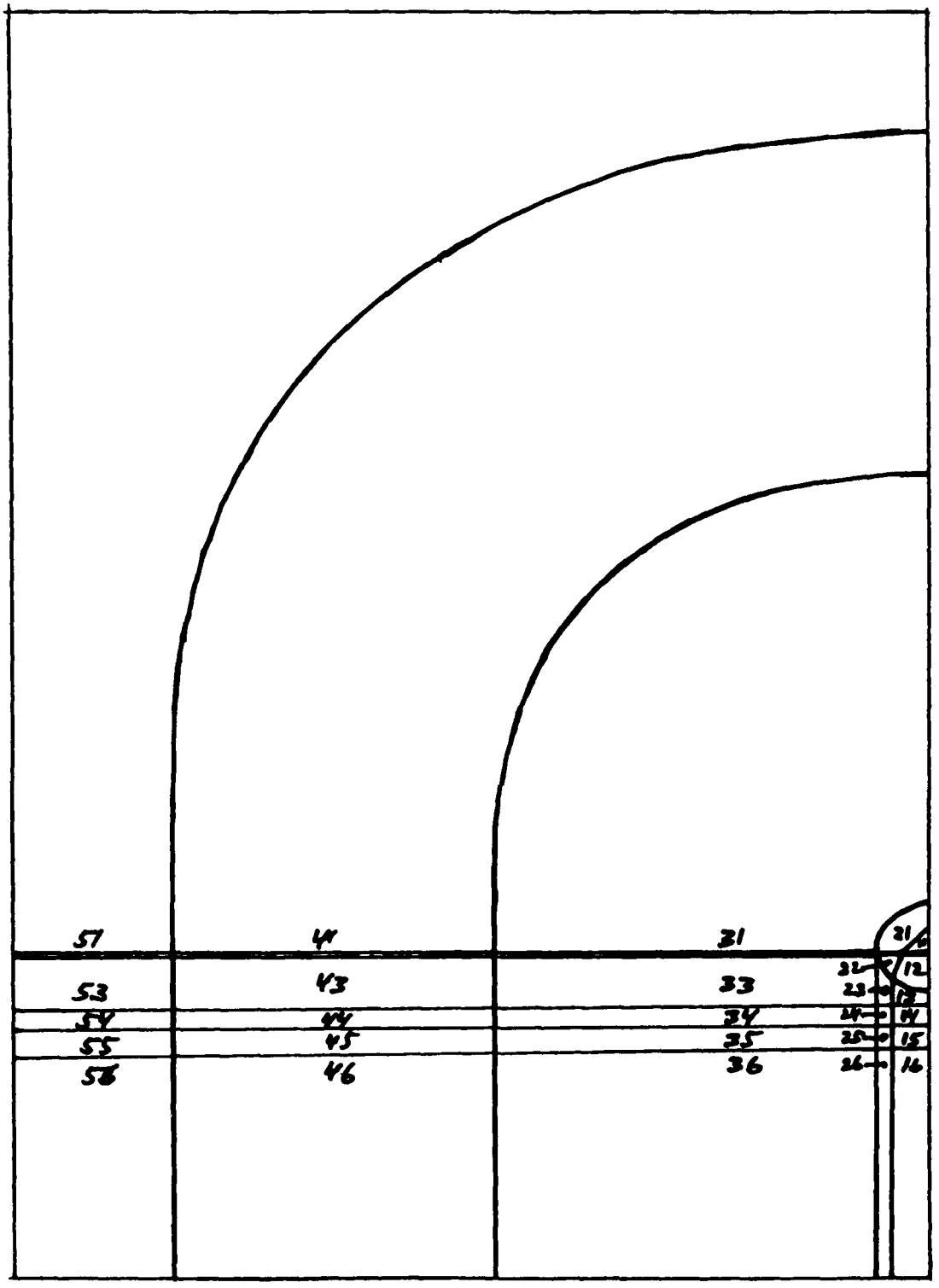

Figure 26. Block-structure at section x = 89.5" (canopy begins).

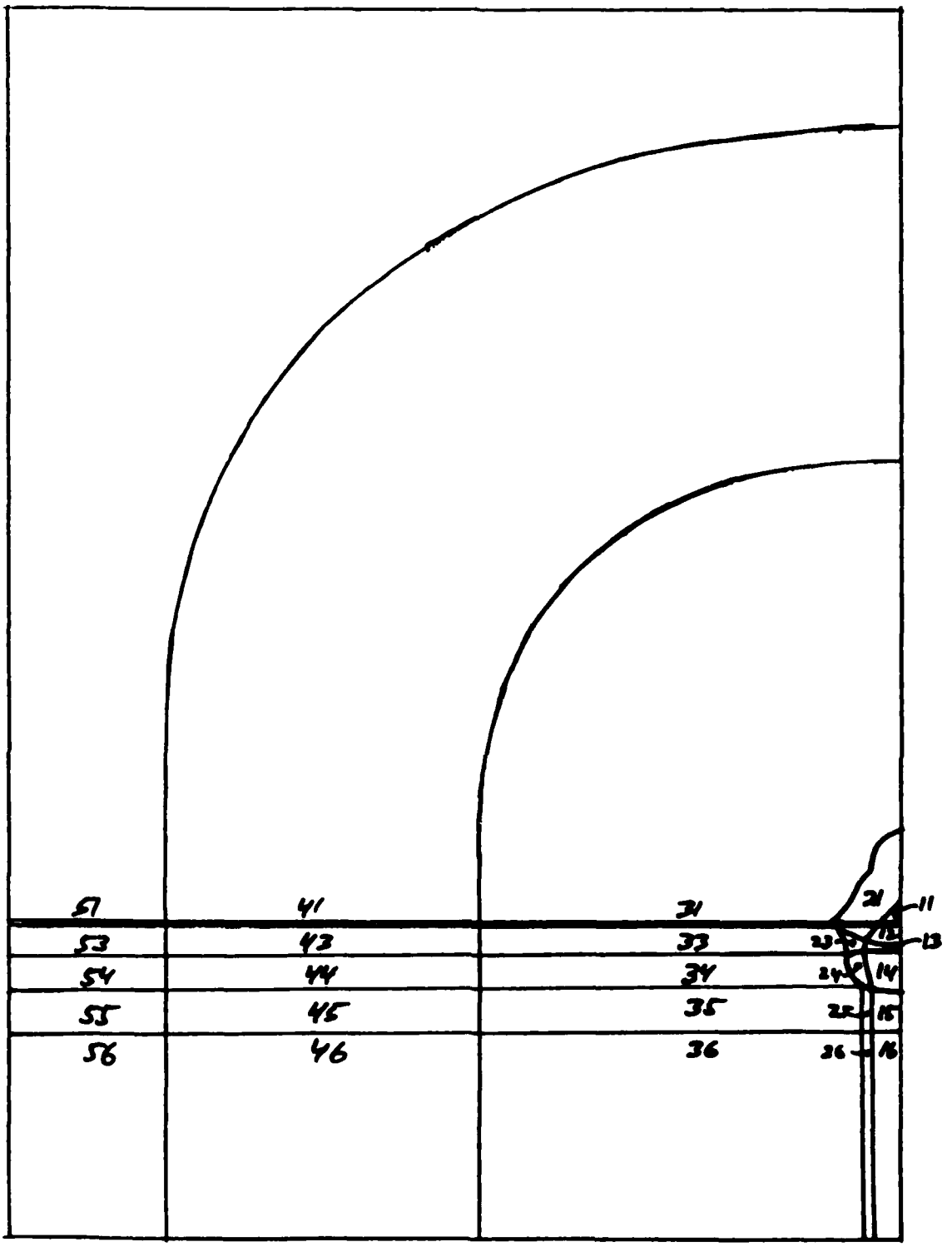

Figure 27. Block-structure at section x = 160" (intake begins).

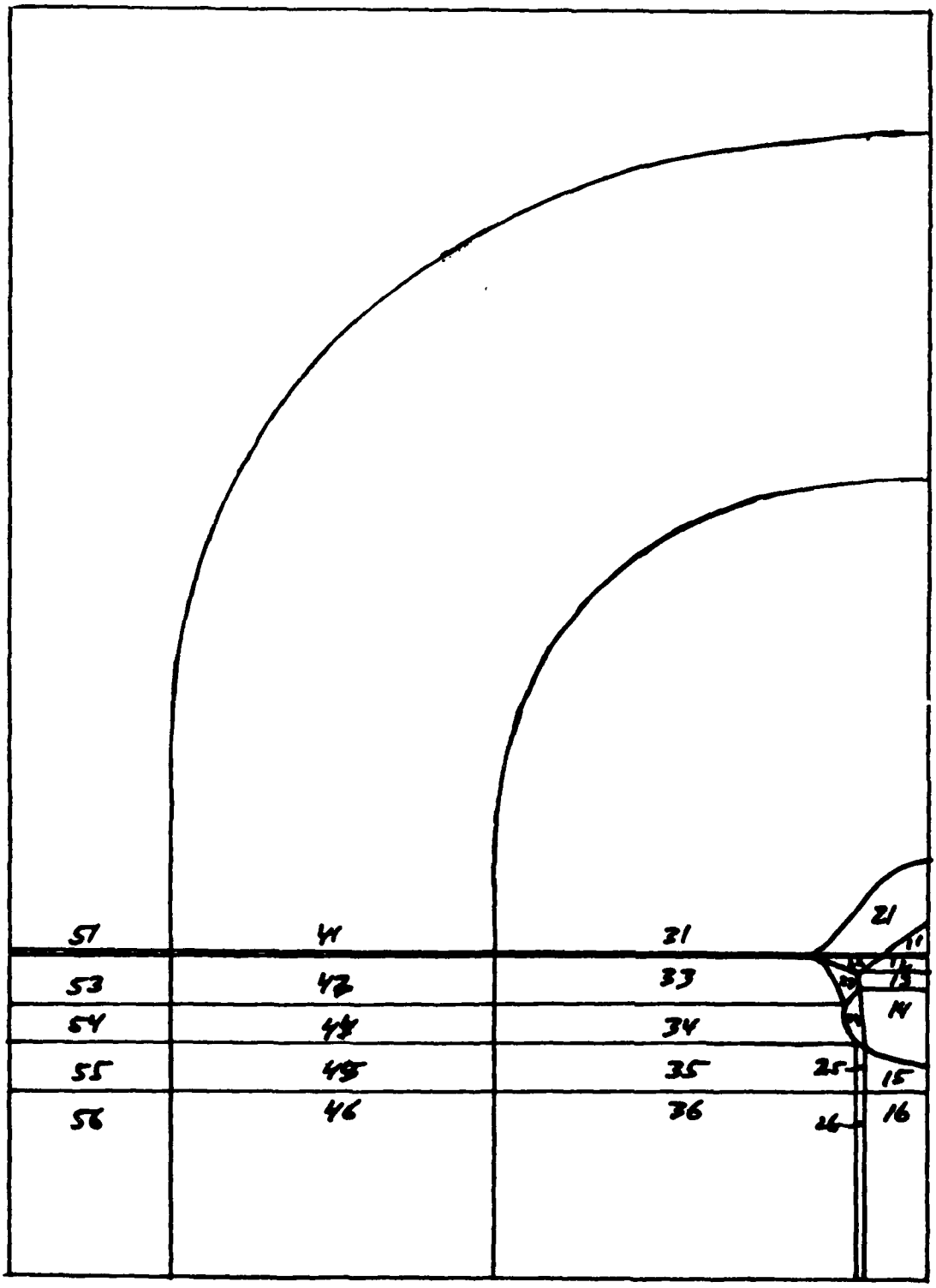

Figure 28. Block-structure at section x = 219.75" (intake notch).

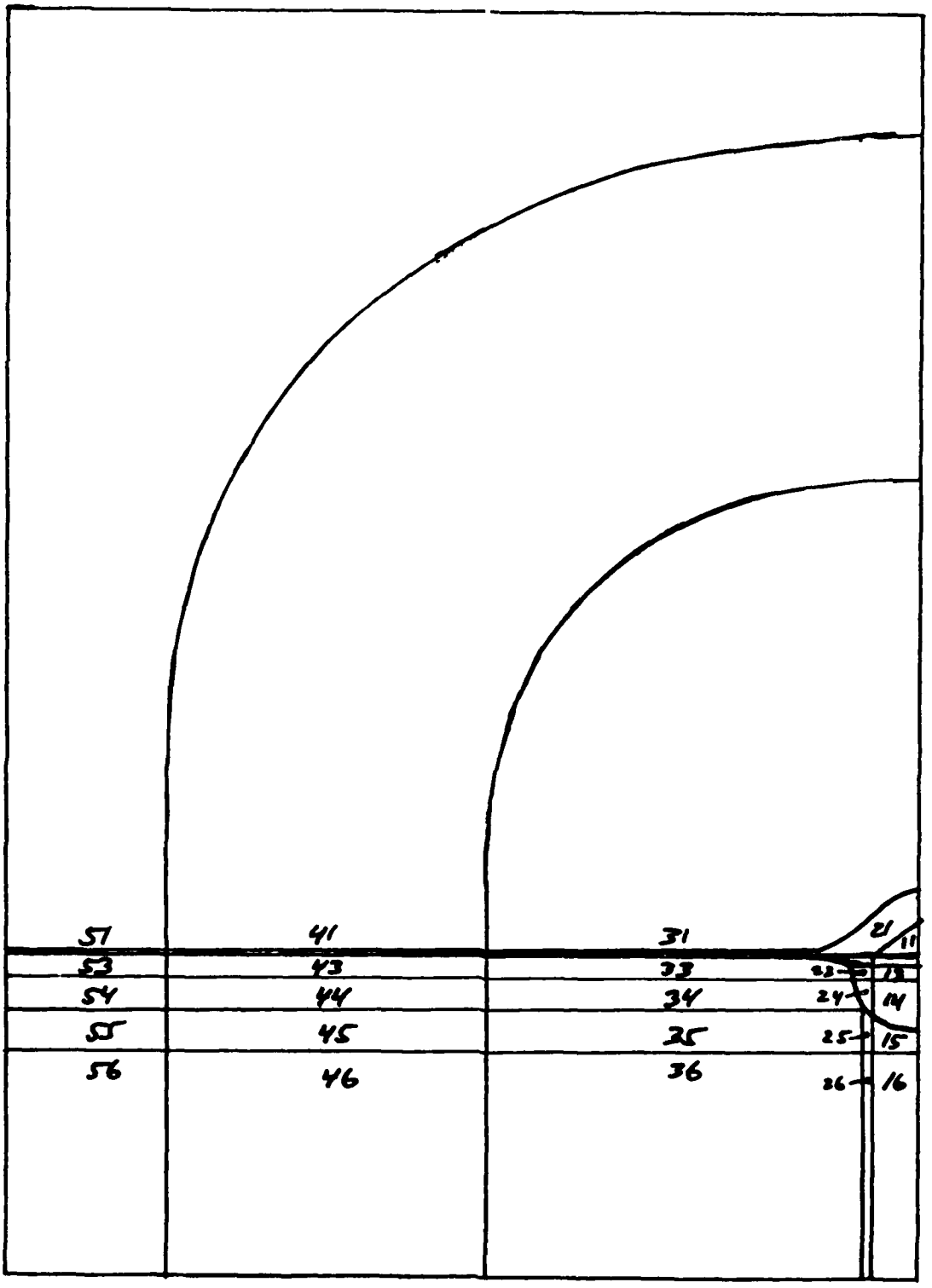

Figure 29. Block-structure at section x = 259.5" (front wing begins).

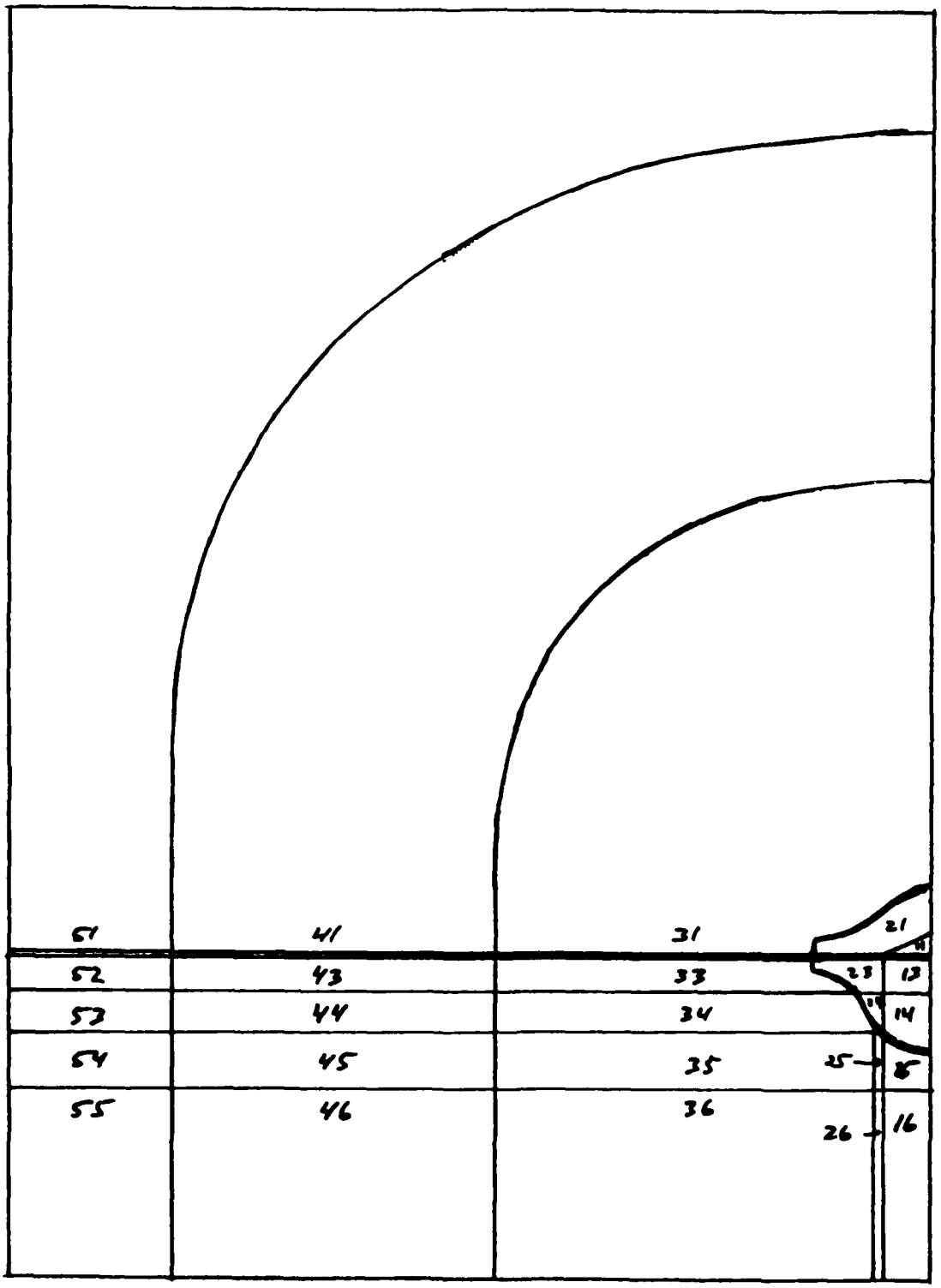

Figure 30. Block-structure at section x = 389" (fin begins).

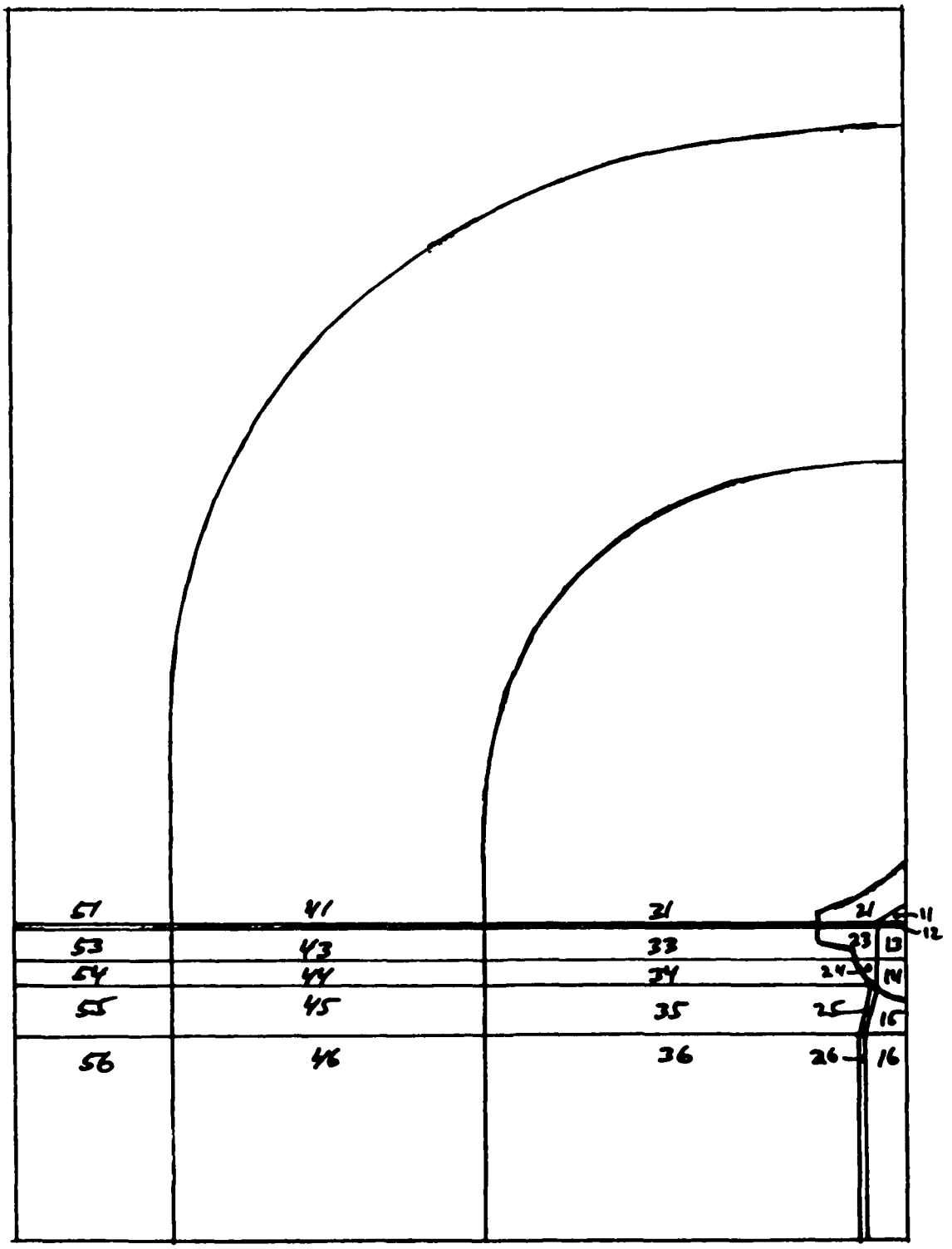

Figure 31. Block-structure at section x = 409" (wing trailing edge).

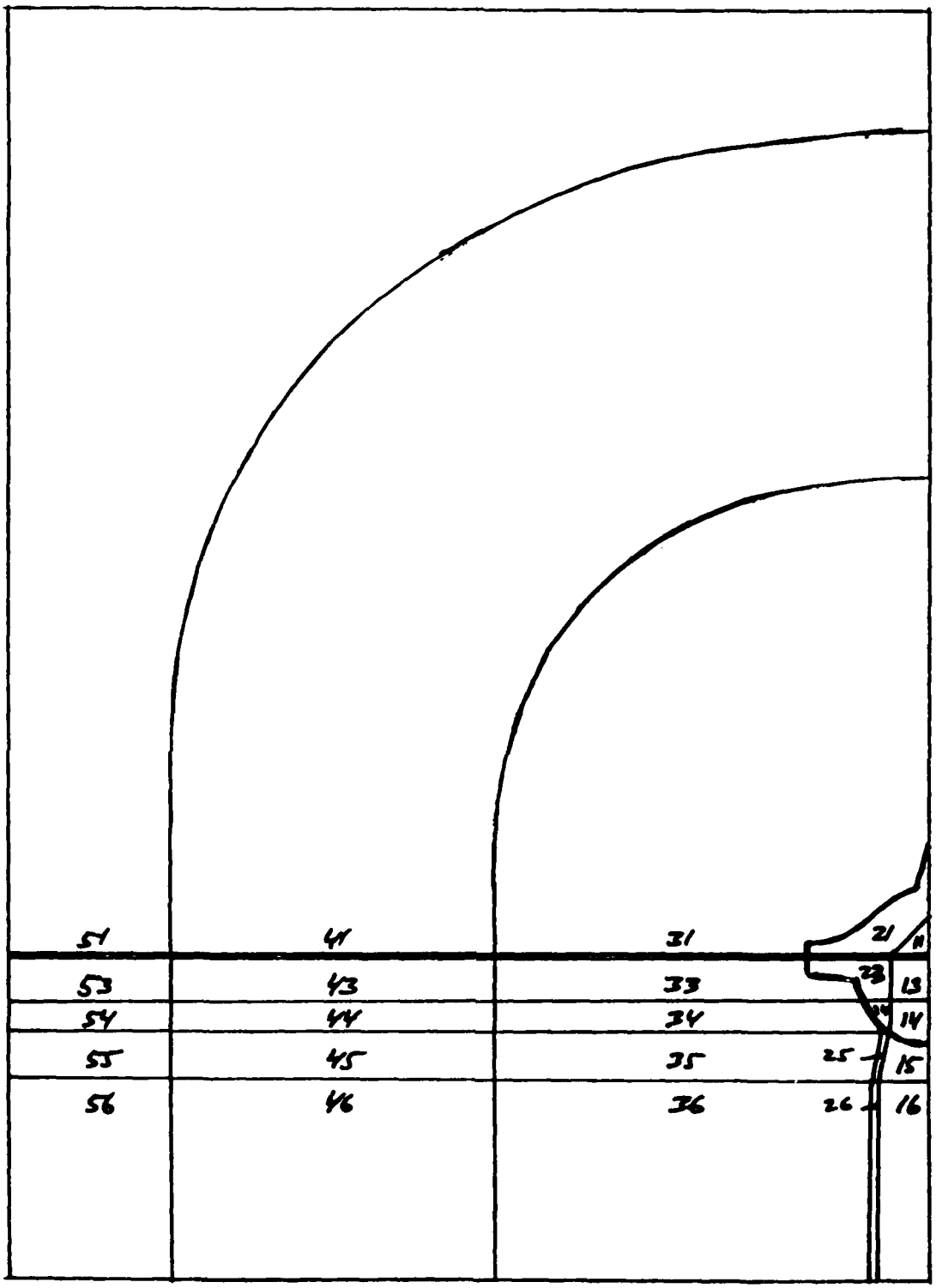

Figure 32. Block-structure at section x = 430" (tail starts).

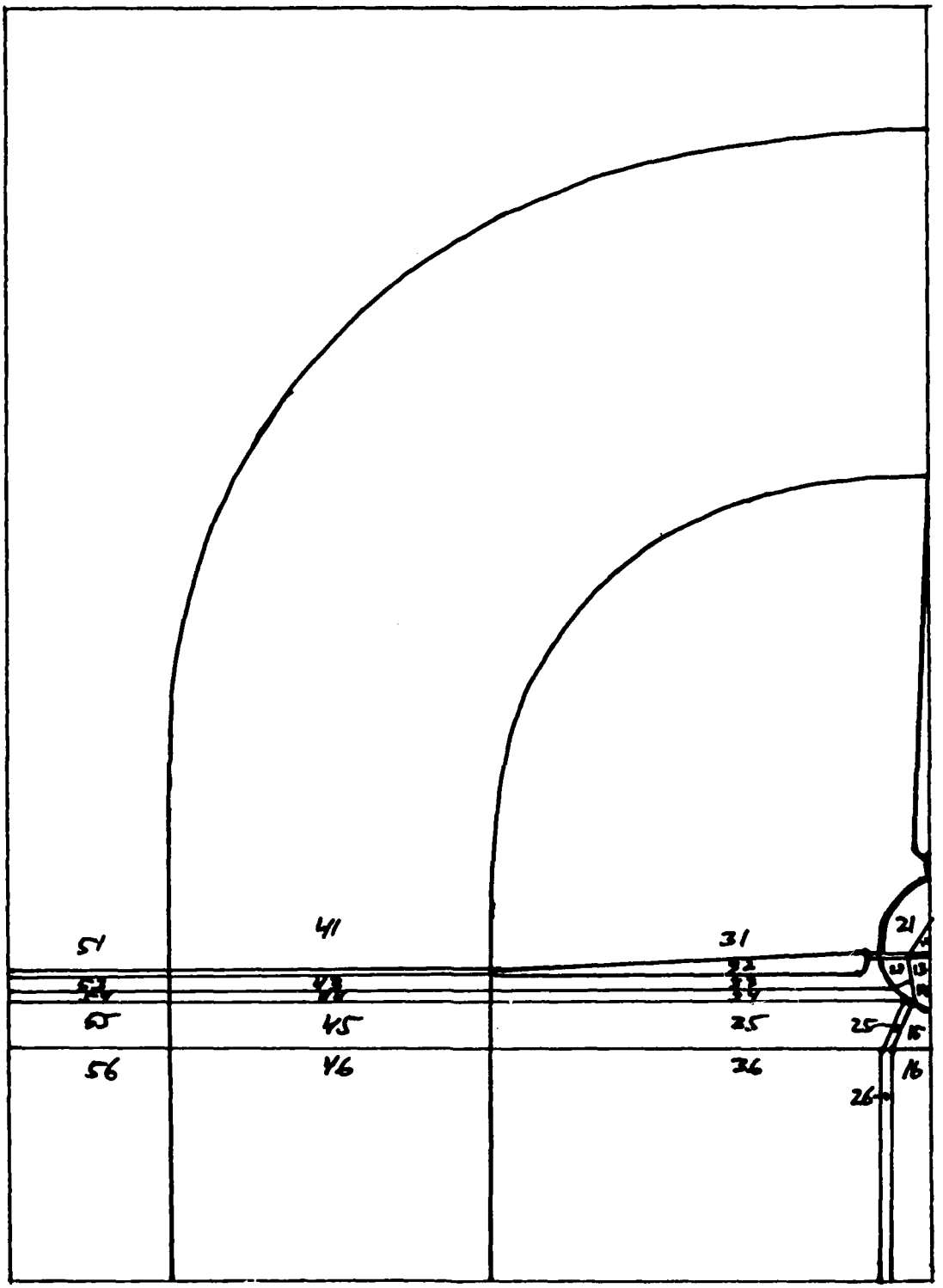

Figure 33. Block-structure at section x = 530" (through r. wing and tail).

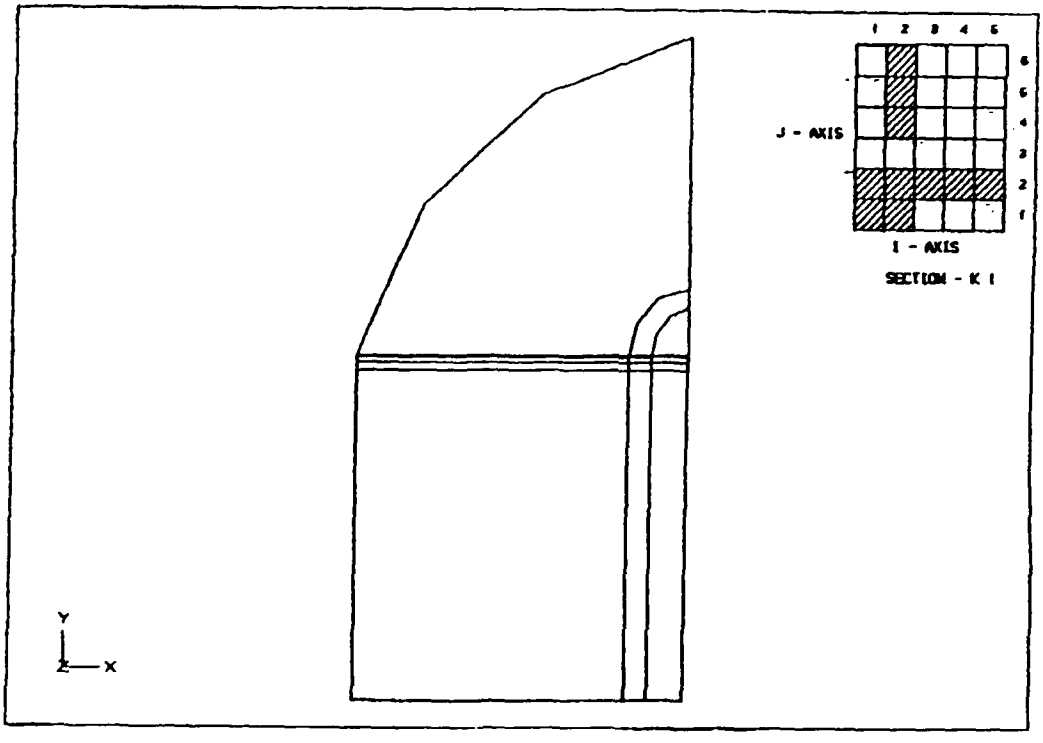

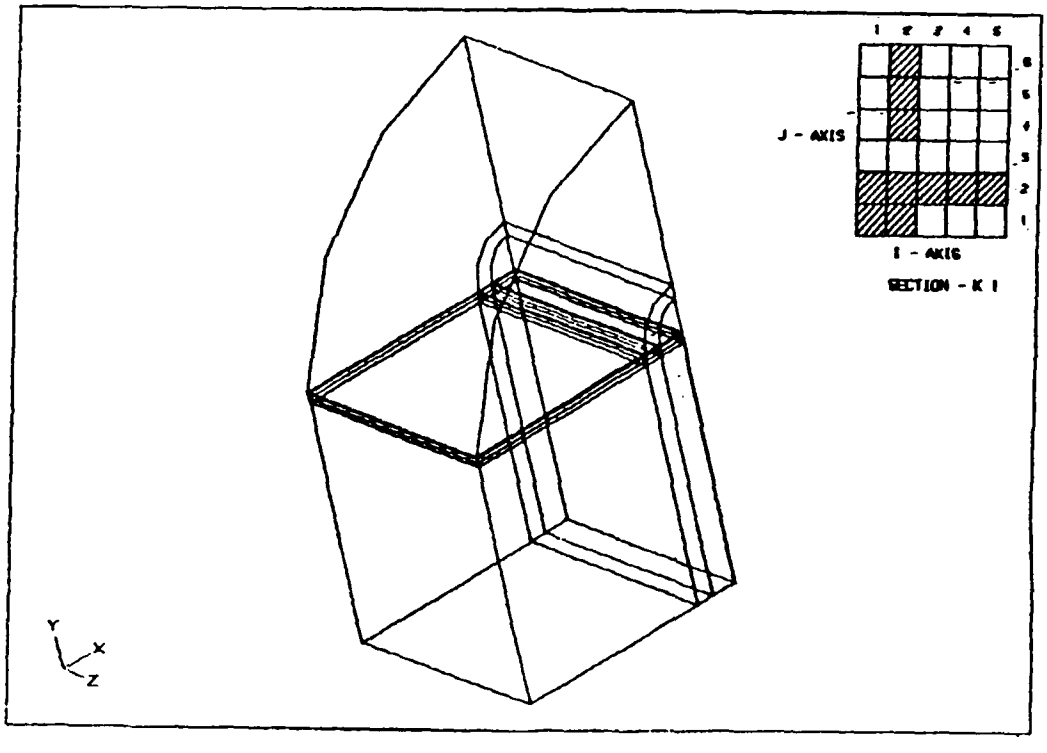

Figure 34. Generation of blocks from one section of the flow field.

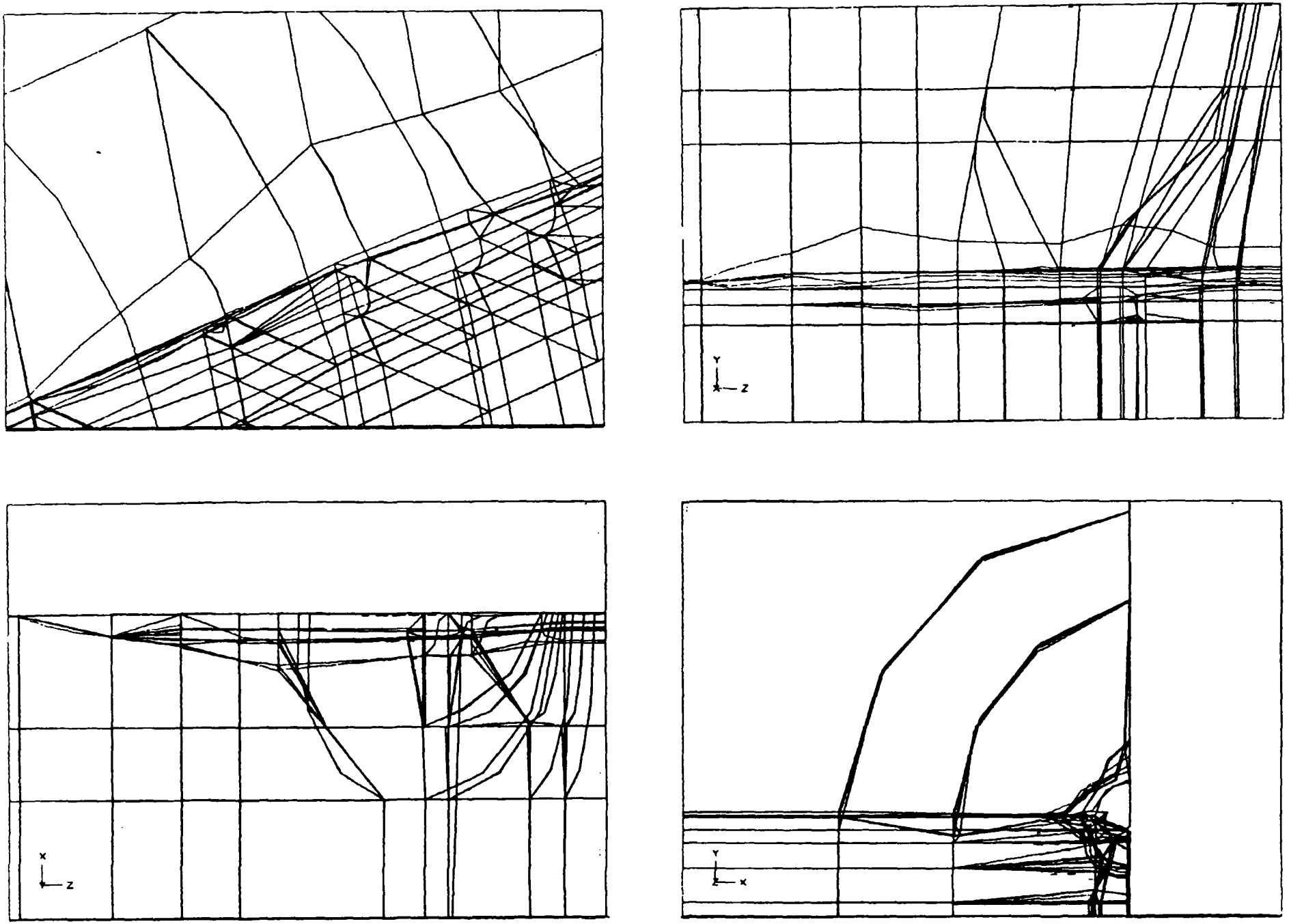

Figure 35. Details of the block-structure around the engine inlet.

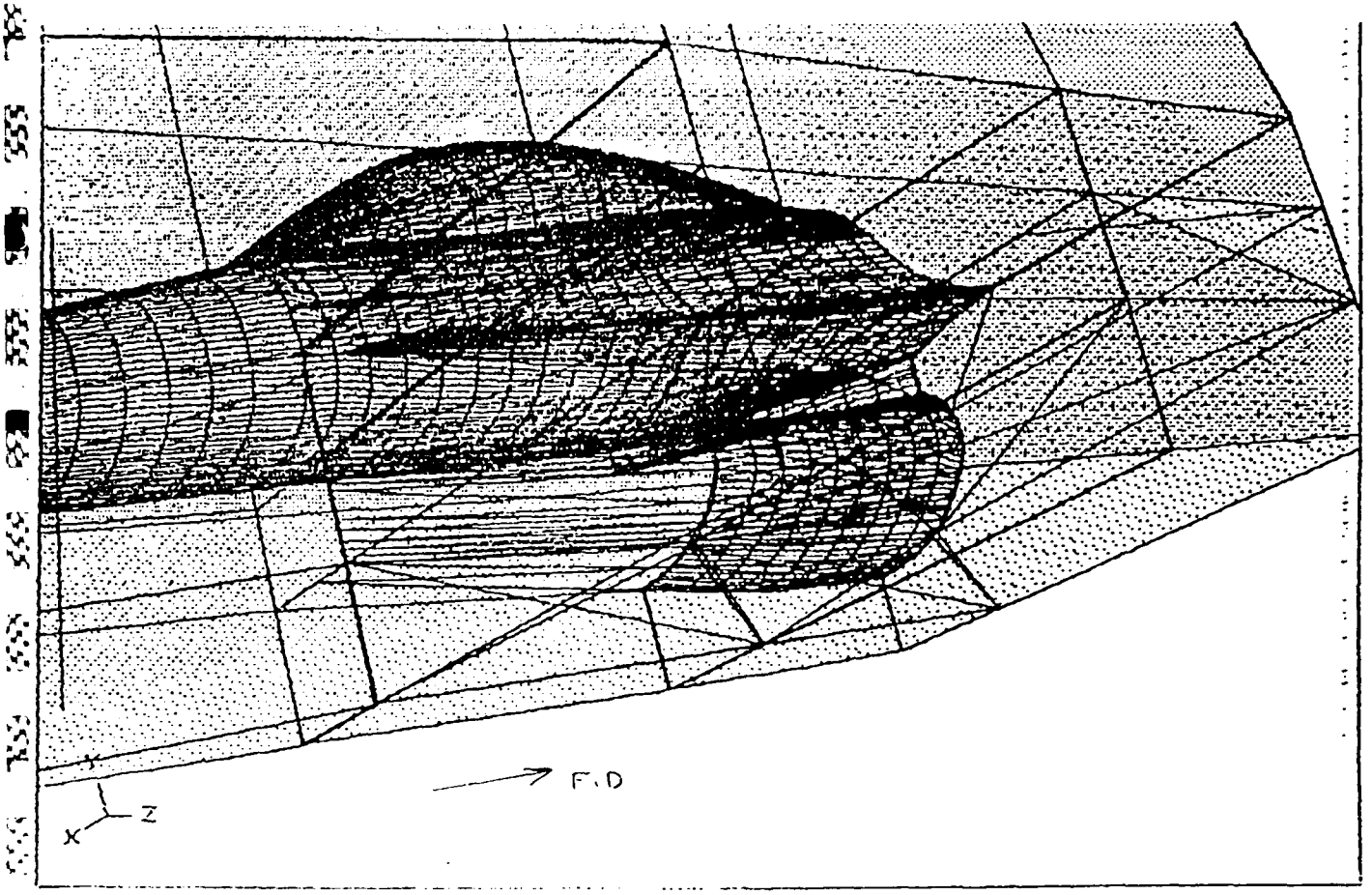

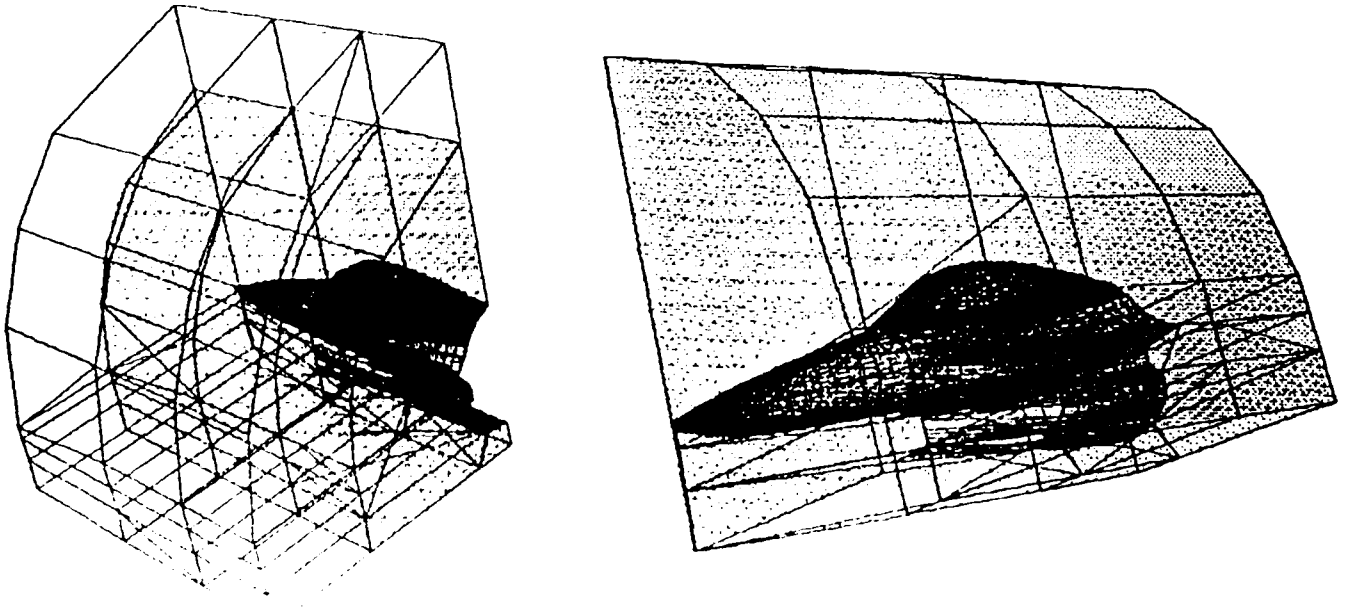

Figure 36. Details of the block-structure around the tail.

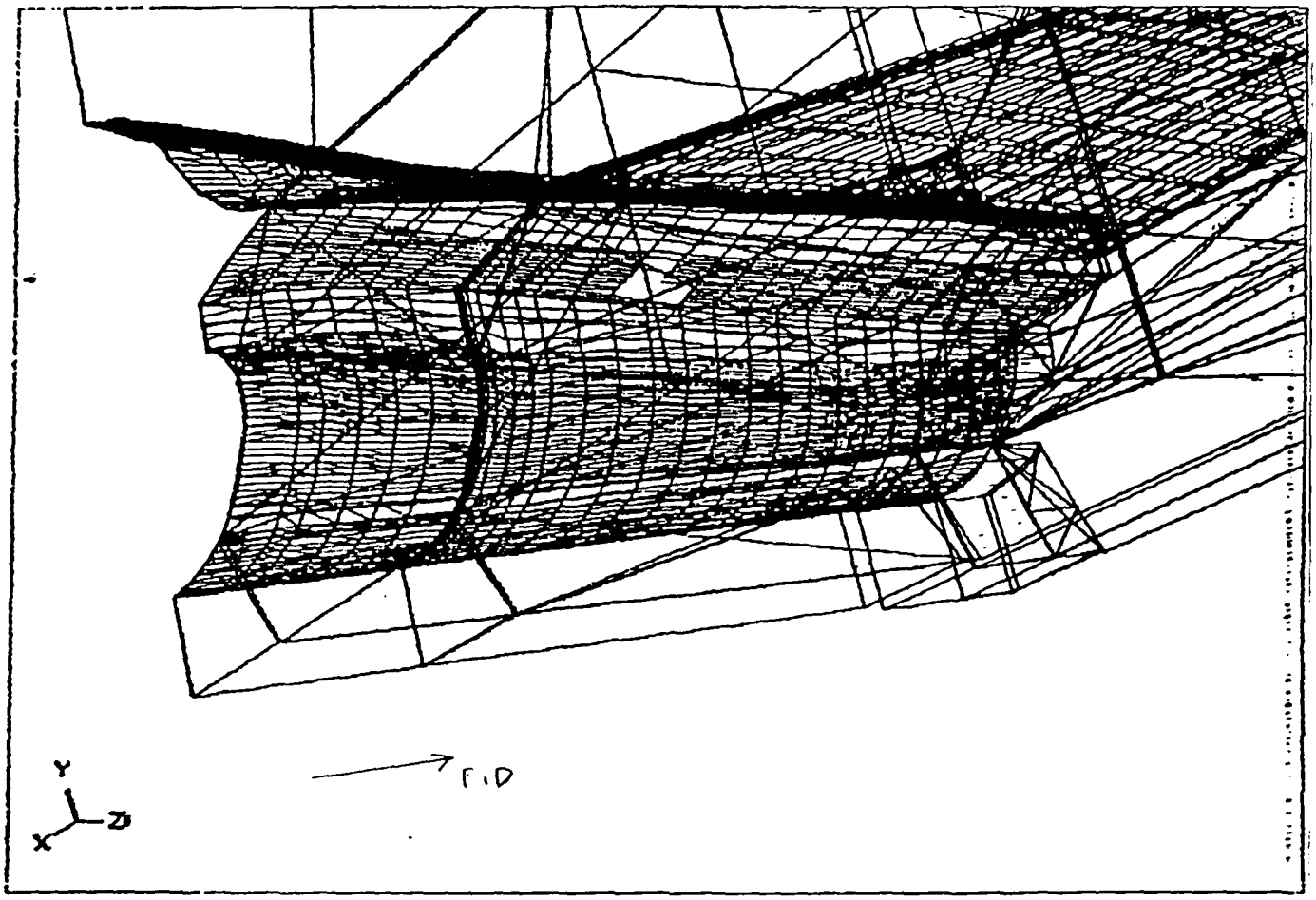

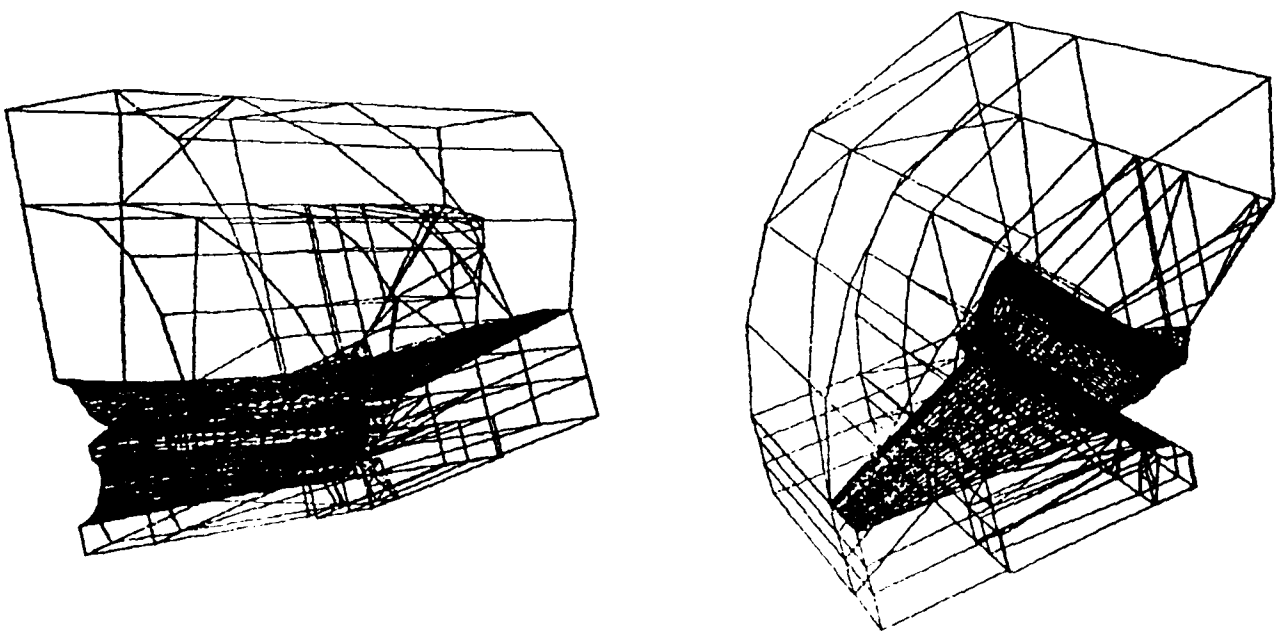

Figure 36 continued. Details of the block-structure around the tail.

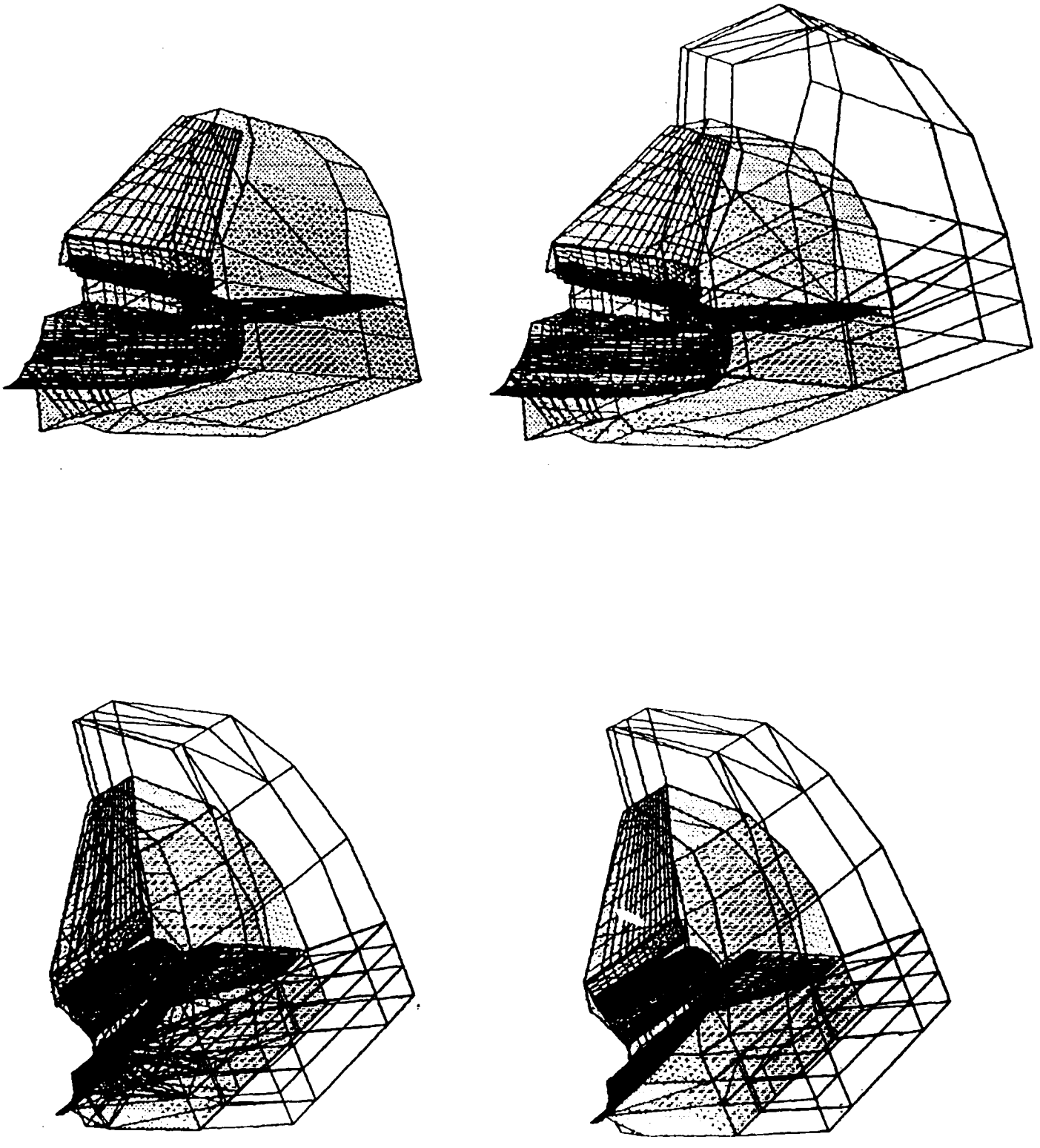

Figure 36 continued. Details of the block-structure around the tail.

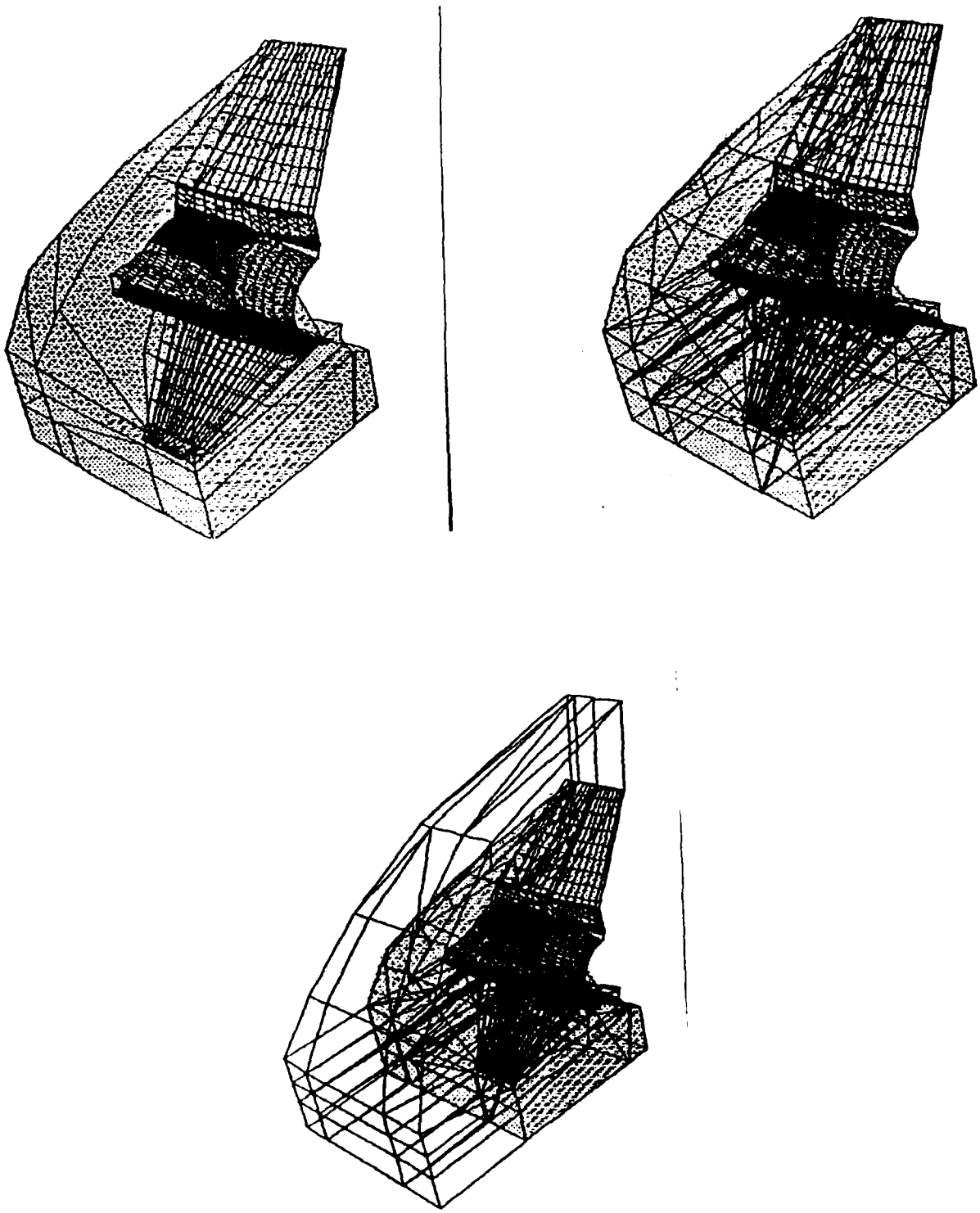

Figure 36 continued. Details of the block-structure around the tail.

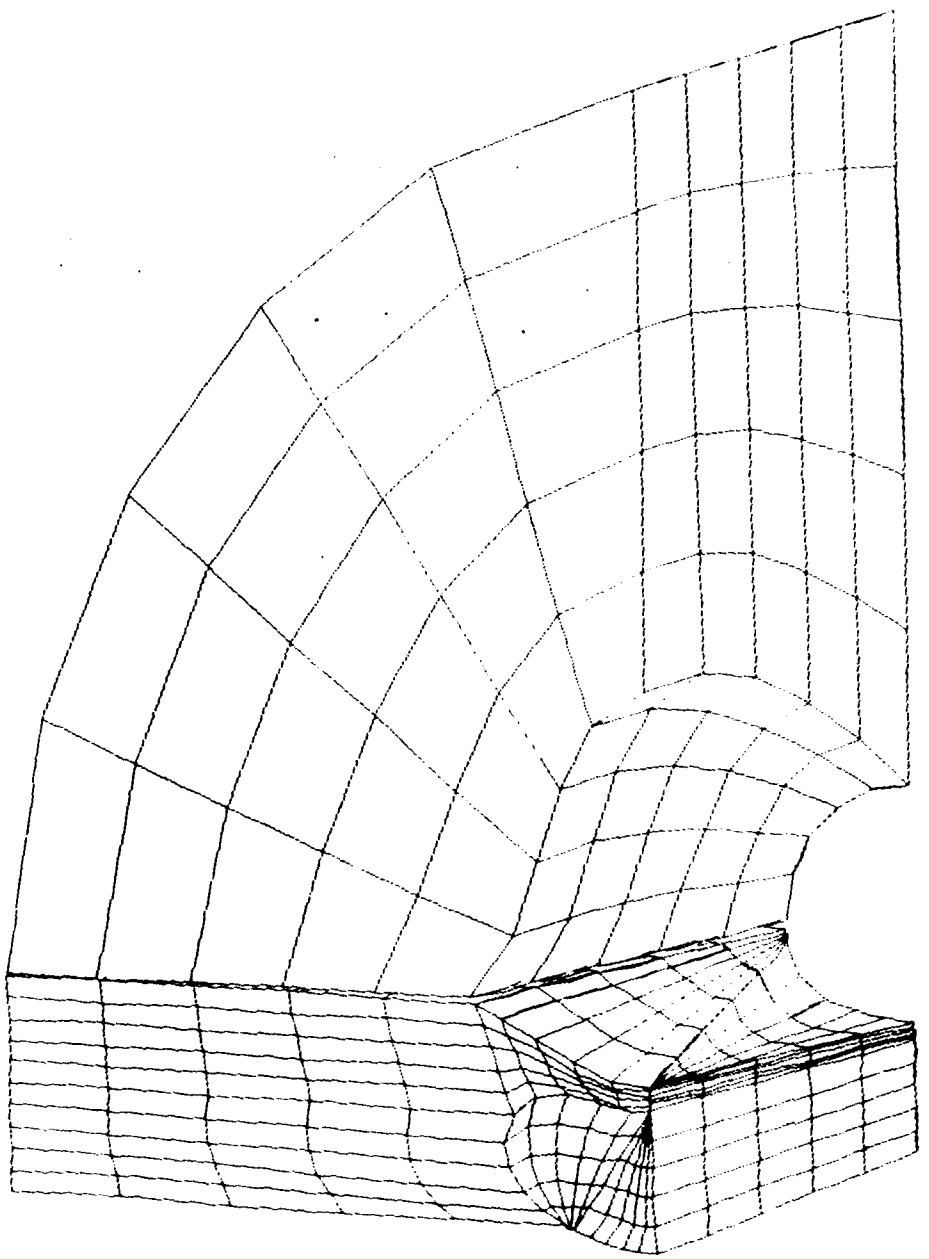

Figure 37. Details of the mesh around the canopy (A coarse mesh to demonstrate the grid topology).

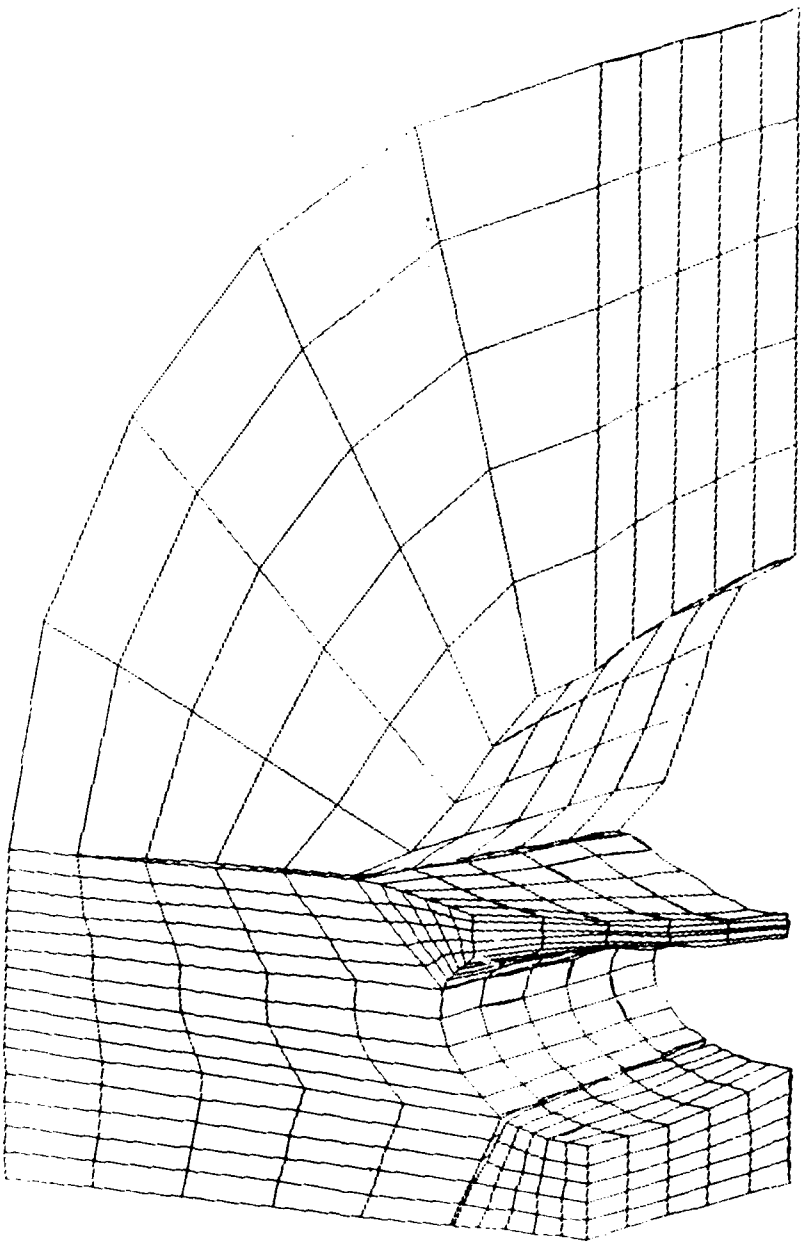

Figure 38. Details of the mesh around the engine intake (A coarse mesh to demonstrate the grid topology).

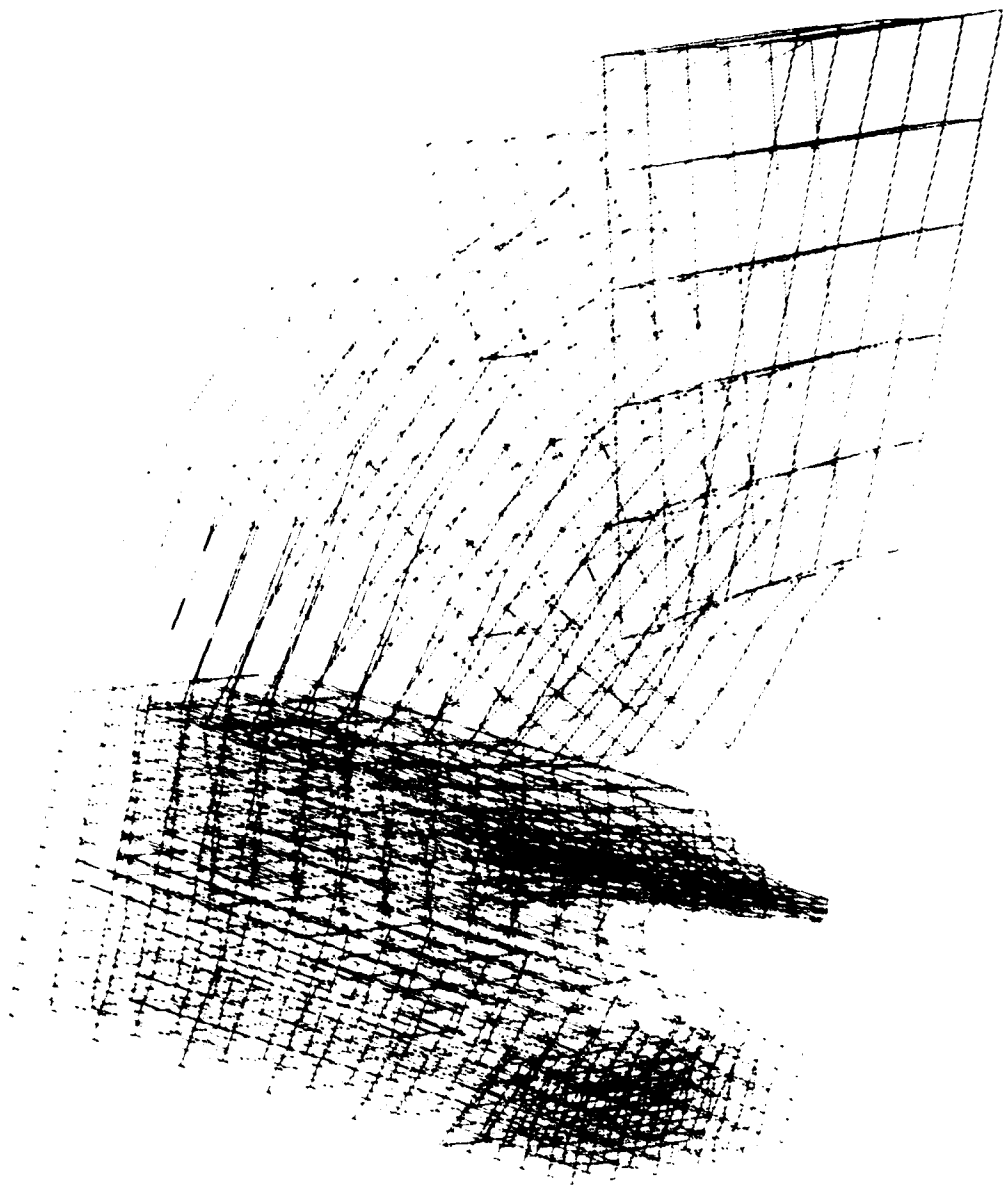

Figure 38 continued. Details of the mesh around the engine inlet
(A coarse mesh to demonstrate the grid topology).

APPENDIX D

GRID GENERATION FOR FLOW AROUND A CAR BODY

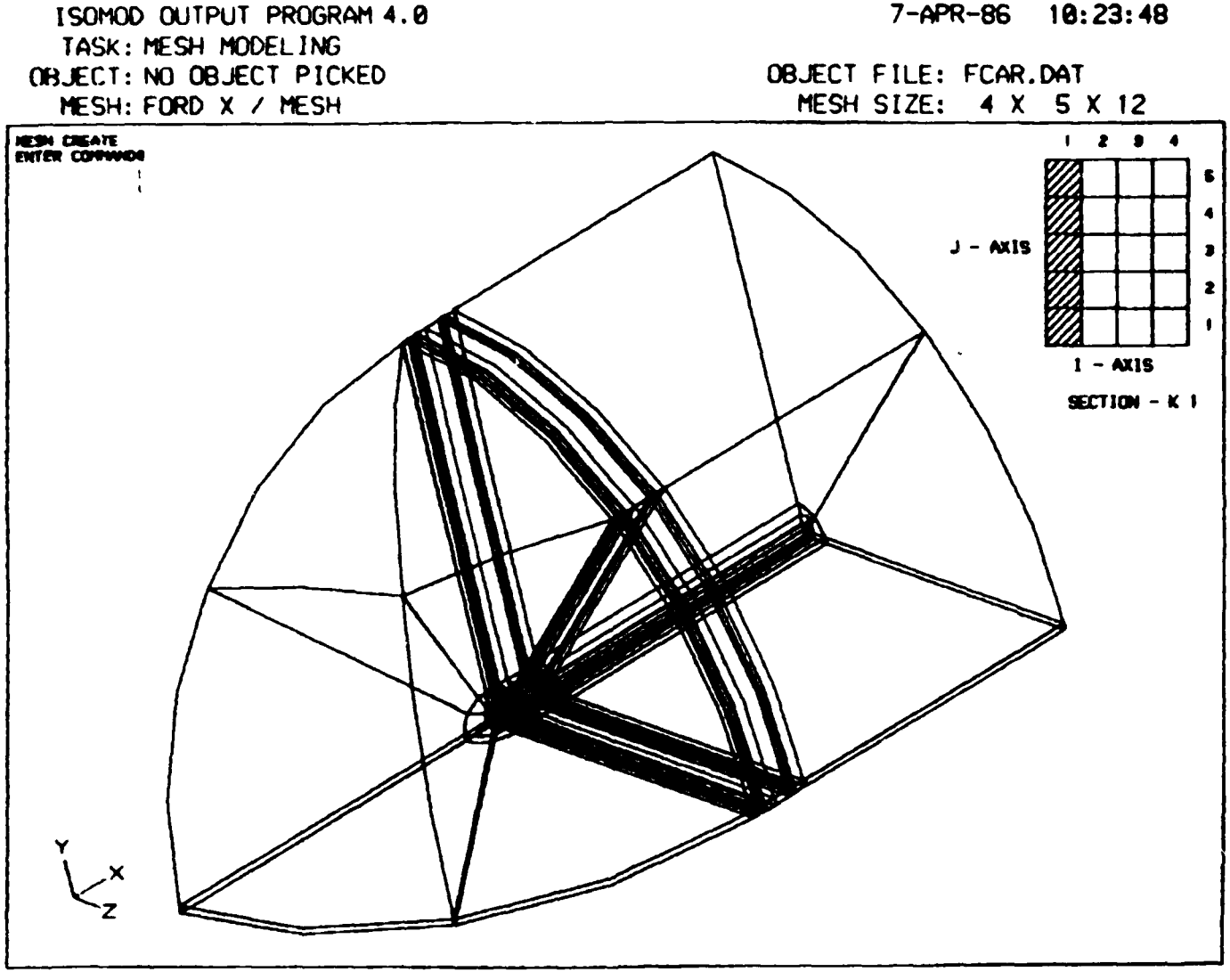

Figure 39. Block-structure around car geometry employing 180 blocks.

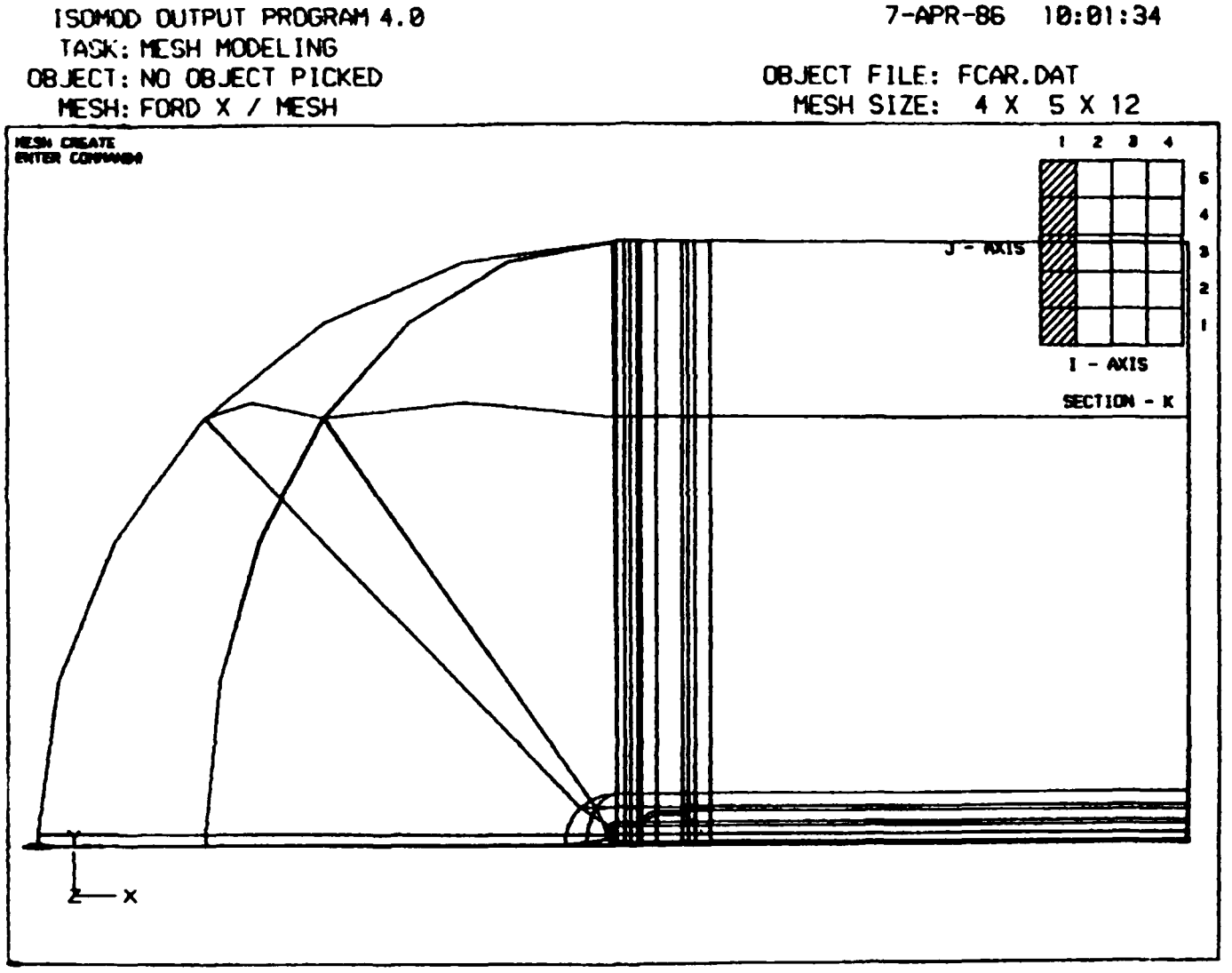

Figure 40. Side-view of the block-structure around car geometry for c-type grids around nose.

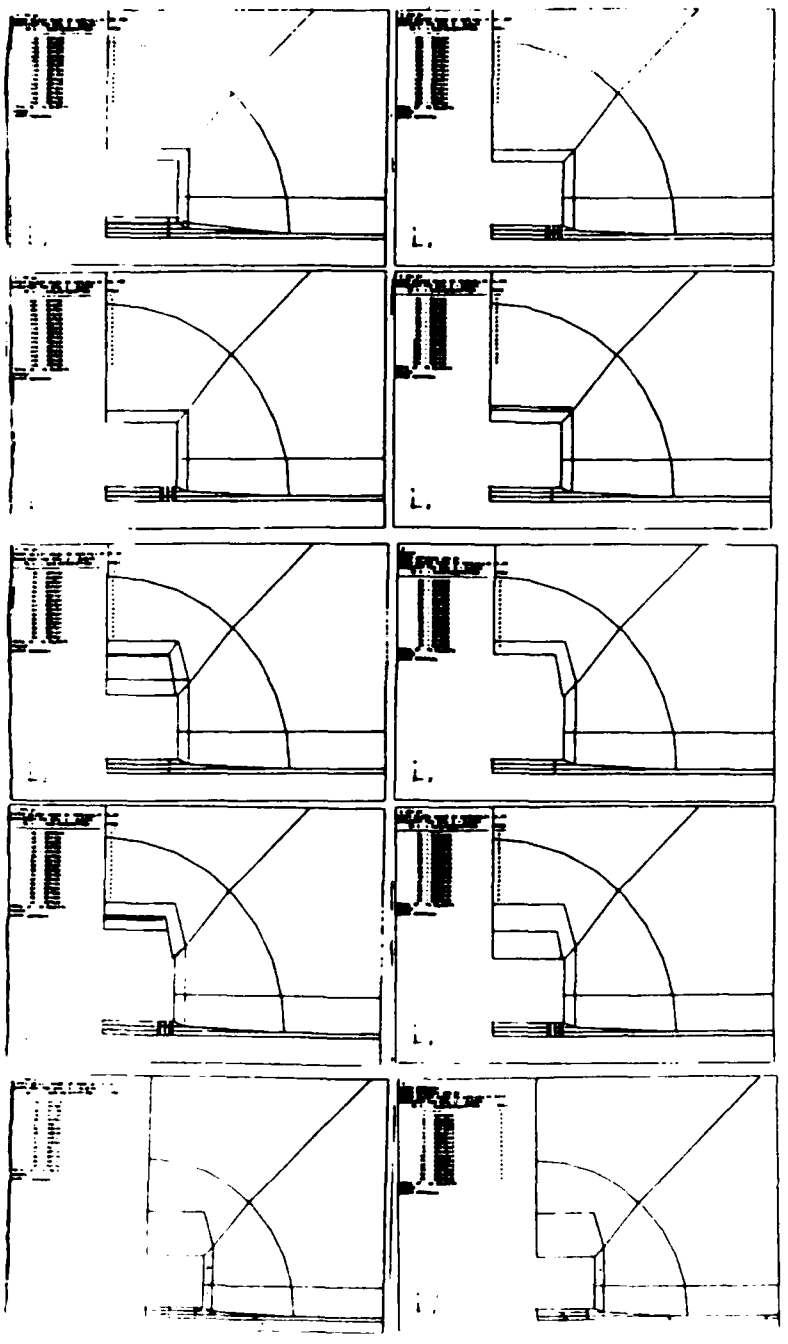

Figure 41. Block-structure at different sections of the car geometry.

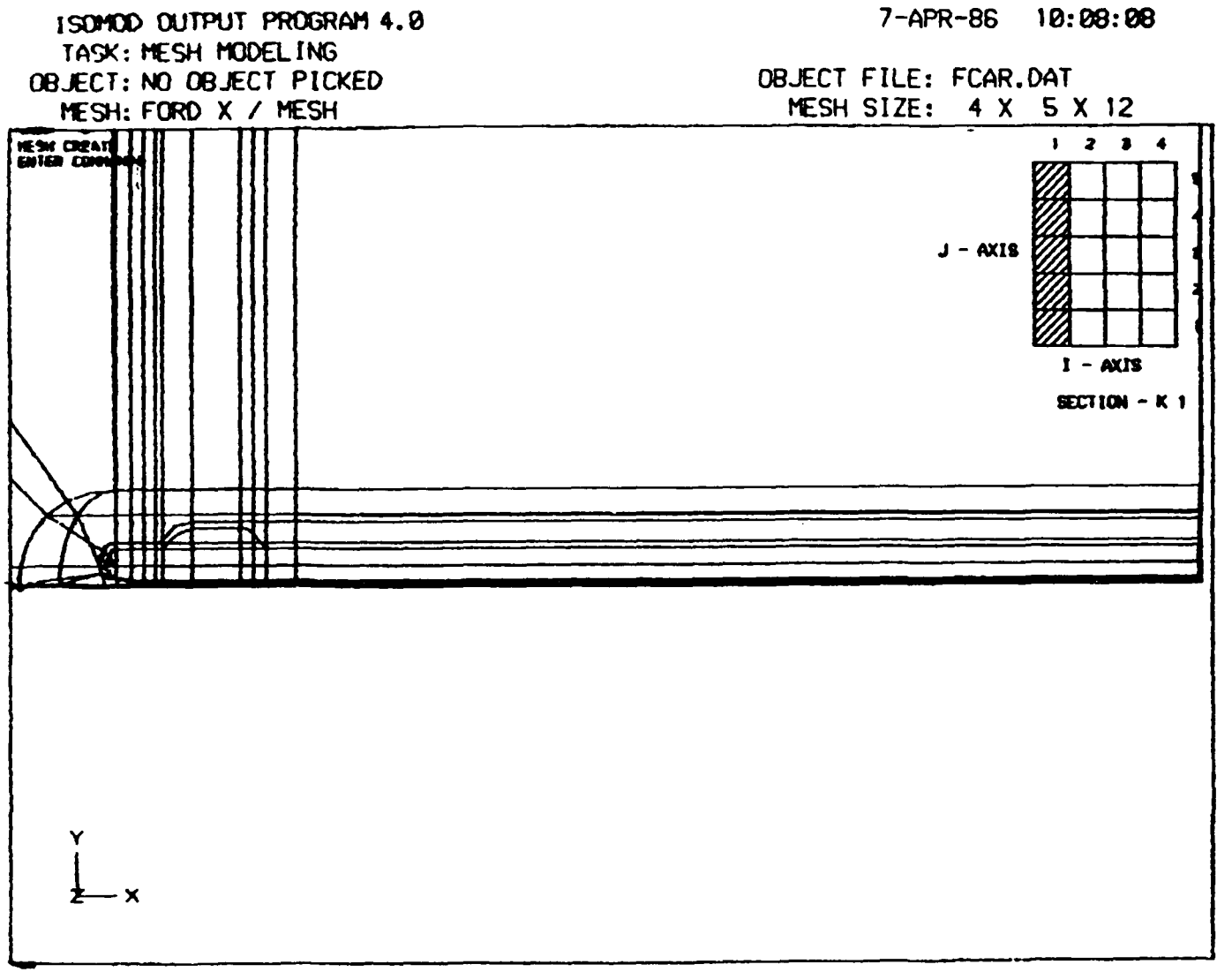

Figure 42. Block-structure at grid farfield.

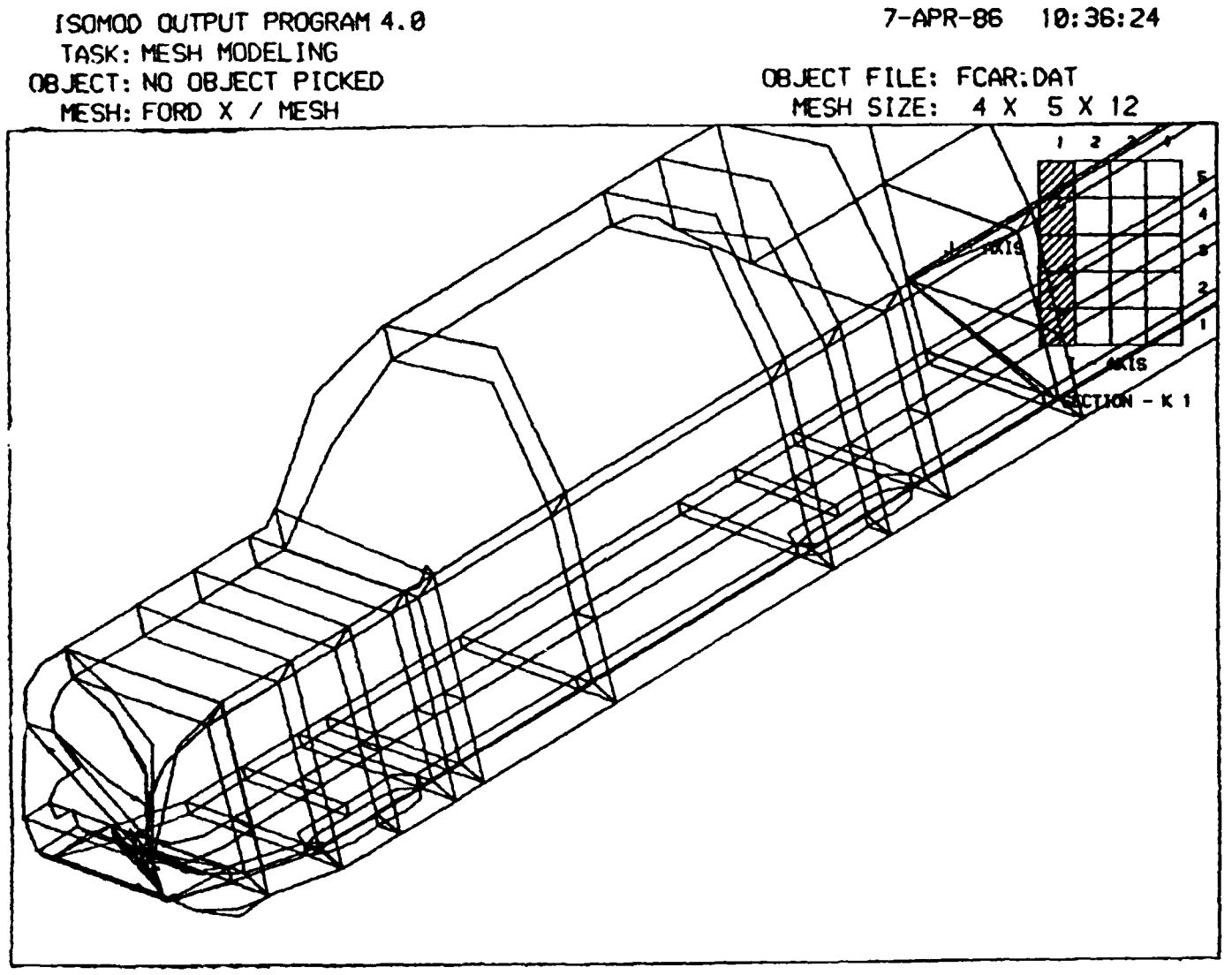

Figure 43. Boundary layer block shell around car geometry.

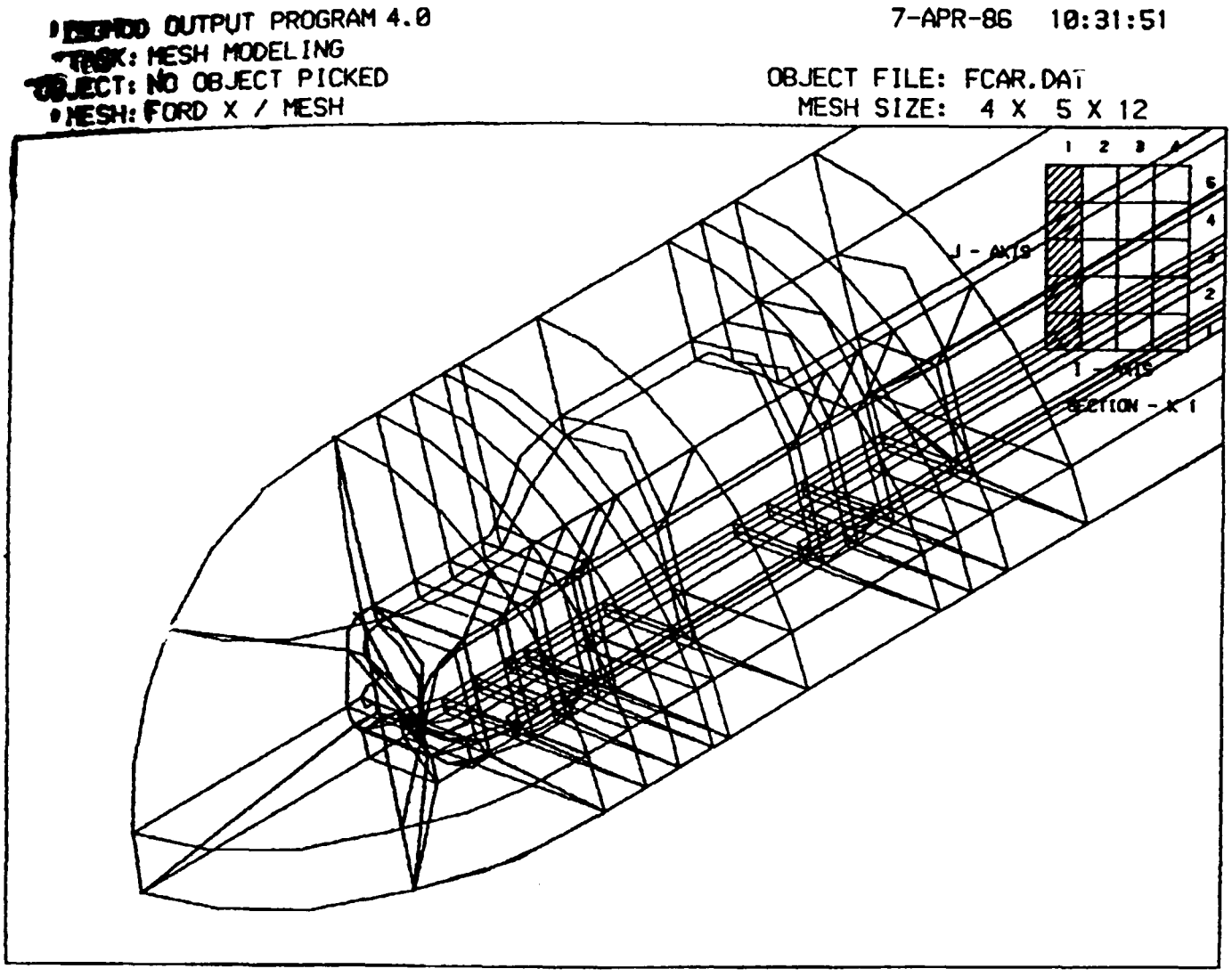

Figure 44. Intermediate block shell around boundary layer shell.

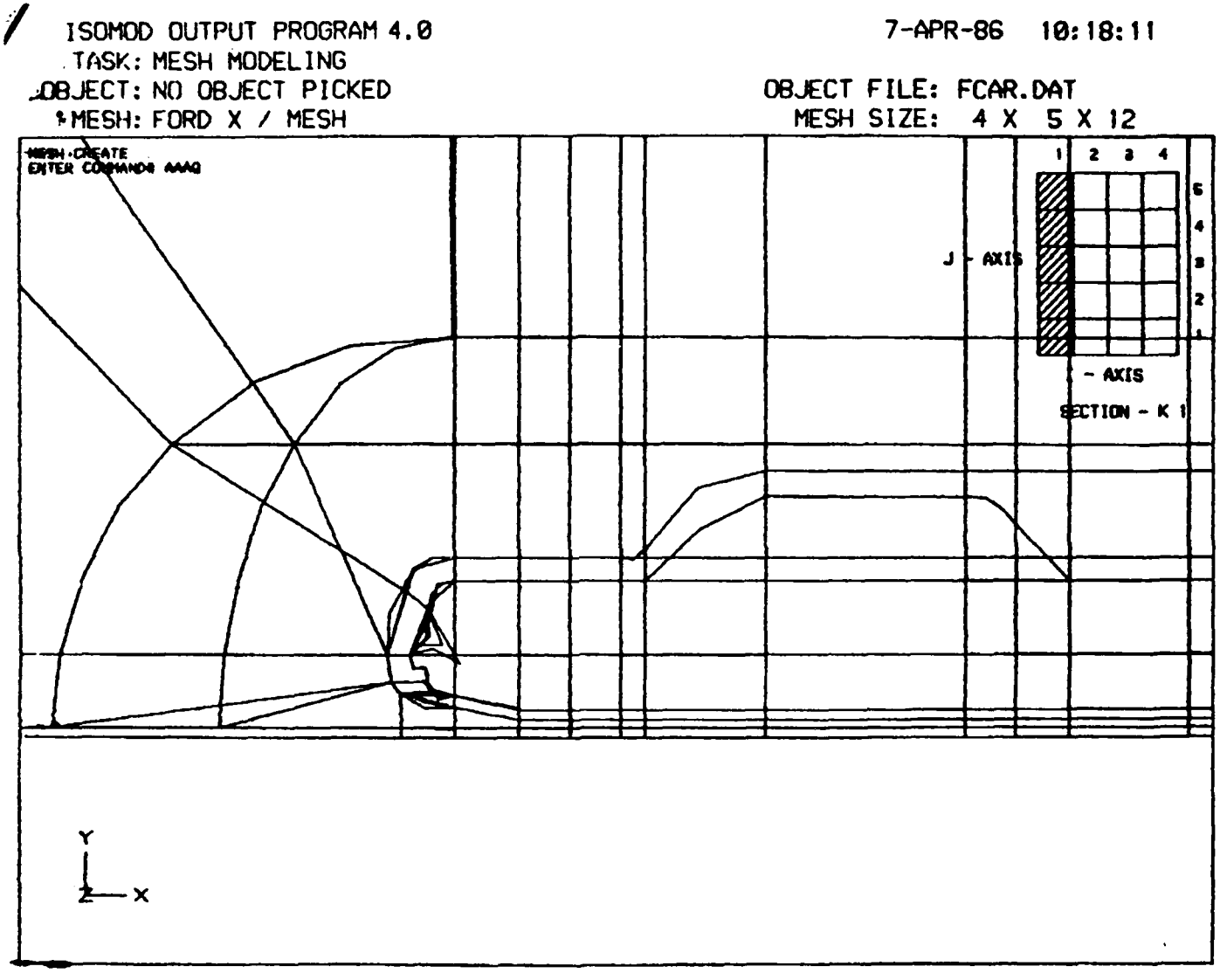

Figure 45. Side view of the intermediate and boundary layer block shells around car geometry.

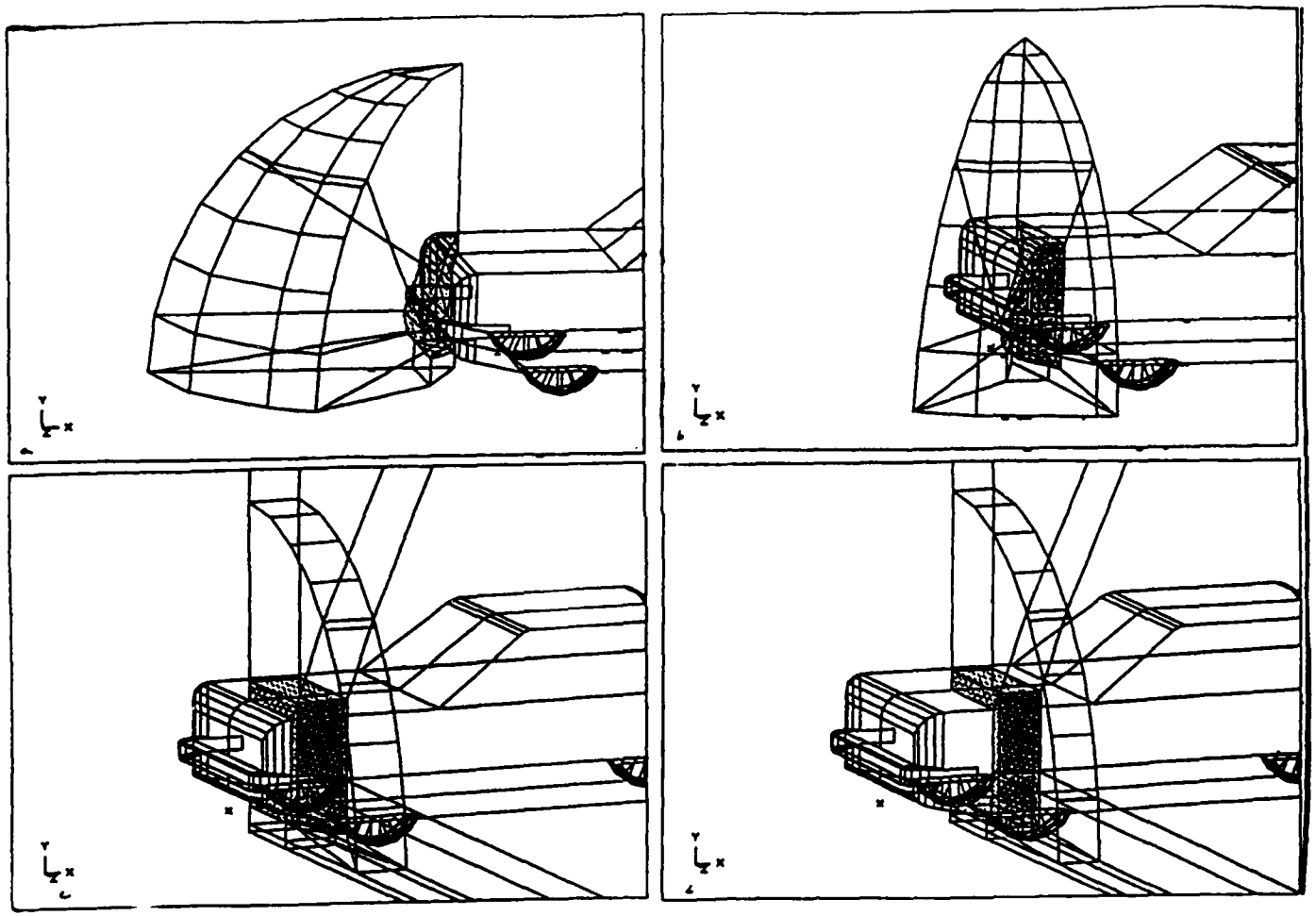

Figure 46. Blocks around car nose section with precise surfaces shaded.

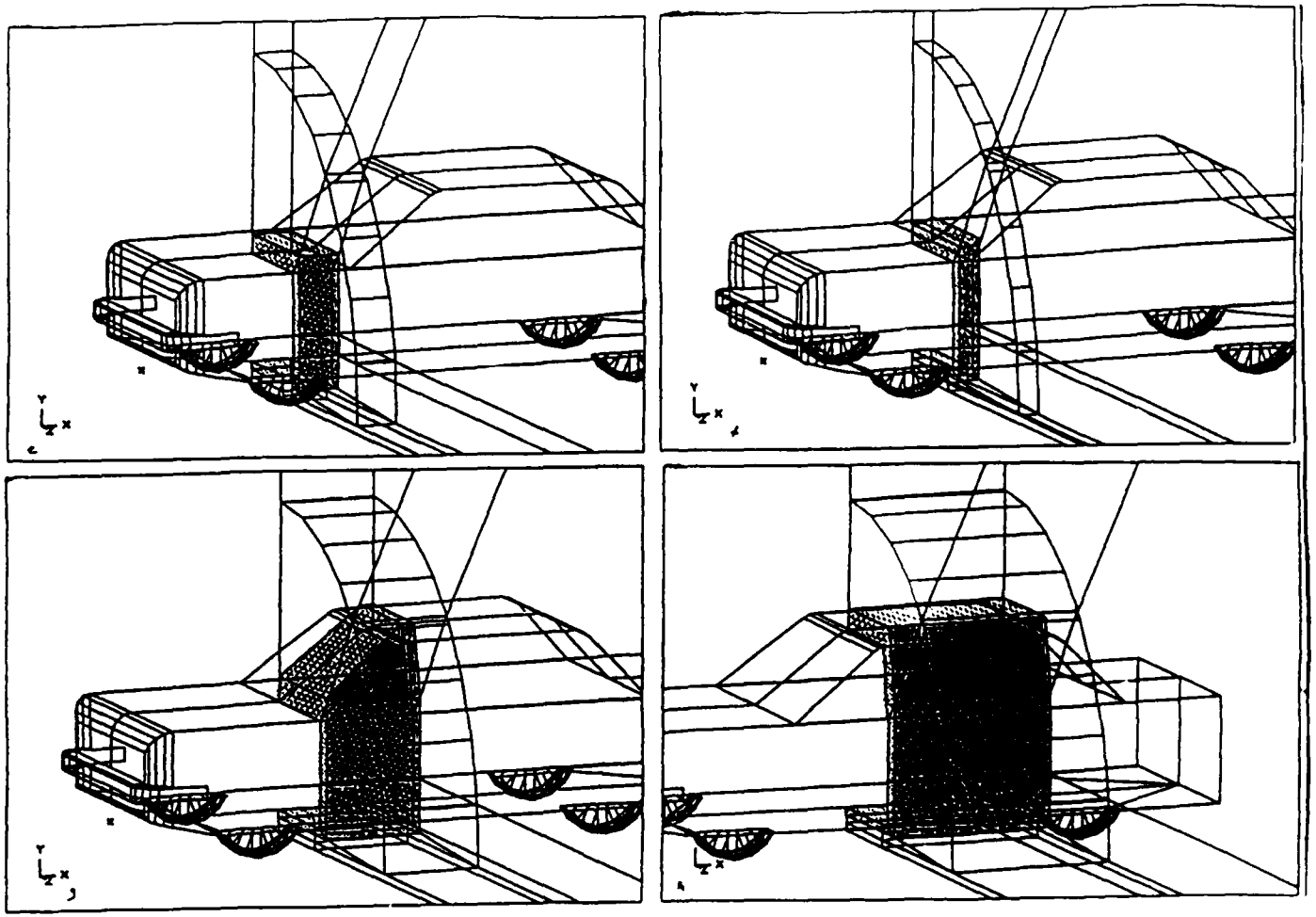

Figure 47. Blocks around car mid-section with precise surfaces shaded.

APPENDIX E

GRID GENERATION FOR THREE-DIMENSIONAL FLOWS THORUGH TURBINE HOUSINGS

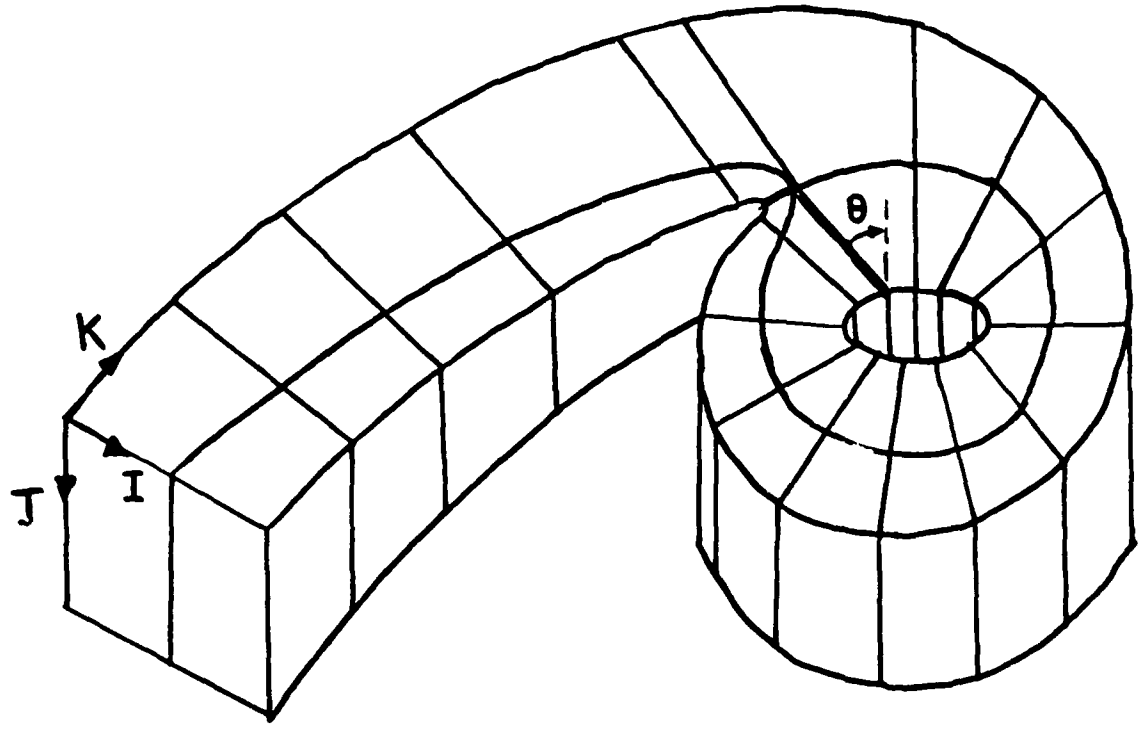

Figure 48. A sketch of block layout for the turbine housing.

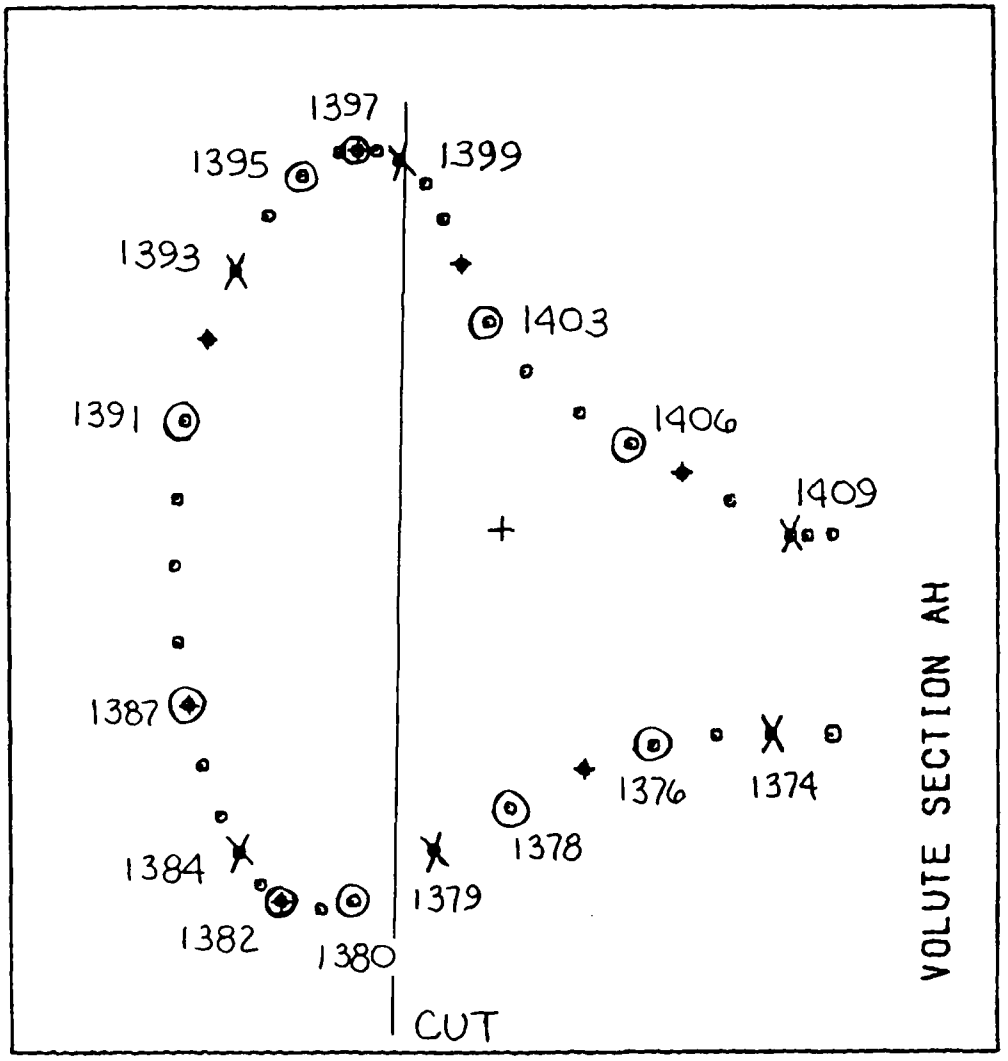

Figure 49. Volute cross-section showing block-defining nodes (numbered).

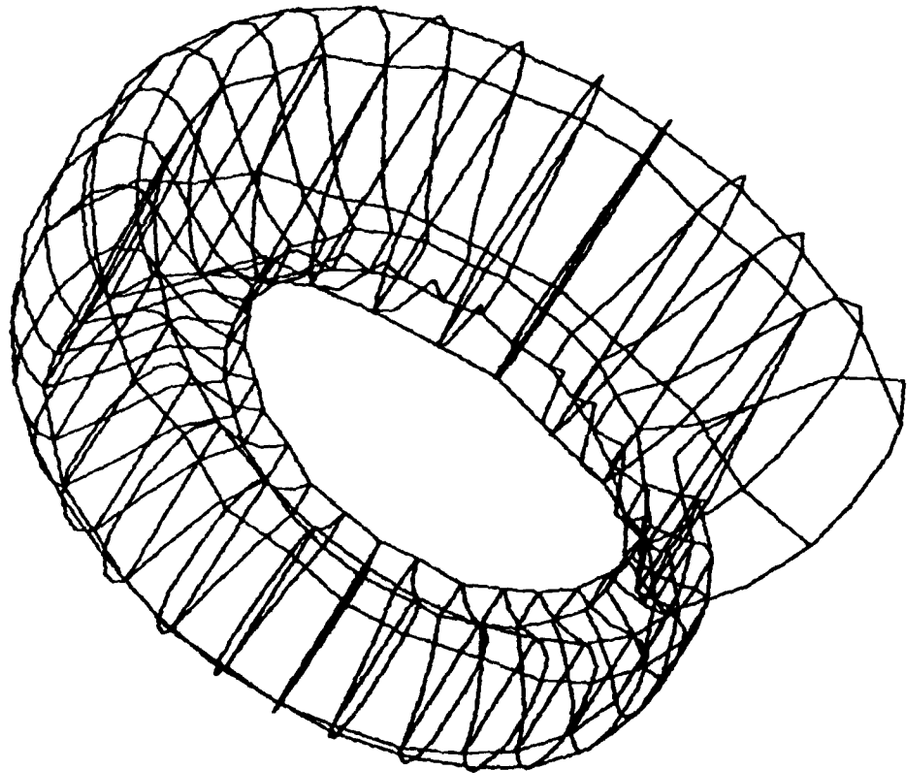

Figure 50. Block-structure for the volute section of the turbine casing.

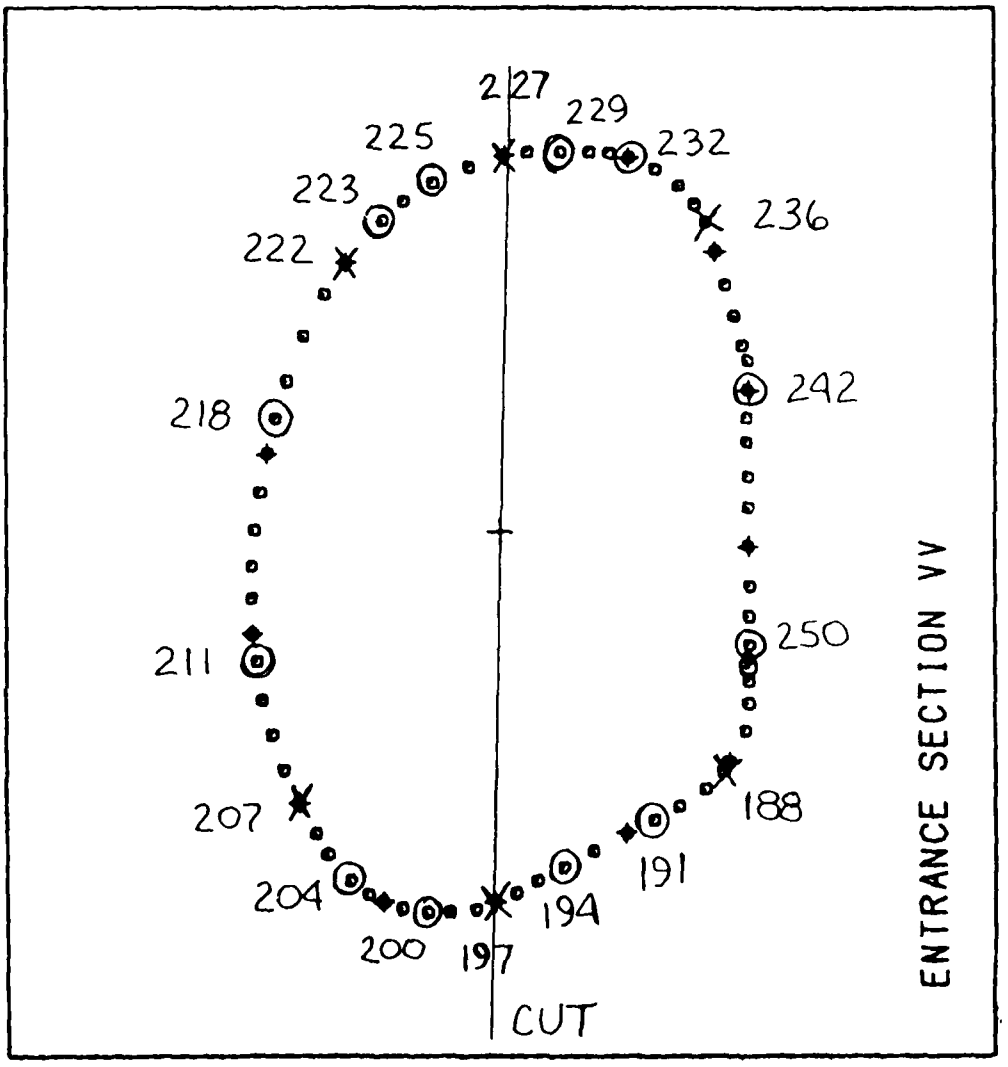

Figure 51. Entrance cross-section showing block-defining nodes (numbered).

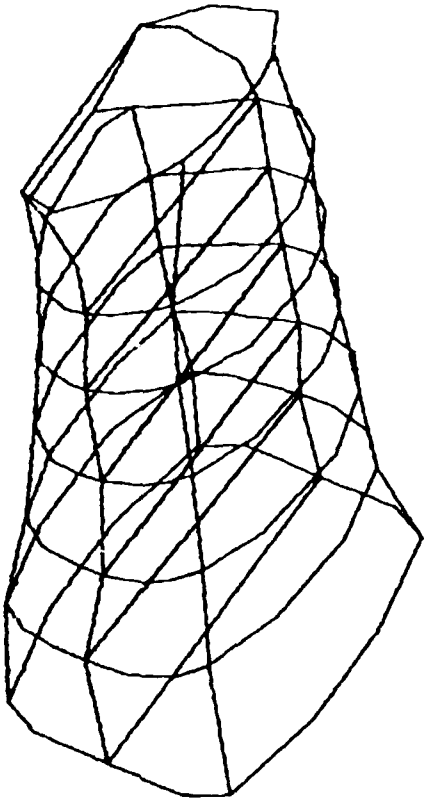

Figure 52. Block-structure for the entrance section.

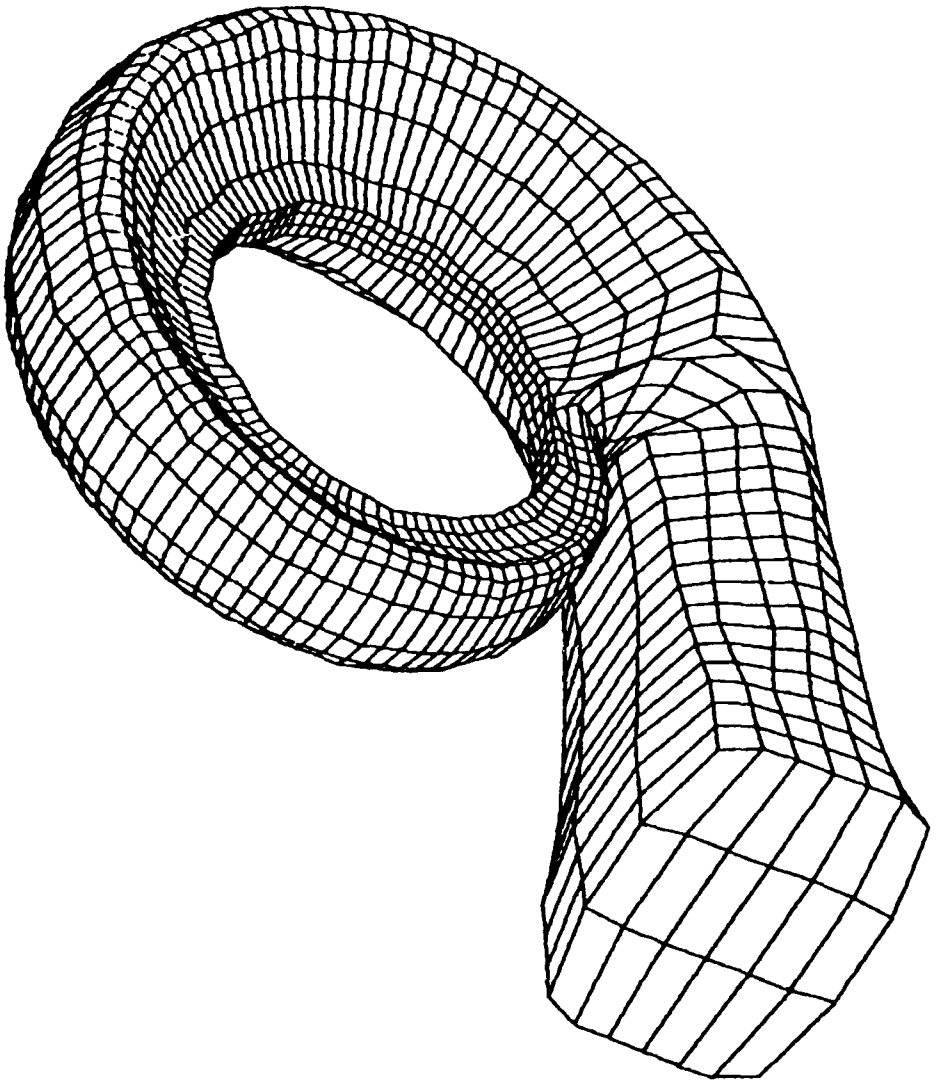

Figure 53. Grid for the entrance and volute sections assembled.

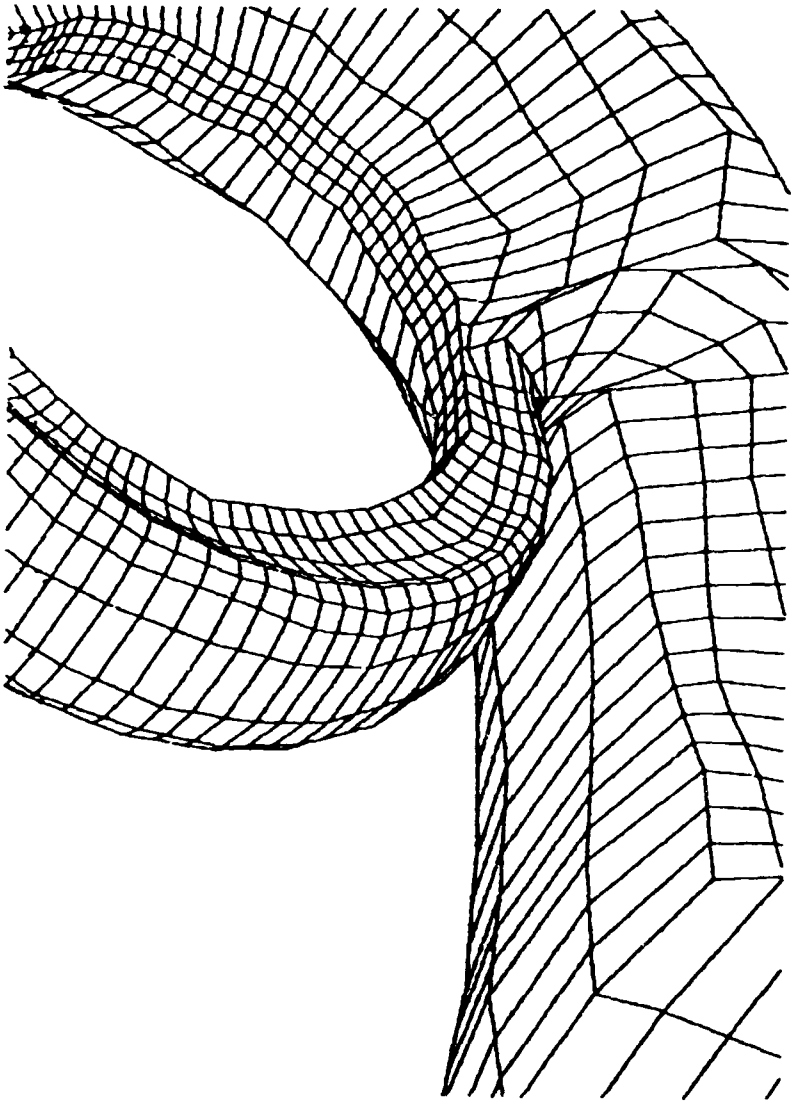

Figure 54. Grid detail at the joining area of the entrance and volute sections.

APPENDIX F

IMPLEMENTATION OF BLOCK-STRUCTURED GRID GENERATION SCHEME ON LARGE COMPUTERS

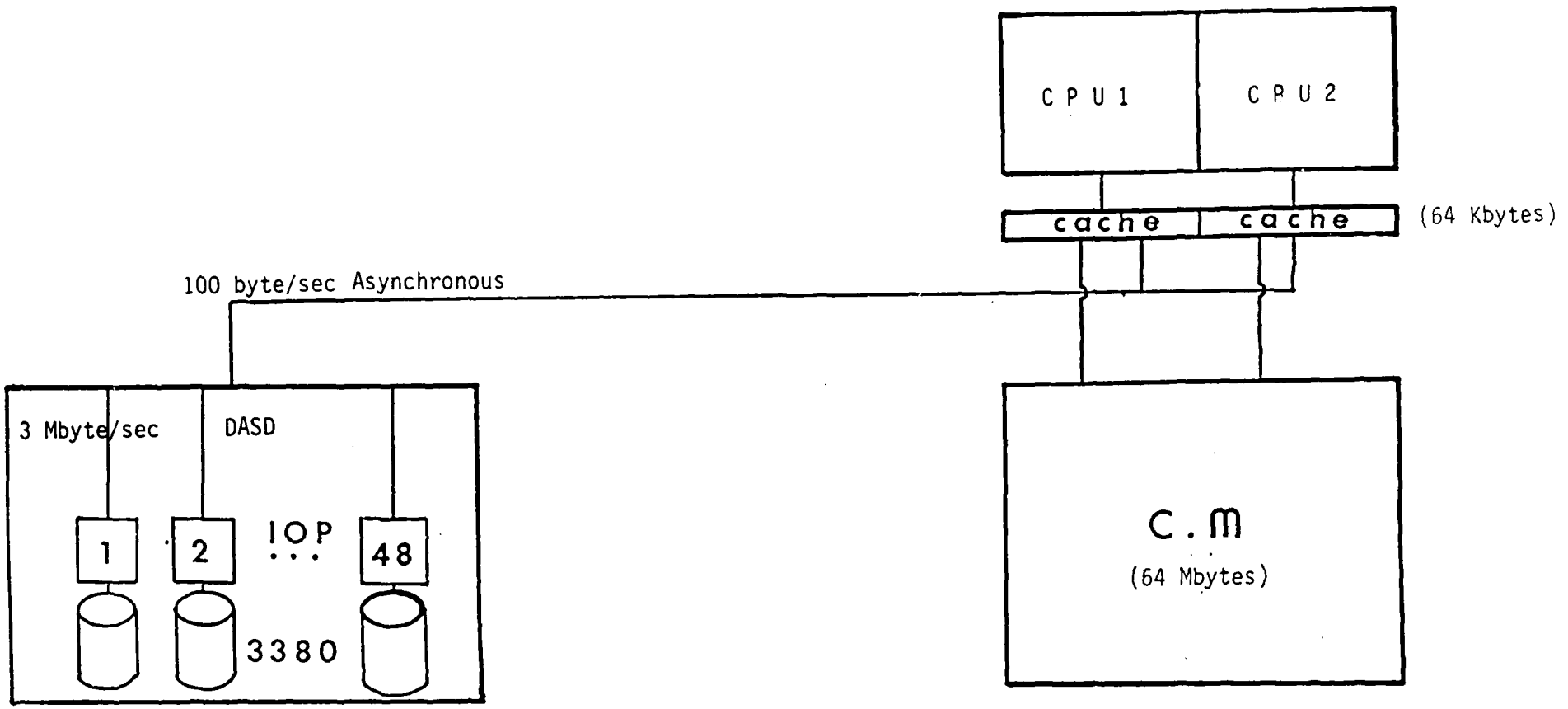

Figure 55. Disk I/O Configuration for IBM-3090 System

Implementation was completed on this system.

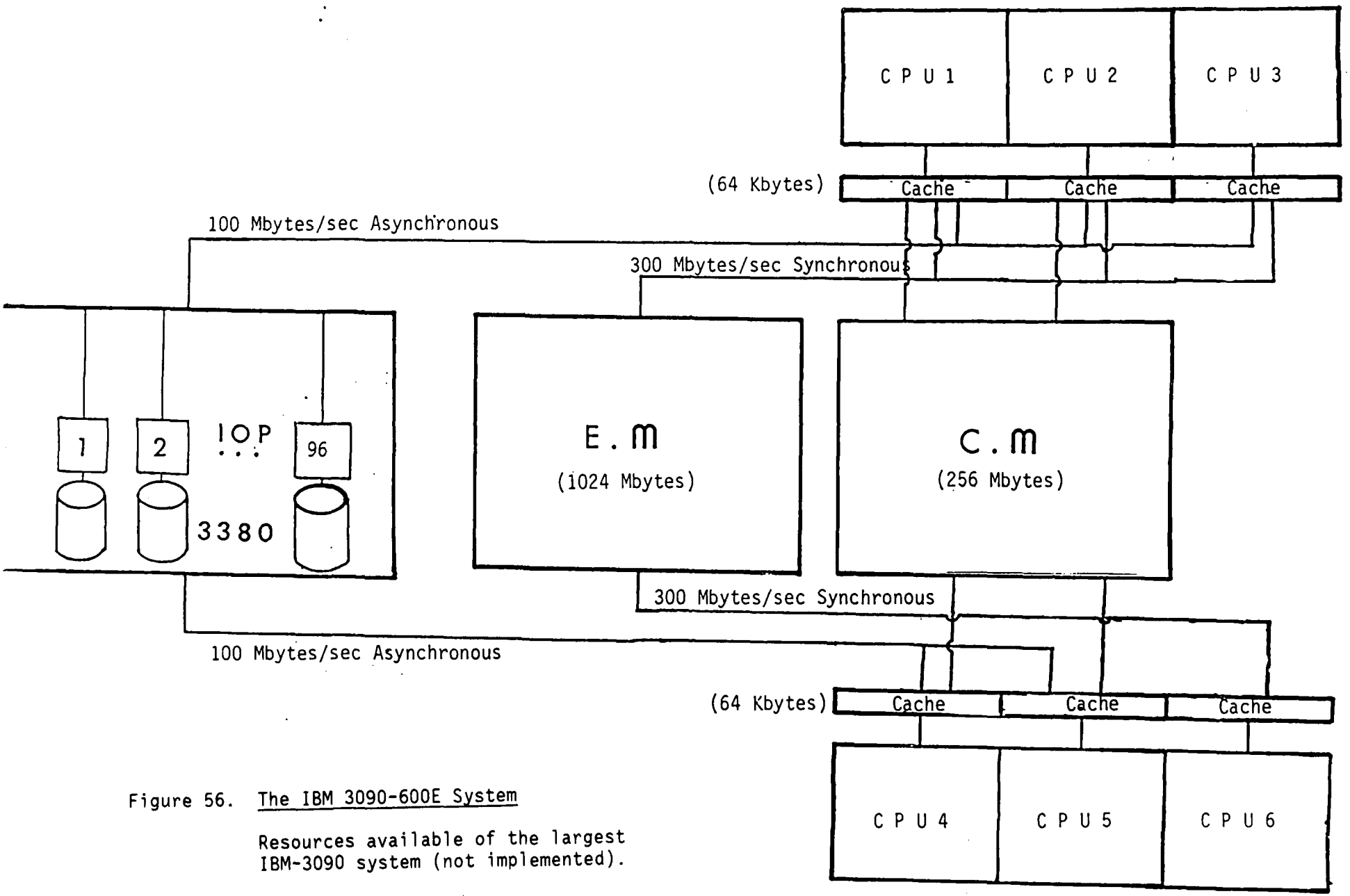

Figure 56. The IBM 3090-600E System

Resources available of the largest IBM-3090 system (not implemented).

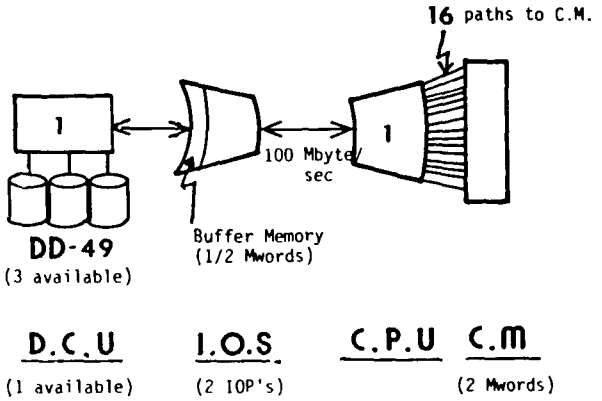

Figure 57. The existing AFWAL Cray X-MP 12 System

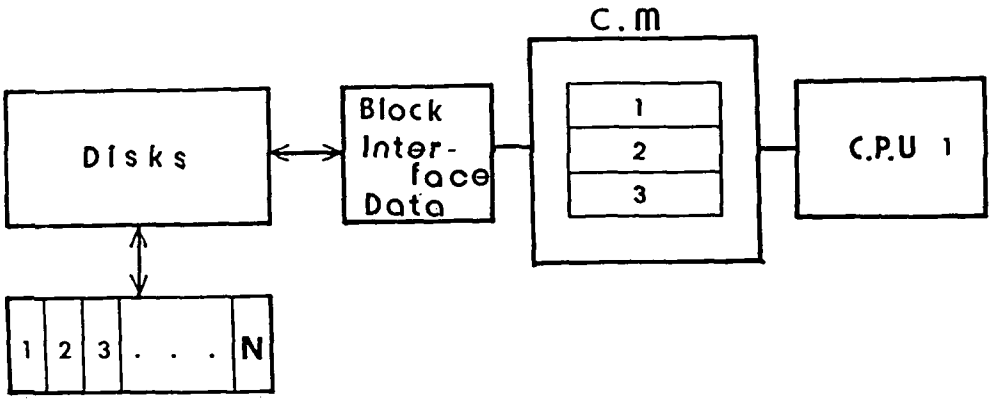

Figure 58. Disk I/O with AFWAL Cray X-MP 12 System

Implementation of the block-structured solution in scheme.

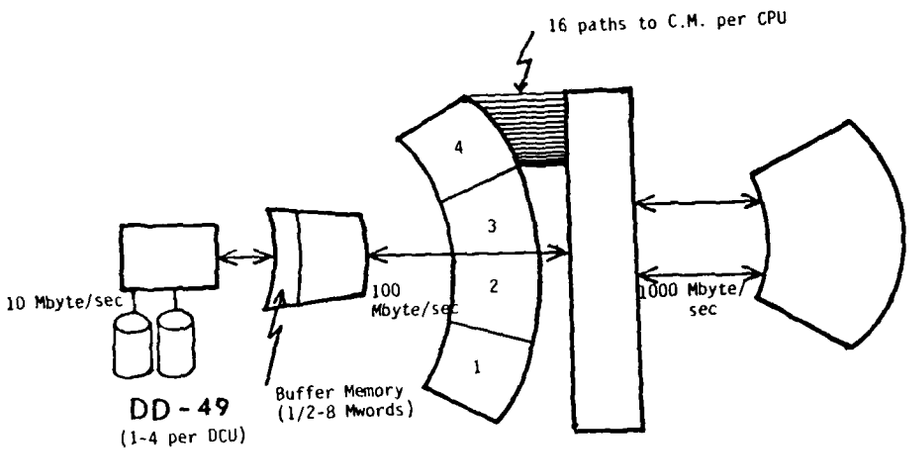

Figure 59. The Cray X-MP 416 System

Resources available on the largest Cray X-MP system.

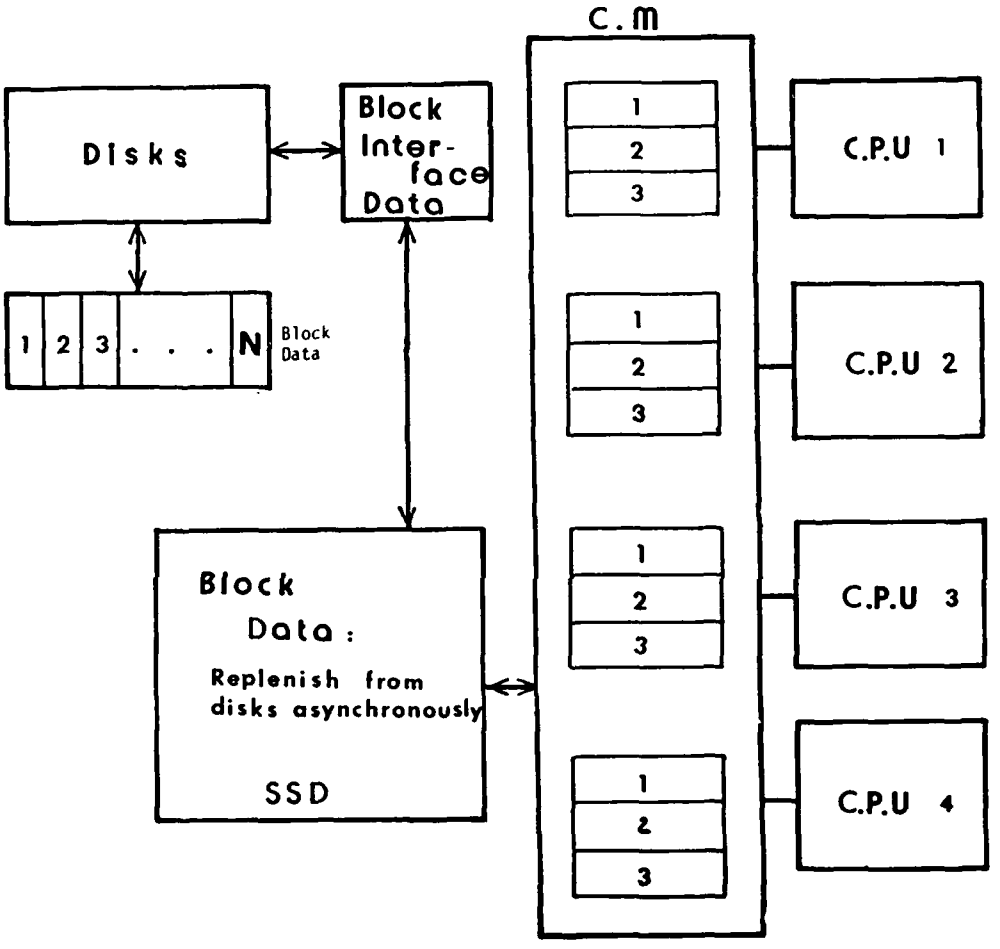

Figure 60. Disk I/O with Cray X-MP 416

Implementation of the block-structured solution scheme on the largest Cray X-MP system (not implemented).

END

12-87

DTIC